
Transect HYD-02A¹

Expedition 325 Scientists²

Chapter contents

Introduction	1
Hole M0040A	1
Hole M0041A	4
Hole M0042A	7
Hole M0043A	11
Hole M0044A	13
Hole M0045A	15
Hole M0046A	15
Hole M0047A	17
Hole M0048A	19
References	23
Transect HYD-02A summary	20
Figures	24
Tables	126

Introduction

During Integrated Ocean Drilling Program (IODP) Expedition 325, cores were recovered from 9 holes (5 sites) at Hydrographer's Passage, comprising transect HYD-02A (Holes M0040A–M0048A) (Fig. F1), with an average transect recovery of 22.45% of the drilled length. Water depths ranged from 50.78 to 126.58 m (lowest astronomical tide) and were taken from tidally corrected EM300 multibeam bathymetry data. Existing data sets were evaluated prior to arrival at each site, and drilling targets and their respective coordinates were chosen from within the agreed area approved by the IODP Environmental Protection and Safety Panel.

Hole M0040A

Operations

Transit to transect HYD-02A

The *Greatship Maya* transited to the survey transect under guidance from the pilot. The vessel crossed Hydrogr Passage in a southeast direction and reached Site 10, Hole M0040A, at 1830 h on 5 March 2010.

Site 10, Hole M0040A

By 1925 h on 5 March 2010, the seabed transponder had been deployed and the *Greatship Maya* had settled on station over Hole M0040A (Table T1). American Petroleum Institute (API) pipe was run to just above the seabed by 2125 h, when the downpipe camera was deployed. The camera survey was completed by 2220 h, and API pipe was run until the seabed was tagged at 2235 h. The first core was on deck at 2250 h, and coring continued until the end of Run 3, when repairs to the driller's shack electrics halted operations between 0030 and 0155 h on 6 March. Operations then restarted for another nine runs until the hole was terminated at 0825 h at 21.5 meters below seafloor (mbsf), with an average recovery of 54.6%.

Three API pipes were tripped to bring the drill string to ~4 m above the seabed. A downpipe camera survey was then conducted between 0850 and 0910 h, prior to the vessel moving 10 m to starboard to the next hole.

¹Expedition 325 Scientists, 2011. Transect HYD-02A. In Webster, J.M., Yokoyama, Y., Cotterill, C., and the Expedition 325 Scientists, *Proc. IODP*, 325: Tokyo (Integrated Ocean Drilling Program Management International, Inc.).
doi:10.2204/iodp.proc.325.104.2011

²Expedition 325 Scientists' addresses.



Sedimentology and biological assemblages

Hole M0040A is divided into six lithostratigraphic units.

Unit 1: Sections 325-M0040A-1R-1 through 1R-CC: unconsolidated mud

The uppermost Unit 1, spanning Sections 325-M0040A-1R-1 through 1R-CC, consists of unconsolidated mud with a small amount of lime sand. Interval 325-M0040A-1R-1, 0–10 cm, is rich in pebble-sized or smaller bioclasts of *Halimeda*, mollusks, foraminifera, and echinoids (spines). Below this interval, bioclasts are rare, except for a few small benthic foraminifera. There are no larger foraminifera or planktonic foraminifera. There are no corals in Unit 1.

Unit 2: Section 325-M0040A-2R-1: unconsolidated fine lime sand and pebbles

Unit 2, consisting only of Section 325-M0040A-2R-1, is composed of 17 cm of pebble-sized or smaller bioclasts of mollusks, larger foraminifera (including *Homotrema*), corals, *Halimeda*, and serpulids, associated with calcareous fine sand. There are a few fragments of *Seriatopora*.

Unit 3: Section 325-M0040A-3R-1: fragments of coralg-al-microbialite boundstone

Unit 3, consisting only of Section 325-M0040A-3R-1, contains 23 cm of fragments of coralg-al-microbialite boundstone. The boundstone is buff colored and composed of bryozoans, nongeniculate coralline algae, and microbialites. Because the material was fragmented by the drilling process, the succession of lithologies in the unit cannot be determined. There are no corals in Unit 3.

Unit 4: Sections 325-M0040A-4R-1 through 4R-CC: unconsolidated bioclasts and lithoclasts

Unit 4, spanning Sections 325-M0040A-4R-1 through 4R-CC, consists of pebble-sized and smaller bioclasts of mollusks, corals (hermatypic and solitary corals), foraminifera, and lithoclasts of microbialite boundstone (and packstone). Corals are associated with microbialites.

There are a few *Seriatopora* fragments throughout Unit 4, with some larger *Seriatopora* fragments and a piece of massive *Goniopora*(?) in Section 325-M0040A-4R-CC.

Unit 5: Sections 325-M0040A-5R-1 through 9R-1: microbialite boundstone

Unit 5, spanning Sections 325-M0040A-5R-1 to 9R-1, 36 cm, consists mainly of microbialite with an interlayer of bioclastic packstone/rudstone in interval 7R-1, 9–40 cm (Fig. F2). Coralg-al boundstone in interval 325-M0040A-9R-1, 0–14 cm (Fig. F3) and bioclastic rudstone in interval 9R-1, 14–37 cm (Fig. F4) occur at the base of Unit 5. Microbialites have a range of different fabrics, from massive and laminated to thrombolitic. Corals are common, but nongeniculate coralline algae are rare. Cavities of uncertain origin are partly filled with consolidated and unconsolidated fine-grained (silt-sized) internal sediment (Fig. F5). The packstone/rudstone and rudstone intervals are rich in bioclasts of mollusks, echinoids, corals, *Halimeda*, and, to a lesser extent, bryozoans.

The main corals are thin encrusting to submassive layers of *Porites*, *Montipora*(?), and Agariciidae (Figs. F6, F7). Associated corals include massive *Goniopora*(?), Acroporidae, and Faviidae, as well as encrusting to branching *Seriatopora*, *Goniopora*, *Porites*, *Tubipora musica*, Pocilloporidae, and Acroporidae. Fragments include *Seriatopora*, *Porites*, *Tubipora musica*, *Montipora*(?), Acroporidae, Agariciidae, and Poritidae.

Unit 6: Sections 325-M0040A-9R-CC through 12R-CC: unconsolidated sediment

The lowermost Unit 6, spanning Sections 325-M0040A-9R-CC through 12R-CC, consists mainly of unconsolidated fine- to medium-grained lime sand that contains molluscan shell fragments and a few bryozoans. Very coarse sands from interval 325-M0040A-10R-1, 20–25 cm, contain fragmented specimens of *Operculina* and Soritinae, as well as abraded specimens of Rotallidae (*Amphistegina*?). Well-preserved or fragmented specimens of *Operculina* and Soritinae are common in fine to medium sands from interval 325-M0040A-11R-1, 70–75 cm, whereas similar fine to medium sands from interval 12R-1, 70–75 cm, contain sparse but well-preserved specimens of *Operculina*, Miliolidae, *Amphistegina*, and Soritinae. A few well-preserved specimens of *Operculina* and Miliolidae also exist in fine to medium sands from interval 325-M0040A-12R-2, 50–55 cm. There are no corals in Unit 6.

Physical properties

Hole M0040A was cored to a total depth of 21.50 m drilling depth below seafloor (DSF-A), of which

11.73 m was successfully recovered (54.56% recovery). Physical property data for this hole are summarized in Table T2.

Density and porosity

Gamma density varies from 1.01 to 2.44 g/cm³ in cores from Hole M0040A (Fig. F8). The cores are characterized by sections dominated by fracturing and by the fact that the cores are undersaturated. This is particularly evident in the fluctuating gamma bulk density values in Sections 325-M0040A-5R-1 through 9R-2. Fourteen discrete samples from Hole M0040A (Fig. F9) yield bulk density measurements in the range 1.83 to 2.33 g/cm³. Between 0 and 1.5 m core depth below seafloor (CSF-A), sandy lime mud and lime sand samples exhibit high porosity (49%–53%). From 3.5 to 12.69 m CSF-A, fragments of numerous lithologies include, but are not limited to, coralgal microbialite boundstone and bioclastic packstone with mollusks. The porosity of these sediments is lower, with a mean value of 26%. Below 12.69 m CSF-A to total depth, the lime sand has a higher porosity (37%–48%).

P-wave velocity

P-wave velocity measurements taken on whole cores offshore range from 1522 to 1829 m/s (Fig. F8). However, cores were frequently undersaturated and underfilled, which implies these values may be an underestimate of the in situ values (see “Physical properties” in the “Methods” chapter). P-wave velocity is at its highest at ~16 m CSF-A (Sections 325-M0040A-11R-1 and 11R-2), where fine sediments with some shell fragments are present. Whole-core velocities were not obtained between 2 and 14 m CSF-A in areas mainly composed of coralgal-microbialite and microbialite boundstones. Six core plug samples were taken from Hole M0040A and measured using the discrete P-wave logger. Velocities (mean resaturated values) measured on these samples range from 3727.67 to 4073.00 m/s (Fig. F10A), which are appropriate values for well-lithified porous formations such as these. In the discrete samples measured from Hole M0040A, P-wave velocity mostly increases with increasing bulk density (Fig. F10B).

Magnetic susceptibility

Recovered core from Hole M0040A exhibits a range of magnetic susceptibility values, from -1.69×10^{-5} to 34.44×10^{-5} SI (Fig. F8). Values are dominantly in the -1.69×10^{-5} to 2×10^{-5} SI range. Intervals of higher magnetic susceptibility include the uppermost 1 m of the hole, which has values in the region

of 16×10^{-5} SI, which decreases stepwise to the dominant hole value (note that the stepwise nature of this change may be indicative of a sporadic sensor [80 mm loop] issue (see “Physical properties” in the “Methods” chapter). The two other highs occur in Sections 325-M0040A-10R-1 (14.06 m CSF-A) and 12R-2 (20.19 m CSF-A).

Electrical resistivity

Electrical resistivity measured on whole cores is highly variable and ranges from 0.56 to 26.54 Ω m (Fig. F8). Values are primarily affected by lithology, pore fluid, and salinity, as well as core liner saturation. Resistivity values are most reliable in the upper and lower portions of the borehole where the values are the lowest (~0–2 m CSF-A and between ~15.60 m CSF-A and the base of the hole). The recovered cores are fractured and undersaturated where they are dominated by microbialite (Sections 325-M0040A-5R-1 through 9R-2), so resistivity values must therefore be considered with caution.

Digital line scans and color reflectance

All cores from Hole M0040A were measured using a digital line scan system with all data recorded at a resolution of 150 pixel/cm as both images and red-green-blue (RGB) values. Appropriate cores were also scanned for color reflectance (Fig. F11). Color reflectance in this hole varies between 50.27% and 72.73%. Measurements from shallower lithologies, which correspond to units mostly composed of fine sands and mud, have lower reflectance than coarser sediments such as coral fragments. Reflectance increases from 5 m CSF-A and remains high (53.71%–72.73%) to 10 m CSF-A. When fine sediments are present, the signal for a* is negative, indicating green coloration. Larger grain size gives higher values close to or within the red scale. Values for b* remain in the same range, with high variations within sections. The a*/b* ratio is a good indicator of changes in lithology in this hole, as it captures the trends in a* and b* simultaneously.

Thermal conductivity

Four thermal conductivity measurements were taken in Hole M0040A, and values range from 1.04 to 1.18 W/(m·K) (Fig. F12). No particular trend is visible in this small data set.

Paleomagnetism

Measurements of low-field and mass-specific magnetic susceptibility (χ) were performed on samples taken from the working half of the recovered core using both 1 cm³ and paleomagnetic standard sam-

ples (Fig. F13). Very low to low negative (diamagnetic) susceptibilities occurred throughout the core, ranging from -0.07×10^{-8} to -5.0×10^{-8} m³/kg with an arithmetic mean value of -1.29×10^{-8} m³/kg. In addition, positive susceptibilities ranging from 0.00 to 131.58×10^{-8} with an arithmetic mean value of 5.45×10^{-8} m³/kg were recorded. The positive susceptibility peaks indicate the presence of ferromagnetic minerals.

Chronology

Two calibrated radiocarbon ages (10 calibrated years before present [cal y BP; years before 1950 AD], Core 325-M0040A-2R; 15 cal y BP, Core 4R) (Fig. F14) and one U-Th age (25 cal y BP, Core 8R) (see Table T10 in the “Methods” chapter) are consistent with their stratigraphic positions. The U-Th age is unaffected by corrections for initial ²³⁰Th (the seawater correction makes the age 0.6 k.y. younger), adding to the confidence in this age interpretation. Therefore, this hole recovered material from the Last Glacial Maximum interval and has captured the early portion of the deglaciation to 10 cal y BP.

Hole M0041A

Operations

Site 10, Hole M0041A

The *Greatship Maya* was on station over Hole M0041A by 0915 h on 6 March 2010, and a precoring downpipe camera survey was conducted (Table T1). The camera was back on deck by 0925 h, and the API pipe tagged the seabed at 0955 h. Coring operations ran smoothly for 12 standard rotary corer runs before the hole was terminated at 1650 h at 22.1 mbsf, with an average recovery of 45.5%.

The API pipe was tripped until it sat ~5 m above the seabed, and the downpipe camera was deployed. However, the camera became stuck in the bottom-hole assembly at 1720 h and could not be recovered. At 1745 h, the decision was taken to cut the camera cable and trip the API pipe, passing the camera cable through each pipe successively in order to retain the camera should it become free while tripping the API pipe. At 2110 h, the camera became free in the pipe above the collars and was recovered. By 2130 h, all API pipe was in the rack/slips and retermination of the camera cable had begun. The seabed transponder was recovered, and the vessel began to transit 6 km landward to Site 2, Hole M0042A, at 2220 h.

Sedimentology and biological assemblages

Hole M0041A is divided into five lithostratigraphic units.

Unit 1: Sections 325-M0041A-1R-1 through 1R-2: unconsolidated mud and very fine sand

The uppermost Unit 1, spanning Sections 325-M0041A-1R-1 through 1R-2, consists of 200 cm of unconsolidated mud and very fine sand, with rare bioclasts of larger foraminifera and mollusks. The uppermost 3 cm in Section 325-M0041A-1R-1 is rich in molluscan shells. Interval 325-M0041A-1R-1, 14–19 cm, contains a few well-preserved specimens of *Amphistegina* and Miliolidae. There are no visible corals in Unit 1.

Unit 2: Sections 325-M0041A-1R-CC to 4R-1, 8 cm: fragmented boundstone/packstone and unconsolidated lime sand and gravel

Unit 2, spanning Sections 325-M0041A-1R-CC, 0 cm, to Section 4R-1, 8 cm, consists of angular, pebble-sized lithoclasts of coralgall boundstone and bioclastic packstone, with sand- to pebble-sized bioclasts of corals, mollusks, and, to a lesser extent, larger foraminifera (Fig. F15). Sediments from interval 325-M0041A-1R-2, 70–75 cm, only contain small benthic foraminifera. Lithoclasts are stained dark gray.

Except for one massive *Porites*, most corals are broken pieces of encrusting to massive Acroporidae and Poritidae. Smaller fragments include *Porites*, *Acropora*(?), *Isopora*(?), *Montipora*(?), and Pocilloporidae.

Unit 3: Sections 325-M0041A-4R-1, 8 cm, to 7R-1, 21 cm: microbialite boundstone

Unit 3, spanning Sections 325-M0041A-4R-1, 8 cm, to 7R-1, 21 cm, mainly consists of (coralgall) microbialite with varying amounts of coralline algae, but its nature is difficult to determine because the recovered material is broken into many fragments, possibly by drilling disturbance. A well-preserved sample of microbialite from interval 325-M0041A-6R-1, 13–31 cm, has both thrombolitic and laminated fabrics (Fig. F16). Laminar microbialites also form columns (~1–2 cm in diameter and ~6 cm in height), and cavities in the microbialites are filled with bioclastic packstone.

Pieces of Acroporidae(?) and Poritidae(?) dominate the upper parts of Unit 3, whereas Agariciidae and Faviidae dominate toward the base. Coral fragments are largely unidentifiable in the upper parts of the unit, but fragments toward the base include *Seriatopora*, *Tubipora musica*, Acroporidae, Agariciidae, Poritidae(?), and free-living *Heterosammia cochlea*.

Unit 4: Sections 325-M0041A-7R-1, 21 cm, to 10R-1, 8 cm: very coarse lime sand with coral clasts

Unit 4, spanning Sections 325-M0041A-7R-1, 21 cm, to 10R-1, 8 cm, consists of very coarse lime sand with pebble-sized clasts of corals (Fig. F17). The very coarse lime sand is composed mainly of bioclasts of corals along with mollusks, with lesser amounts of *Halimeda* and larger foraminifera. Muddy medium sands from interval 325-M0041A-8R-1, 40–45 cm, include many well-preserved specimens of *Operculina* and *Alveolinella* and abraded specimens of *Amphistegina*. Fragmented specimens of *Operculina*, *Alveolinella*, *Amphistegina*, and Elphidiidae are common in muddy medium sands from interval 325-M0041A-10R-1, 34–39 cm.

Larger coral clasts are pieces of massive Faviidae (including *Favites*). Smaller clasts and fragments include *Plesiastrea*(?), *Montipora* or *Porites*, *Seriatopora*, and *Turbinaria*.

Unit 5: Sections 325-M0041A-10R-1, 8 cm, through 12R-CC: unconsolidated fine to medium sand

The lowermost Unit 5, spanning Sections 325-M0041A-10R-11, 8 cm, through 12R-CC, consists mainly of unconsolidated fine to medium lime sand with larger foraminifera (e.g., *Operculina*), molluscan shell fragments, and rare coral clasts. Some interlayered lithologies consist mainly of pebble-sized bioclasts of mollusks, larger foraminifera, and smaller benthic foraminifera (including *Homotrema rubrum*). There are well-preserved and fragmented specimens of *Operculina* (Fig. F18) in muddy medium-grained sands from intervals 325-M0041A-11R-1, 55–60 cm, 12R-1, 64–69 cm, and 12R-2, 24–29 cm.

Corals are scarce but include small fragments of *Porites*, *Montipora*(?), *Seriatopora*, free-living *Heterocyathus cochlea*, and solitary ahermatypic corals.

Physical properties

Hole M0041A was cored to a total depth of 22.10 m CSF-A, of which 10.06 m was successfully recovered (45.52% recovery). As with other holes from this transect, physical property measurements for this hole are compiled in Table T2.

Density and porosity

Bulk density varies from 1.13 to 2.41 g/cm³ in cores from Hole M0041A (Fig. F19). The uppermost 2 m and bottommost 5 m of the hole are characterized by relatively stable bulk density values in the range of 1.92 to 2.21 g/cm³. The middle part of the hole has more erratic bulk density values, which are likely a function of core length and core quality (see “Physical properties” in the “Methods” chapter). Twelve samples were taken from Hole M0041A for discrete moisture and density analysis (Fig. F20). High porosity (52% and 53%) sandy lime mud and lime sand is present between 0 and 1.5 m CSF-A. From 3.5 to 13.20 m CSF-A, there are fragmented units (lime sand and lime pebbles) where the porosity ranges from 27% to 37%. Below 13.20 m CSF-A, there is a lime sand unit of higher porosity (42%–50%). Beyond this, porosity changes with depth in a similar manner to that found in Hole M0040A. This is probably due to the fact that the boreholes are in close proximity to one another and at a similar water depth. Similar to Hole M0040A, grain density varies from 2.74 to 2.79 g/cm³, whereas bulk density ranges from 1.83 to 2.32 g/cm³. There are no downhole trends evident from the density data.

P-wave velocity

In Hole M0041A, whole-core *P*-wave velocity measurements taken offshore range from 1508.59 to 1700.41 m/s (Fig. F19). The lower values are too close to the value of *P*-wave velocity of water, indicating a problem with the validity of these data points. This problem is probably due to core quality issues (see “Physical properties” in the “Methods” chapter). Multisensor core logger *P*-wave velocity data are restricted to the uppermost 2 m and bottommost 5 m, with the lower interval exhibiting a decrease in value with depth. The absence of data from the central portion of Hole M0041A is a function of core quality and the potential for acoustic coupling across the *P*-wave velocity transducers. One discrete *P*-wave velocity measurement was taken on a sample from Hole M0041A cores, giving a value of 3841 m/s (mean value for resaturated core).

Magnetic susceptibility

In Hole M0041A, magnetic susceptibility values range from -1.00×10^{-5} to 67.34×10^{-5} SI, with most values falling between -1×10^{-5} and 1×10^{-5} SI (Fig. F19). Magnetic susceptibility highs occur in the bottom half of the hole at 12.98 CSF-A (15.57×10^{-5} SI), 16.24 CSF-A (22.92×10^{-5} SI), 17.77 CSF-A (67.34×10^{-5} SI), and 19.19 CSF-A (43.05×10^{-5} SI). No evidence of a downhole trend in the values exists.

Electrical resistivity

Similar to the density and *P*-wave data sets, resistivity data are relatively good and continuous at the top and bottom of the hole but erratic in the central section. Electrical resistivity measured on whole cores varies from 0.58 to 5.03 Ωm (Fig. F19). Resistivity values are most reliable in the upper and lower portions of the borehole, where the values are the lowest. Overall, there are no obvious downhole trends.

Digital line scans and color reflectance

All cores from Hole M0041A were digitally scanned, and, where appropriate, cores were measured for color reflectance. Color reflectance in Hole M0041A ranges from 44.71% to 73.7%. Hole M0041A exhibits a similar trend to Hole M0040A (Fig. F21). The uppermost 2 m of the hole is characterized by color reflectance values between 50.05% and 63.64% where muddy lime and pebbles were detected. A slightly higher reflectance was detected below 3 m CSF-A, reaching a maximum of 66.88% at 5.7 m CSF-A. Below this depth, the reflectance of the materials decreases with a higher dispersion of data corresponding to lime-sand areas. The presence of mollusk shells in certain areas could explain a higher dispersion of the data at ~13 m CSF-A. Where lime and muddy sand was present, values for the index a^* became negative (green color), and values were positive when coarser sediments, corresponding to broken coral fossils, were present. The value of b^* was positive in all cases, showing higher dispersion in depth within the same range. This indicated a yellow color in the samples.

Thermal conductivity

Three thermal conductivity measurement points were taken for Hole M0041A, with values ranging from 1.06 to 1.09 W/(m·K).

Paleomagnetism

Measurements of low-field and mass-specific magnetic susceptibility (χ) were performed on all samples taken from the working half of the recovered core using both 1 cm³ and paleomagnetic standard samples (Fig. F22). Very low to low negative (diamagnetic) susceptibilities occur throughout the entire core, ranging from -0.03×10^{-8} to -2.87×10^{-8} m³/kg with an average of -1.21×10^{-8} m³/kg. In addition, positive susceptibilities range from 0.00 to 58.18×10^{-8} m³/kg with an arithmetic mean of 3.94×10^{-8}

m³/kg. Two prominent susceptibility peaks are located at 14.15 and 15.63 mbsf with values of 9.16×10^{-8} and 58.18×10^{-8} m³/kg, respectively. These positive susceptibilities may indicate the presence of paramagnetic and/or ferromagnetic minerals.

Preliminary results obtained from the paleomagnetic study of a U-channel taken from Section 325-M0041A-12R-1 (transect HYD-02A) are also presented (Figs. F23, F24). The noisy natural remanent magnetization (NRM) demagnetization paths are attributed to the relatively low intensity of magnetizations (1.08×10^{-9} to 2.19×10^{-7} A/m with a mean of 2.02×10^{-8} A/m). A limited number of samples are characterized by high NRMs, and these are associated with lithologic layers of high magnetic susceptibility. Consistency of NRM inclinations of the discrete cubes measured can also be correlated with the intensity of magnetization results.

The generally positive and high inclination values obtained for Expedition 325 samples are not what is expected for the low paleolatitude of the sampling sites (latitude = 15°–20°S) with corresponding geocentric axial dipole values of ~28° to 36°S. One interpretation of the results is that a significant portion of the drilling overprint remains on the majority of samples studied. Alternatively, there may be a pervasive present-field overprint that was not possible to remove with alternating-field demagnetization experiments.

Anhyseretic remanent magnetization (ARM) values ($n = 134$) have an arithmetic mean of 5.16×10^{-8} A/m (Fig. F23D). Values $>3 \times 10^{-8}$ A/m occur in interval 325-M0041A-12R-1, 3–20 cm, with an average of 2.69×10^{-7} A/m. The rest of the core shows an arithmetic mean of 2.16×10^{-8} A/m. Therefore, the uppermost ~20 cm of Section 325-M0041A-12R-1 has ARM of over an order higher than the rest of the section. This interval at the top of the section testifies that depositional or preservation conditions are different here than in the rest of the section. We do not exclude the contamination of this interval during the drilling operations, which may have biased the magnetic properties.

Chronology

This hole has a single calibrated radiocarbon age of 17 cal y BP from Core 325-M0041A-2R (Fig. F25). The dated sample is from the top of the hole, indicating that this hole may have captured part of the early deglaciation. There are 10 cores beneath this 17

cal y BP section, indicating that this hole may have also recovered material from the Last Glacial Maximum, and possibly older.

Hole M0042A

Operations

Site 2, Hole M0042A

The *Greatship Maya* arrived at Site 2 at 2330 h on 6 March 2010 and began to settle on dynamic positioning. The seabed template was secured in the moonpool, repairs to the camera cable continued, and the API pipe was run to just above the seabed. At 0145 h on 7 March, the downpipe camera was deployed. The first standard rotary corer (ALN) core was recovered at 0330 h, and operations continued until 0500 h, when repairs to a latch head dog stopped coring for 55 min. After ALN Run 5 was recovered at 0715 h, it was decided that the API was spudded into the seabed firmly enough to switch to HQ coring. By 1020 h, the seabed template was secured in the moonpool with steel wires, the API pipe was set in the elevators, and the HQ rods were ready to be run. The first HQ core (Run 6) was recovered at 1240 h. However, the API pipe was sinking in the hole (1.5 m), presumably because of soft sediments, so hole stabilization using a thicker mud continued until 1330 h. During Run 7, the bit became blocked, requiring flushing. However, the API pipe started sinking again, now resting on the elevators, and it was believed that swabbing the hole was causing further instability. The decision was made to trip the HQ rods and return to API coring until a harder formation was encountered in which to set the API pipe.

At 1500 h, a sample was recovered from the HQ bottom-hole assembly and curated as a wash sample. Between 1540 and 1700 h, the API pipe was reconnected and the elevator removed. ALN coring restarted at 1710 h and continued until 0705 h on 8 March, when the hole was terminated at 46.4 mbsf with an average recovery of 23.6%.

Downhole logging was conducted following coring operations, and mobilization of the drill floor and logging equipment continued until 1010 h. Between 1010 and 1150 h, the through-pipe gamma log was run. On completion, the API pipe was tripped to 7 mbsf, and conditioning of the hole continued until 1340 h. The seabed template was then lowered onto the seabed, and the dual induction logging sonde was deployed at 1410 h. Following this, the acoustic borehole image, spectral gamma, magnetic susceptibility, sonic, optical borehole image, and caliper sondes were deployed at 1530, 1710, 1845, 2000,

2125, and 2320 h, respectively. Some hole caving was noted, with the tools logging from 45.07, 43.98, 39.93, 38.49, 33.23, 38.84, and 38.58 wireline log matched depth below seafloor (WMSF), respectively. By 0030 h on 9 March, all downhole logging had been completed and demobilization of the equipment and securing of the drill floor for transit had begun. At 0130 h, the seabed template was recovered, and by 0345 h, all API pipe had been tripped. The seabed transponder was onboard and secured by 0400 h, and the vessel began the 6.5 km transit seaward to Site 12, Hole M0044A.

Over the course of coring and logging this hole, three separate remotely operated vehicle dives were conducted, viewing the drill string, the small entry hole, and the dispersion of drill cuttings.

Sedimentology and biological assemblages

Hole M0042A is divided into 10 lithostratigraphic units.

Unit 1: Section 325-M0042A-1R-1: modern lime sand and algal bindstone

The uppermost Unit 1, consisting only of Section 325-M0042A-1R-1, is composed of algal bindstone and bioclastic packstone fragments, with lime sand containing fragments of *Halimeda*, mollusks, larger foraminifera, and coralline algae. Coralline algae form an open framework of thin plants. Fragments of coralline algal bindstone with worm tube and brownish stains in the uppermost 4 cm of Section 325-M0042A-1R-1 probably represent the modern seafloor. Interval 325-M0042A-1R-1, 14–19 cm, contains larger benthic foraminifera in muddy coarse sands.

The only coral is a fragment of a solitary Fungiidae in the uppermost 5 cm of the section.

Unit 2: Sections 325-M0042A-1R-CC through 3R-1: coralgall boundstone

Unit 2, spanning Sections 325-M0042A-1R-CC through 3R-1, contains pieces of coralgall boundstone (Fig. F26). The boundstone consists mainly of massive corals covered with coralline algae and minor microbialite crusts and has some internal sediments and fragments of mollusks and bryozoans. All components are bioeroded locally. The coralline algal crust in interval 325-M0042A-2R-1, 5–7 cm, has a “reddish” surface.

Large corals are mainly submassive to massive Faviidae (*Favia*(?) and *Platygyra*(?)) and one branching *Acropora*. Fragments include *Acropora*, *Cyphastrea*, *Porites*, *Montipora*(?), and various Faviidae.

Unit 3: Sections 325-M0042A-3R-CC through 5R-CC: coralg-al-microbialite boundstone

Unit 3, spanning Sections 325-M0042A-3R-CC through 5R-CC, consists of coralg-al-microbialite boundstone. Coralline algae alternate with microbialite crusts and appear to trap bioclasts. Coralline algae occur as thick crusts on top of corals or as irregular, contorted structures intergrown with microbialites. Microbialites can be several centimeters thick and are usually dark colored (Fig. F27) with a succession from laminated textures at the base to digitate forms at the top. Some internal bioclastic sediments, containing *Halimeda* and mollusks, occur throughout Unit 3. All components of the boundstone are bioeroded by bivalves and sponges. The geopetal filling of an intraskeletal void at Section 325-M0042A-4R-1, 40 cm, is probably microbialite.

The upper part of Unit 3 is dominated by medium to robustly branching *Acropora* (Fig. F28) and encrusting to submassive *Porites*. Associated corals are *Seriatopora*, *Tubipora musica*, encrusting *Porites*, and Faviidae. The only corals toward the base of Unit 3 are fragments of *Porites* and *Montipora*.

Unit 4: Sections 325-M0042A-8W-1 to 11R-1, 20 cm: unconsolidated sediment

Unit 4, spanning Section 325-M0042A-8W-1 through interval 325-M0042A-11R-1, 1–20 cm, consists of unconsolidated lime granules and pebbles. Major components are coral fragments (as large as 9 cm), coralg-al-microbialite boundstone fragments, *Halimeda*, larger foraminifera, mollusks, and coralline algae. Coralline algae occur both as crusts in boundstone fragments and as loose branching plants. Fragments from the overlying boundstones and fresh mollusk shells clearly indicate downhole contamination.

Larger corals are mainly massive *Isopora* and *Montipora*, with some branching to massive *Porites*. Diverse fragments include branching Pocilloporidae (*Pocillopora*, *Seriatopora*, and *Stylophora*), branching *Acropora*, and some pieces of *Montipora*, *Isopora*, *Platygyra*, *Porites*, *Montastrea*(?), and *Platygyra*.

Unit 5: Sections 325-M0042A-11R-1, 20 cm, through 13R-CC: grainstone

Unit 5, spanning Sections 325-M0042A-11R-1, 20 cm, through 13R-CC, is a yellowish grainstone to rudstone rich in larger foraminifera, *Halimeda*, mollusks, and coral fragments (Fig. F29). Granules and

pebbles from downhole contamination are present only in Section 325-M0042A-12R-1. The grainstone in Sections 325-M0042A-13R-1 and 13R-CC is highly fragmented (shattered by drilling). Muddy coarse sands from interval 325-M0042A-13R-1, 26–31 cm, contain sparse abraded *Heterostegina* and *Amphistegina*.

The few large corals are submassive *Porites*. Diverse fragments include *Pocillopora*, *Seriatopora*, *Stylophora*, *Acropora*, *Porites*, and possibly *Montipora*.

Unit 6: Sections 325-M0042A-14R-1 through 16R-CC: unconsolidated sediment

Unit 6, spanning Sections 325-M0042A-14R-1 through 16R-CC, consists of unconsolidated lime granules and pebbles. Major components are coral fragments, coralg-al-microbialite boundstone fragments, mollusks, and larger foraminifera. Fragments of overlying boundstones and other particles indicate downhole contamination.

There are no large corals. Numerous small fragments include Acroporidae, Pocilloporidae, *Porites*, and *Porites*(?) or *Montipora*(?).

Unit 7: Sections 325-M0042A-17R-1 through 325-M0042A-19R-1: grainstone with rhodoliths

Unit 7, spanning Sections 325-M0042A-17R-1 through 19R-1, consists of yellowish grainstone to rudstone rich in rhodoliths (i.e., nodules composed mainly of coralline algae). Rhodoliths are small (<3 cm) to very small (<1 cm) and subelliptical. Larger foraminifera, mollusks, and coral fragments are also common. There is widespread dissolution of clasts, creating moldic porosity.

The only corals are small to tiny fragments, mostly unidentifiable, that include Pocilloporidae, *Porites*, and possibly *Montipora*. The nucleus of one rhodolith is an acroporid. A piece of octocoral spiculite near exists the base of the unit.

Unit 8: Sections 325-M0042A-20R-1 to 21R-1, 10 cm: unconsolidated sediment

Unit 8, spanning Sections 325-M0042A-20R-1 to 21R-1, 10 cm, consists of unconsolidated lime granules and pebbles. Major components are coral fragments, coralg-al-microbialite boundstone fragments, mollusks, and larger foraminifera. Fragments of overlying boundstones and fresh mollusk shells clearly indicate downhole contamination.

Corals consist of fragments that include *Acropora*, *Isopora*, *Montipora*(?), *Seriatopora*, and possibly other Pocilloporidae.

Unit 9: Sections 325-M0042A-21R, 1 cm, through Section 22R-1: gray rudstone

Unit 9, spanning Sections 325-M0042A-21R-1, 10 cm, through 22R-1, consists of fragments of gray-colored rudstone rich in larger foraminifera, *Halimeda*, and coral and bivalve fragments. Aragonitic components are partially dissolved (Fig. F30).

Recognizable corals are mainly molds of *Acropora*, *Isopora*, and *Seriatopora*. Fragments are mainly Pocilloporidae and Acroporidae.

Unit 10: Sections 325-M0042A-22R-CC through 29R-CC: rudstone with brown stains

The lowermost Unit 10, spanning Sections 325-M0042A-22R-CC through 29R-CC, consists of yellowish rudstone to grainstone with large rhodoliths and coral fragments (Fig. F31). *Halimeda* segments, larger foraminifera, and mollusks are other major components. Rhodoliths are as wide as 8 cm in maximum diameter (Figs. F32, F33), and some have coral fragments as nuclei. Aragonite clasts are largely dissolved (Fig. F34). The deposit has brown staining locally (Fig. F35) and contains root remains (rhizoliths) in interval 325-M0042A-25R-1, 55–57 cm, indicating subaerial exposure (Fig. F36). A brown carbonate crust covers some fragments in Section 325-M0042A-22R-CC, at the top of Unit 10, and may represent a calcrete or speleothem developed on the original rudstone. Interval 325-M0042A-29R-CC, 0–5 cm, contains larger foraminifera in muddy, very coarse sands.

Because of extensive alteration and dissolution, most corals are not identifiable (Fig. F37). Nuclei of some rhodoliths include Acroporidae, Poritidae, and Pocilloporidae.

Physical properties

A total of 10.94 m of core was successfully recovered from Hole M0042A, which was cored to a total depth of 46.4 m DSF-A (23.58% recovery). Physical property data are summarized in Table T2.

Density and porosity

In Hole M0042A, bulk density measured on whole cores varies from 1.03 to 2.49 g/cm³ (Fig. F38). Core recovery is such that it was not possible to acquire data for three quarters of the hole. This lack of data, combined with the majority of the cores being <0.2 m in length and composed of rubbly material, results in poor data quality for Hole M0042A. It is impossi-

ble to comment on trends downhole. However, it was possible to measure 17 samples from the hole for discrete moisture and density analysis (Fig. F39). Discretely sampled bulk density data varies from 1.51 to 2.45 g/cm³, whereas porosity values in the hole range from 16% to 72%. These results for porosity and bulk density are difficult to compare with lithology. There is boundstone between 0 and 7.5 m CSF-A and principally lime pebbles and lime granules between 7.5 m and 45 m CSF-A. In terms of grain density, values range from 2.70 to 2.81 g/cm³ (Fig. F39). Owing to the questionable quality of the bulk density data in this hole, it is difficult to draw comparisons between the two data sets.

P-wave velocity

Multisensor core logger *P*-wave velocity measurements range from 1510.50 to 1865.90 m/s (Fig. F38). The lower values of the range could be due to poor core quality (see “Physical properties” in the “Methods” chapter). Three discrete *P*-wave velocity measurements were taken on samples from Hole M0042A cores, with values ranging from 3772 to 4223 m/s (mean value for resaturated core). There are no clear downhole trends with this data set (Fig. F40A) and there is no obvious relationship between bulk density and discrete *P*-wave velocity measurements (Fig. F40B).

Magnetic susceptibility

Core recovery in Hole M0042A was such that the cores are generally short; therefore, identification of any downhole trends is difficult. Magnetic susceptibility values range from -12.42×10^{-5} to 38.73×10^{-5} SI (Fig. F38).

Electrical resistivity

Similar to the other data sets, resistivity data have suffered because of short core length and discontinuous recovery downhole, resulting in an erratic profile for resistivity downhole. Electrical resistivity measured on whole cores varies from 0.76 to 40.36 Ωm (Fig. F38).

Digital line scans and color reflectance

All cores from Hole M0042A were digitally scanned, and, where appropriate, cores were measured for color reflectance. Hole M0042A was the deepest hole, recovering the oldest material in transect HYD-02A. Color reflectance in Hole M0042A varies between 52.1% and 93.02% L* (Fig. F41). Variations in color reflectance parameters show some dispersion for individual sections, especially in the uppermost 20 m, corresponding with lime lithologies. From 20

to 30 m CSF-A, the values obtained were in the same range with a very small dispersion in individual sections due to the presence of larger fragments of corals and rudstone. From 34 to 45 m CSF-A, values were highly variable within sections, ranging from 65% to 85% with some outliers. The extremely high value present at 40.38 m CSF-A is probably due to the presence of liquid water and drilling mud contamination. The low reflectance values measured at the base of the hole are due to the presence of shattered rudstone. No significant variations in color indexes were noticed. Values of a^* were mainly positive (red color), and values of b^* were always positive (yellow color). The a^*/b^* ratio did not indicate additional information in these cases because of the small variation in the values of a^* and b^* .

Paleomagnetism

Measurements of low-field and mass-specific magnetic susceptibility (χ) were performed on all samples taken from the working half of the recovered core (Fig. F42). Very low negative (diamagnetic) susceptibilities occur throughout the entire core, ranging from -3.07×10^{-8} to -0.90×10^{-8} m³/kg with an arithmetic mean value of -1.03×10^{-8} m³/kg. Three positive values at 4.04, 22.09, and 40.42 mbsf were recorded, with magnetic susceptibilities of 0.95×10^{-8} , 0.58×10^{-8} , and 0.07×10^{-8} m³/kg, indicating the presence of paramagnetic and/or ferromagnetic minerals.

Chronology

Two calibrated radiocarbon ages (10 cal y BP, Core 325-M0042A-1R; 13 k. y. cal. BP, Core 10R) (Fig. F43) and one U-Th age (169 cal y BP, Core 24R) (see Table T10 in the “Methods” chapter) are consistent with their stratigraphic positions. The U-Th age is unaffected by corrections for initial ²³⁰Th, adding to the confidence in this age interpretation. Therefore, the upper portions of this hole have recorded the middle part of the deglaciation, whereas the lower cores seem to have recovered material from the Pleistocene. Specifically, this hole contains material from marine isotope Stage 6, but there are five cores below the 169 cal y BP section that may contain older material and 13 cores between the 169 and 13 cal y BP sections that may record younger periods of the Pleistocene.

Downhole measurements

Downhole logging operations were completed in Hole M0042A to a maximum depth of 45.69 m WMSF (seafloor picked from the log data) with the ANTARES Spectral Natural Gamma Probe (ASGR)

sonde (see “Downhole logging” in the “Methods” chapter for detailed tool information). Recovery in Hole M0042A was just over 23.58%; therefore, the continuous downhole measurements provide a useful tool to fill in data gaps. Downhole logging was conducted in an API hole, the diameter of which is beyond the maximum working size for the acoustic and optical tools (ABI40 and OBI40). However, the full tool suite (with the exception of the IDRONAUT) was run downhole. Chronologically the tools deployed were

1. ASGR 256 (through API pipe),
2. DIL45 (conductivity in open hole),
3. ABI40 (API hole diameter too great to obtain acoustic images),
4. ASGR 256 (spectral gamma ray in open hole),
5. EM51 (magnetic susceptibility in open hole),
6. Sonic (centralizers undersized so that the tool would fit through the API bit; therefore, tool not optimally centralized in the hole and so errors were introduced into the measurements),
7. OBI40 (optical tool; API hole diameter too great and mud caking prevented good image collection), and
8. Caliper (borehole diameter).

Hole stability for open-hole logging was relatively good. The open-hole stage of logging began with 44.17 m WMSF available hole and ended with the caliper tool (CAL3) (last tool run) logging 37.76 m WMSF of open hole.

From the logging data, four main logging units were identified in Hole M0042A (Fig. F44):

1. Unit I (0–13.96 m WMSF; Cores 325-M0042A-1R through 10R) is characterized by low total gamma ray (TGR) counts (through-pipe and open hole) and high conductivity (457 mmho). Magnetic susceptibility is very low, fluctuating around 0.6 mSI (maximum = ~0.65 mSI; minimum = ~0.575 mSI). Velocities measured in the unit are all just above 1500 m/s and are therefore similar to that of seawater. Borehole diameter was extremely large in this unit (as wide as 40 cm), which may have been caused by movement of the bottom of the API bottom-hole assembly and/or may reflect the nature of the borehole formation. A number of lithostratigraphic units have been described in the depth range of this logging unit. Lithologies observed from shallow to deep are lime sand and algal bindstone (Section 325-M0042A-1R-1), coralgall boundstone (Sections 1R-CC through 3R-1), coralgall-microbialite boundstone (Sections 3R-CC through 5R-CC), and unconsolidated sediment (lime granules and pebbles).

2. Unit II (13.96–24.26 m WMSF; Cores 325-M0042A-11R through 17R) is defined by TGR counts measured in open hole between 14 and 32 cps, conductivity values of ~350 mmho (minimum = ~155.79 mmho; maximum = ~425.78), magnetic susceptibility between 0.6 and 0.63 mSI, and borehole diameter in gauge. Sonic velocity values are unreliable in this portion of the hole, with values lower than that of seawater (1500 m/s). Within this defined logging unit, lithostratigraphic units vary from grainstone (Sections 325-M0042A-11R-1 through 13R-CC) to unconsolidated sediment (lime granules and pebbles; Sections 14R-1 through 16R-CC) to grainstone with rhodoliths. These lithologic changes are reflected most in the conductivity data.
3. Unit III (24.26–35.36 m WMSF; Cores 325-M0042A-18R through 24R) is characterized by increasing values of TGR counts downhole, with values starting at 20 cps and increasing to ~56 cps. Conductivity undulates around ~450 mmho throughout the unit; however, *P*-wave velocity values seem to differentiate between two units, the upper having velocities of ~1700 m/s and the lower with velocities of ~1900 m/s. Caliper data show that the hole remains in gauge throughout. Lithostratigraphic units observed over this logging unit interval are grainstone with rhodoliths (Sections 325-M0042A-18R-1 through 19R-1), unconsolidated sediment (lime granules and pebbles; Sections 20R-1 through 21R-1), gray rudstone (Sections 21R-1 through 22R-1), and rudstone with brown staining (Sections 22R-CC through 24R-1). It is possible that the velocity log is differentiating between the unconsolidated unit and the gray rudstone beneath it.
4. Unit IV (35.36–45.47 m WMSF; Cores 325-M0042A-25R through 29R) represents a zone of reduced TGR counts with values of ~25 cps (where open-hole data are present); additionally, conductivity exhibits a decrease to 100 mmho at the very top of Unit IV and then a gradual increase to a maximum of ~682 mmho at ~40.6 m WMSF. Magnetic susceptibility fluctuates between a minimum value of 0.57 and 0.62 mSI. The caliper tool registers the hole as in gauge. The sole lithology found within this logging unit is rudstone with brown staining (Sections 325-M0042A-25R-1 through 29R-CC). Conductivity data suggest that there may be an increase in pore space concentration and or pore space size and connectivity as depth increases to ~40.6 m WMSF.

Hole M0043A

Operations

Site 12, Hole M0043A

The seabed transponder was deployed at 0455 h on 9 March 2010, and by 0515 h the *Greatship Maya* was on station at Site 12 (Hole M0043A) (Table T1). The seabed template was adjusted in the moonpool, and at 0550 h the API pipe started running to just above the seabed. A downpipe camera survey was conducted at 0740 h, and coring operations (standard rotary corer) started at 0815 h, continuing until 2350 h, when the hole was terminated at 35 mbsf with an average recovery of 17.3%. The API pipe was tripped to 7 m above the seabed, and a downhole camera survey was completed by 0115 h on 10 March 2010. The seabed transponder was recovered at 0115 h and the camera remained inside the pipe while the vessel slowly moved 52 m under dynamic positioning to Site 8, Hole M0044A.

Sedimentology and biological assemblages

Hole M0043A is divided into five lithostratigraphic units.

Unit 1: Sections 325-M0043A-1R-1 through 2R-CC: coralg boundstone (modern at the top)

The uppermost Unit 1, spanning Sections 325-M0043A-1R-1 through 2R-CC, consists of boundstone dominated by a framework of thin coralline algae and worm tubes (Fig. F45). Internal sediments have fragments of larger foraminifera and mollusks. The boundstone is stained reddish brown, and all components are bioeroded locally. In interval 325-M0043A-1R-1, 0–10 cm, remains of a recent sponge overlie lime mud containing worm tubes and mollusks (Fig. F46). Fragmented specimens of *Amphistegina* and *Heterostegina* are rare in muddy gravels from interval 325-M0043A-2R-1, 20–25 cm.

The main corals are medium thickness branching *Goniopora*(?), submassive *Porites*, and massive Favidae. Fragments are mainly fine branching Pocilloporidae (*Seriatopora*?).

Unit 2: Sections 325-M0043A-3R-1 through 17R-CC: coralg-microbialite boundstone

Unit 2, spanning Sections 325-M0043A-3R-CC through 17R-CC, consists of coralg-microbialite boundstone in which coralline algae alternate with microbialite crusts that trap bioclasts (Fig. F47). Coralline algae occur as thick crusts on top of corals or

as thinner structures intergrown with microbialites (Fig. F48). Microbialites reach several centimeters in thickness, and they are usually dark colored and poorly laminated (Fig. F49). Some digitate growths occur at the top of microbialite crusts, whereas some internal bioclastic sediments with *Halimeda* and mollusks occur throughout this unit. All boundstone components are bioeroded by bivalves and sponges.

The main corals forming the framework are massive *Isopora*, branching *Acropora* (Figs. F50, F51), massive Faviidae (Fig. F47), and colonies of fine-branching *Seriatopora* embedded in microbialite (Fig. F48). Associated corals are *Porites*, *Goniopora*, *Montipora*(?), and Faviidae, including branching *Echinopora*. All of these taxa except *Echinopora* are common as fragments, which also include *Tubipora musica* and Agariciidae(?).

Unit 3: Sections 325-M0043A-18R-1 through 21R-CC: unconsolidated sediment

Unit 3, spanning Sections 325-M0043A-18R-1 through 21R-CC, consists of unconsolidated lime granules and pebbles. Major components are coral fragments (as large as 6 cm), coralgal-microbialite boundstone fragments, *Halimeda*, larger foraminifera, mollusks, bryozoans, echinoids, and worm tubes. Medium to coarse sands from interval 325-M0043A-18R-1, 10–15 cm, contain abundant specimens of abraded *Baculogypsina* and *Calcaria*. Fragments of the overlying boundstones and fresh mollusk shells clearly indicate downhole contamination.

A few massive *Isopora* are associated with encrusting *Porites* and Agariciidae. Coral fragments are diverse and include *Acropora*, *Isopora*, *Seriatopora*, *Porites*, *Pocillopora*(?), *Tubipora musica*, Fungiidae, Agariciidae, and one small solitary ahermatypic coral.

Unit 4: Section 325-M0043A-22R-CC: packstone overlain by worm tube boundstone

Unit 4, represented only by Section 325-M0043A-22R-CC, is a 5 cm thick blackened boundstone of thin foliose coralline algae and worm tubes overlying a dark packstone (Fig. F52). It also contains larger foraminifera, *Halimeda*, mollusks, and coral fragments. Corals are fragments of *Seriatopora* and *Acropora*.

Unit 5: Section 325-M0043A-23R-CC: lime sand

The lowermost Unit 5, consisting only of Section 325-M0043A-23R-CC, consists of medium to coarse lime sand rich in larger foraminifera and black granules. Interval 325-M0043A-23-CC, 5–10 cm, contains fragmented specimens of *Operculina*. The black

grains probably originate from the overlying deposits, and indicate downhole contamination.

Apart from a few fragments of *Isopora*(?) in the uppermost parts of the unit, there are no visible corals.

Physical properties

Hole M0043A yielded 6.04 m of core from a total penetration depth of 35.0 m DSF-A (17.26% recovery). Table T2 summarizes physical property data collected for this hole.

Density and porosity

Bulk density measured on Hole M0043A cores varies from 1.05 to 2.40 g/cm³ (Fig. F53). Similar to Hole M0042A, recovery and core length has impacted the amount and quality of gamma density data for this hole (see “Physical properties” in the “Methods” chapter). Again, it is impossible to comment on trends downhole. However, it was possible to measure 16 samples from Hole M0043A for discrete moisture and density. Bulk density data from these analyses vary from 1.83 to 2.39 g/cm³, whereas porosity values in the hole range from 22% to 53% (Fig. F54). Disturbed lime pebbles lie between 0 and 8 m CSF-A, with porosity decreasing from 52% to 32% downhole. Between 10 and 21 m CSF-A, where the lithology is principally coralgal-microbialite boundstone, porosity varies between 22% and 43%. Below 21 m CSF-A, lime pebbles have a porosity varying between 24% and 53%. Similar to Holes M0040A and M0041A, grain density varies from 2.74 to 2.82 g/cm³.

P-wave velocity

Offshore *P*-wave velocity measurements range from 1526.84 to 1895.75 m/s (Fig. F53). The minimum values are too low for the type of sediment observed, likely because of the poor core quality (see “Physical properties” in the “Methods” chapter). The multi-sensor core logger *P*-wave data come from only one of the recovered core sections, with data absent from the rest of the hole. There were no discrete *P*-wave velocity measurements taken on core from Hole M0043A. The combination of an extremely limited *P*-wave velocity data set with questionable validity of those data renders it impossible to make any sort of interpretation.

Magnetic susceptibility

Cores from Hole M0043A have magnetic susceptibility values ranging from -12.76×10^{-5} to 9.82×10^{-5} SI (Fig. F53). Similar to Hole M0042A, data are limited; therefore, identifying any trends is difficult. Three

sections suggest intervals of relatively high magnetic susceptibility: Sections 325-M0043A-2R-1 (with a value of 9.82×10^{-5} SI at 2.34 CSF-A), 6R-1 (with a magnetic susceptibility peak value of 5.27×10^{-5} SI at 8.76 CSF-A), and 12R-1 (with a value of 4.87×10^{-5} SI at 17.13 CSF-A).

Electrical resistivity

Similar to the other data sets, short core lengths and discontinuous recovery downhole means the resistivity profile makes little sense on its own. Electrical resistivity measured on whole cores varies from 0.75 to 93.27 Ωm (Fig. F53).

Digital line scans and color reflectance

All cores from Hole M0043A were digitally scanned, and, where appropriate, cores were measured for color reflectance. Color reflectance in Hole M0043A varies between 41.17% and 83.95% L^* (Fig. F55). Reflectance values were highly dispersed for most of the borehole sections. The more dispersed sections correspond to the thick coralgal-microbialite boundstone unit, mainly between 10 and 20 m CSF-A. Less dispersed values were present in the lowermost 5 m of the hole, corresponding to blackened boundstone, unconsolidated, and packstone units. In the uppermost 1 m of the hole, values were negative where bindstone and lime pebbles were present. Below 2 m CSF-A, color values showed a downhole trend, from positive a^* values (red) to negative ones (green). Lower b^* values were also found in the lowermost few meters, although they were always in the positive range (yellow). The trend in color is more obvious in the a^*/b^* ratio.

Paleomagnetism

Measurements of low-field and mass-specific magnetic susceptibility (χ) were performed on samples taken from the working half of the recovered core (Fig. F56). Low negative (diamagnetic) susceptibilities occur throughout the core, ranging from -2.76×10^{-8} to -0.17×10^{-8} m^3/kg with an arithmetic mean of -0.92×10^{-8} m^3/kg . Four positive measurements were taken from samples located at 0.07, 2.28, 8.79, and 15.15 mbsf with susceptibilities of 0.245, 3.36, 0.14, and 0.01×10^{-8} m^3/kg , respectively, indicating the presence of paramagnetic and/or ferromagnetic minerals.

Chronology

Two calibrated radiocarbon ages (15 cal y BP, Core 325-M0043A-2R; 18 cal y BP, Core 9R) (Fig. F57) and one U-Th age (20 cal y BP, Core 18R) (see Table T10 in the “Methods” chapter) are consistent with their

stratigraphic positions. The U-Th age is unaffected by corrections of initial ^{230}Th , adding to the confidence in this age interpretation. This hole recovered material from the Last Glacial Maximum and early deglaciation to 15 cal y BP. There are five cores below the 20 cal y BP section, indicating that there may be more material representing the Last Glacial Maximum or even older Pleistocene deposits in this hole.

Hole M0044A

Operations

Site 8, Hole M0044A

The seabed transponder was deployed at 0140 h on 10 March 2010, and the vessel was on station over Hole M0044A by 0155 h (Table T1). The downpipe camera survey was completed by 0225 h, and the barrel was prepared as API pipe was run to tag the seabed. The first core (standard rotary corer [ALN]) was recovered at 0320 h. On recovering the second core at 0415 h, the ALN polycrystalline diamond bit was found to be damaged and the stabilizer housing was deformed. The bit was changed for a short impregnated ALN bit, and coring continued. At 0800 h, the vessel lost a forward thruster for 5 min without affecting coring operations. At 0905 h, the seabed template was lowered in the moonpool in an attempt to dampen drill string vibration. At 1120 h, the ALN barrel became stuck in the bottom-hole assembly (BHA) during Run 9. Attempts were made to recover the barrel, but at 1310 h, the wireline failed. In order to recover the barrel and overshot, the API pipe had to be tripped, terminating Hole M0044A at 11 mbsf with an average recovery of 15.2%. The ALN was recovered from the BHA at 1645 h. The barrel and BHA were checked, and the overshot wire was repaired.

The API pipe was run in to just above the seabed by 1850 h, and a downpipe camera survey was conducted. The vessel repositioned over ~2.5 m under dynamic positioning to Hole M0045A.

Sedimentology and biological assemblages

Hole M0044A is divided into two lithostratigraphic units.

Unit 1: Section 325-M0044A-1R-1: fragments of bioclastic packstone

The uppermost Unit 1, consisting only of interval 325-M0044A-1R, 0–21 cm, is composed of a packstone ranging in color from buff to gray (Fig. F58). The packstone is composed of bioclasts of corals, bryozoans, encrusting foraminifera, nongeniculate coralline algae, and mollusks. Some fragments have

brown (to gray) staining. Cavities of unknown origin are common in the gray fragments, and some of the cavities are partly to fully filled with silt-sized gray internal sediment. The few coral clasts are extensively altered and unidentifiable.

Unit 2: Sections 325-M0044A-2R-CC through 9R-CC: coralgal-microbialite boundstone

The lowermost Unit 2, spanning Sections 325-M0044A-2R-CC through 9R-CC, is composed mainly of microbialites (Figs. F59, F60). Corals are covered with nongeniculate coralline algae, which are, in turn, encrusted with laminated microbialites. Nongeniculate coralline algae are usually thin (<1 mm) and volumetrically less abundant than microbialites and corals. Corals are common, and some are bioeroded by bivalve mollusks with borings partly filled with unconsolidated silt-sized internal sediment (Fig. F61).

Dominant corals are *Acropora* with thick bases and medium thickness branches (Fig. F62), branching *Porites* and *Pocillopora*, and massive *Isopora* and Faviidae. Most fragments are branching *Acropora*, with some *Porites* and *Pocillopora*.

Physical properties

Total penetration depth for Hole M0044A was 11 m DSF-A with 1.67 m of recovered core (15.18% recovery). Core petrophysical data for this hole are summarized in Table T2.

Density and porosity

Multisensor core logger bulk density measurements from Hole M0044A cores vary from 1.00 to 2.28 g/cm³ (Fig. F63). Downhole trends are not obvious in this limited data set. Discrete moisture and density measurements were taken for two samples, which gave bulk density values of 2.46 and 2.32 g/cm³. Porosity values of the same samples were 19% and 26%, respectively. Grain density values were, respectively, 2.79 and 2.77 g/cm³.

P-wave velocity

Offshore multisensor core logger P-wave velocity measurements yielded no data. However, two discrete P-wave velocity measurements were taken on cores from Hole M0044A with mean values for the samples of 3874 and 4870 m/s (mean resaturated values) (Fig. F64).

Magnetic susceptibility

Cores from Hole M0044A have magnetic susceptibility values ranging from -0.86×10^{-5} to 13.36×10^{-5} SI (Fig. F63). Measurements from the top of the hole (0–5.5 m CSF-A) are dominantly positive ($\sim 3 \times 10^{-5}$ to 13×10^{-5} SI), whereas measurements from the bottom of the hole are dominantly negative. This delineation of magnetic susceptibility values corresponds to the division of the hole into two distinct lithostratigraphic units: an upper bioclastic packstone (fragmented) and a lower coralgal-microbialite boundstone.

Electrical resistivity

Electrical resistivity values range from 2.39 to 44.84 Ω m (Fig. F63). A systematic change in resistivity downhole is not obvious, but this may be due to poor recovery. However, the highest values are present toward the base of the hole (an opposite trend to the magnetic susceptibility values).

Digital line scans and color reflectance

Cores from Hole M0044A were digitally scanned, and, where appropriate, cores were measured for color reflectance. Color reflectance in Hole M0044A varies between 53.37% and 80.34% for L* (Fig. F65). Cores from the top of Hole M0044A yielded the lower values in this range, which are associated with a bioclastic packstone. The presence of fractured *Acropora* sp. boundstone in the remainder of the hole produced dispersed values for all color reflectance spectrophotometry parameters.

Paleomagnetism

Measurements of low-field and mass-specific magnetic susceptibility (χ) were performed on samples taken from the working half of the recovered core (Fig. F66). Low negative (diamagnetic) susceptibilities occur throughout the core, ranging from -3.70×10^{-8} to -0.10×10^{-8} m³/kg with an arithmetic mean value of -1.17×10^{-8} m³/kg. Two positive sample measurements, taken from samples located at the same depth of 5.61 mbsf, display susceptibility values of 1.45×10^{-8} and 0.48×10^{-8} m³/kg, indicating the presence of paramagnetic and/or ferromagnetic minerals.

Chronology

Two calibrated radiocarbon ages (14 cal y BP, Core 325-M0044A-2R; 17 cal y BP, Core 8R) (Fig. F67) are consistent with their stratigraphic positions. This

hole has recovered material from the early deglaciation to 14 cal y BP.

Hole M0045A

Operations

Site 8, Hole M0045A

The *Greatship Maya* was on station over Hole M0045A in 4 min, with the downpipe camera still deployed (Table T1). A precoring camera survey was conducted, and the camera was recovered to deck by 1910 h. The seabed was tagged at 1945 h, and coring commenced. However, after initially appearing to core, the drill string then dropped 3 m abruptly. It was believed that the drill string was skipping down the side of the target coral pinnacle, so the vessel was moved 2 m closer to Hole M0044A before trying another run. The seabed was again tagged, and the drill string appeared to be compensating at 2115 h. However, the first and second standard rotary corer runs again appeared to skip down the side of the pinnacle, with the drill string dropping quickly and with no apparent force. The last 70 cm of the third run appeared to drill very hard material. However, while recovering the barrel, the drill string fell abruptly by 8 m—it was thought that the string had reentered Hole M0044A. If this was so, the drill string should have stopped at the total depth for Hole M0044A of 11 mbsf, but it continued to freefall until 14.6 “mbsf.” As it was not clear whether the API string had actually penetrated the target pinnacle or was skipping down its side, the decision was made to abandon Hole M0045A and move the vessel. Two API pipes were tripped by 0025 h on 11 March, and the *Greatship Maya* was moved 3 m under dynamic positioning to the opposite side of Hole M0044A.

Hole M0046A

Operations

Site 8, Hole M0046A

The *Greatship Maya* was on station above Hole M0046A by 0050 h on 11 March 2010 (Table T1). The first three standard rotary corer runs all appeared to skip down a slope, freefalling to 10.8 “mbsf.” However, coring then continued, with seabed corals appearing in the liner at ~10.8 “mbsf” in Run 4. While recovering Run 10 from a depth of 25.2 “mbsf,” there was a partial hole collapse, so the uppermost 1 m of core from Run 11 represents infill. The hole was terminated after Run 13 at 1040 h at 31.20 “mbsf,” with an average recovery of 8.9%. Depth corrections were made at the Onshore Science Party to account for the actual water depth in which

the seabed was penetrated and, in turn, the final cored depth. Runs 1R and 2R are thus seen as negative depths, to account for the drill string falling through the water column along the side of a pinnacle, with Run 3R penetrating the seabed for the last 1.2 m of a 3 m run. The final depth cored stands at a corrected depth of 20.4 mbsf. The API pipe was tripped back to Joint 11 in preparation for transit to the next site, and the seabed transponder was recovered. The vessel began the move to Site 12, Hole M0047A, at 1145 h.

Sedimentology and biological assemblages

Hole M0046A is divided into three lithostratigraphic units.

Unit 1: Sections 325-M0046A-1R-1 through 3R-1: modern deposits scraped from the seafloor

The uppermost Unit 1, spanning Sections 325-M0046A-1R-1 through 3R-1, is interpreted (from consideration of drilling logs) as being scrapings from the seafloor down the side of a pinnacle. Unit 1 consists of pebble-sized fragments of bioclastic packstone with corals. This packstone has brown and gray staining. Bioclasts of corals, larger foraminifera, and *Homotrema rubrum* are also present. A wood fragment covered with a living sponge lies at the base of Section 325-M0044-3R-1.

Large corals are bioeroded *Favites* and platy *Porites*, with a few large submassive fragments of *Cyphastrea* and one ahermatypic *Dendrophylliidae*.

Unit 2: Sections 325-M0046A-4R-1 through 325-M0046A-9R-CC: coralgall boundstone

Unit 2, spanning Sections 325-M0046A-4R-1 to 9R-1, 13 cm, consists mainly of coral boundstone interlayered with two distinct packstone intervals: 325-M0046A-4R-CC, 0–10 cm, and 5R-CC, 0–10 cm. The boundstone is composed of coralgall framework with a gray packstone matrix (Fig. F68). Cavities of uncertain origin are partly filled with gray fine-grained sediment. No larger foraminifera are present in interval 325-M0046A-6R-CC, 5–10 cm. The upper part of Section 325-M0046A-5R-1 contains ~10 cm of coral-line algal-encrusted spiculite (Fig. F69).

Framework corals are massive to submassive *Acroporidae*, *Montipora*(?), *Porites*, and *Platygyra*(?), mainly in lower parts of the unit. Fragments include submassive to massive *Favites*, *Goniopora*, *Coscinarea*, and branching *Acropora*, *Pocillopora*, *Seriatopora*, and *Stylophora*.

Unit 3: Sections 325-M0046A-10R-CC through 13R-CC: coral boundstone

The lowermost Unit 3, from Section 325-M0046A-10R-CC through 13R-CC, consists of granule- to pebble-sized (rarely cobble-sized) clasts of corals (Fig. F70) without crusts of nongeniculate coralline algae. This unit is likely to be a coral boundstone that was disturbed by drilling.

The only large coral is a massive *Echinopora* in Section 325-M0046A-11R-CC. All other corals are fragments that include numerous branching Pocilloporidae, *Acropora*, and especially *Seriatopora*, along with some pieces of *Porites* and *Montipora*(?).

Physical properties

The total penetration depth for Hole M0046A was 20.40 m DSF-A corrected depth with 2.52 m of recovered core (12.35% corrected recovery). Data acquired as part of the core petrophysics measurement plan for this hole are summarized in Table T2.

Density and porosity

Bulk density multisensor core logger measurements for Hole M0046A cores vary from 1.03 to 2.35 g/cm³ (Fig. F71). Downhole trends are not obvious in this limited data set. Discrete moisture and density measurements were not performed on any cores from Hole M0046A.

P-wave velocity

Offshore P-wave velocity measurements yielded no data, and no samples were selected for discrete P-wave velocity measurement from Hole M0046A.

Magnetic susceptibility

Cores from Hole M0046A have whole core magnetic susceptibility values ranging from -0.12×10^{-5} to 12.76×10^{-5} SI. Similar to values obtained for Hole M0044A, the top of the hole (above 5 m CSF-A) is dominated by higher, positive measurements as high to 12.76×10^{-5} SI, whereas measurements from deeper in the hole (below 5 m CSF-A) are characterized by lower (3.84×10^{-5} SI) and occasionally slightly negative magnetic susceptibility values (-0.06×10^{-5} and -0.12×10^{-5} SI). This change in magnetic susceptibility does not appear to directly correspond with lithostratigraphic changes observed downhole.

Electrical resistivity

Overall, electrical resistivity decreases downhole, with a delineation of values similar to that observed in the corresponding magnetic susceptibility data. Electrical resistivity values range from 0.96 to 29.21 Ωm (Fig. F71). However, Section 325-M0046A-5R-1 presents a range with higher values from 9.14 to 11.93 Ωm .

Digital line scans and color reflectance

Cores from Hole M0046A were digitally scanned, and, where appropriate, cores were measured for color reflectance. Color reflectance in Hole M0046A varies between 43.82% and 81.24% for L* (Fig. F72). The presence of massive corals in this borehole makes the color reflectance data set less dispersed than in other holes in this transect. The flat surface provided when the massive corals are split is a major factor to consider when evaluating the quality of the data. The variations in a* indicate a value close to zero in sections located between 15 and 21 m CSF-A. Values for b* were more dispersed over the same depths, reaching lower values than the ones at the top and bottom of the borehole.

Paleomagnetism

Measurements of low-field and mass-specific magnetic susceptibility (χ) were performed on samples taken from the working half of the recovered core (Fig. F73). Very low negative (diamagnetic) susceptibilities occur throughout the core, ranging from -1.11×10^{-8} to -0.44×10^{-8} m³/kg with an arithmetic mean of -0.74×10^{-8} m³/kg. Two positive values were recorded in samples taken from 1.71 and 18.46 mbsf with susceptibilities of 0.50×10^{-8} and 1.50×10^{-8} m³/kg, respectively, indicating the presence of paramagnetic and/or ferromagnetic minerals.

Chronology

Two calibrated radiocarbon ages (16 cal y BP, Core 325-M0046A-6R; 16 cal y BP, Core 9R) (Fig. F74) and one U-Th age (17 cal y BP, Core 11R) (see Table T10 in the “Methods” chapter) are consistent with their stratigraphic positions. When rounded to 1 ka, the two calibrated radiocarbon dates give the same age, but the individual age ranges are consistent with their stratigraphic order. The U-Th age is unaffected by corrections for initial ²³⁰Th. Therefore, this hole recovered material from the early deglaciation. There

are, however, five shallower cores, so material younger than 16 cal y BP may also be present.

Hole M0047A

Operations

Site 12, Hole M0047A

The *Greatship Maya* came onto station over Hole M0047A at 1220 h on 11 March 2010 (Table T1). Re-termination of the beacon transponder deployment wire delayed deployment until 1250 h. API pipe was run into just above the seabed, and a downpipe camera survey was conducted. The camera was back on deck at 1335 h, and the API tagged the seabed at 1410 h. The first standard rotary corer core was recovered at 1430 h, and coring continued until 0030 h on 12 March, when the hole was terminated at 33.2 mbsf with an average recovery of 11.4%.

The API pipe was tripped to just above the seabed by 0055 h, and a downpipe camera survey was conducted. The seabed transponder was recovered by 0145 h, and the vessel departed for Site 12, Hole M0048A, under dynamic positioning with 11 API pipes deployed.

Sedimentology and biological assemblages

Hole M0047A is divided into four lithostratigraphic units.

Unit 1: Sections 325-M0047A-2R-1 through 10R-CC: coralgall boundstone

The uppermost Unit 1, spanning Sections 325-M0047A-2R-1 through 10R-CC, consists of rock fragments that appear to be coralgall boundstone, but extensive drilling disturbance and low recovery make it difficult to determine the original lithologies. Unit 1 consists of massive and branching corals covered with coralline algae and minor microbialite crusts. The boundstone forming the uppermost part of Section 325-M0047A-2R-1 consists mainly of a framework of coralline algae and has brown and black staining (Fig. F75). Fragments of bioclastic packstone in Sections 325-M0047A-2R-CC and 3R-CC probably represent lithified internal sediment, consisting of loose fragments of coral, mollusks, bryozoans, larger foraminifera (e.g., well-preserved specimens of *Amphistegina* in interval 325-M0047A-3R-1, 10–15 cm), and *Halimeda*. Sections 325-M0047A-3R-1 through 4R-1 were probably originally richer in sediment than the rest of Unit 1.

Framework corals, mainly toward the base of Unit 1, are massive *Isopora* and *Porites*; submassive or branching *Acropora* (Fig. F76), *Isopora*, *Seriatopora*,

Porites, and Pocilloporidae; and some ahermatypic corals (in upper parts of the interval). Diverse fragments include *Acropora*, *Isopora*, *Seriatopora*, *Pocillopora*, *Stylophora*, *Porites*, *Goniopora*, *Tubipora musica*, *Stylasterina*(?), Agariciidae, Faviidae, Pocilloporidae, and some highly altered Fungiidae or Mussidae.

Unit 2: Sections 325-M0047A-11R-1 through 11R-CC: lime sand

Unit 2, spanning Sections 325-M0047A-11R-1 through 11R-CC, consists of medium to coarse lime sands and pebbles rich in larger foraminifera and *Halimeda*, as well as fragments of mollusks, bryozoans, coral, and coralline algal crust. Abraded specimens of *Calcarina*, *Baculogypsina*, and Soritinae are abundant in very coarse sands from interval 325-M0047A-11R-1, 10–15 cm. Although there may be some degree of downhole contamination, the scarcity of fragments of overlying facies suggests that the lime sand represents the original uncontaminated deposit.

Most corals are branching Pocilloporidae (*Seriatopora* and *Pocillopora*), *Acropora*, and *Tubipora musica*, with submassive *Isopora* and *Porites*. Fragments include all of the same taxa.

Unit 3: Sections 325-M0047A-12R-1 through 13R-CC: unconsolidated sediment

Unit 3, spanning Sections 325-M0047A-12R-1 through 13R-CC, consists of unconsolidated lime granules and pebbles. Major components are coral, coralgall boundstone, and microbialite fragments, plus larger foraminifera and mollusks. Fragments of overlying boundstones indicate some downhole contamination.

The only larger corals are occasional encrusting Siderastreidae and Agariciidae (*Leptoseris*(?)). Common fragments are *Seriatopora*, *Pocillopora*, *Acropora*, *Isopora*, *Leptoseris*(?), *Tubipora musica*, and unidentified Pocilloporidae and Siderastreidae.

Unit 4: Sections 325-M0047A-14R-1 through 14R-CC: unconsolidated sediment rich in *Halimeda*

The lowermost Unit 4, spanning Sections 325-M0047A-14R-1 through 14R-CC, consists of unconsolidated lime granules and pebbles, with coarse sand containing abundant *Halimeda* segments. Other components are coral fragments, mollusks, and a few echinoid spines. Fragments of coralgall boundstone and microbialites are indicative of downhole contamination. Specimens of *Gypsina* are restricted to very coarse grained, gravelly sands from interval 325-M0047A-14R-CC, 0–5 cm.

The only large coral is an encrusting Agariciidae (probably *Leptoseris*) with fragments of *Acropora*, *Iso-pora*, *Seriatopora*, and Agariciidae.

Physical properties

Hole M0047A was drilled to 33.20 m DSF-A. A total of 3.79 m of core was recovered, equating to 11.42% recovery. Petrophysical data acquired from these cores are summarized in Table T2.

Density and porosity

Bulk density values from whole-core multisensor core logger measurements range from 1.15 to 2.33 g/cm³ (Fig. F77). Because of a combination of low core recovery and short cores, it is impossible to identify trends in the data set. Ten bulk density measurements were taken on discrete samples from the hole, with values ranging from 2.04 to 2.37 g/cm³ (Fig. F78). Porosity values for the same samples range from 24% to 43%, whereas the grain density of Hole M0047A samples falls within the 2.77 to 2.81 g/cm³ range (these values are high compared to other holes in the transect). Porosity is difficult to compare with lithology because of the often disturbed or unconsolidated nature of the cores being measured. Because of the heterogeneity in the formations and/or the disturbed nature of the cored material, it is difficult to compare it with multisensor core logger data and/or stratigraphy.

Attempts to correlate data across Holes M0047A and M0043A (attempted because of the close proximity of the holes and similar water depths) were unsuccessful. This may be attributed to the high complexity and variability of fossil coral reef pore systems.

P-wave velocity

Whole-core *P*-wave velocity measurements on Hole M0047A cores were unsuccessful, and no samples were taken for discrete *P*-wave velocity measurement.

Magnetic susceptibility

Magnetic susceptibility data for Hole M0047A are sparse, owing to low core recovery. Values range from -0.83×10^{-5} to 6.38×10^{-5} SI, with highs in Sections 325-M0047A-8R-1 and 11R-1 (Fig. F77).

Electrical resistivity

Similar to the magnetic susceptibility data, the electrical resistivity data set is very small because of poor recovery. Noncontact resistivity measurements taken on whole cores yielded data ranging from 0.66 to

3.32 Ω m (Fig. F77) with no systematic changes downhole.

Digital line scans and color reflectance

Cores from Hole M0047A were digitally scanned, and, where appropriate, measured for color reflectance. Color reflectance in Hole M0047A varies between 51.53% and 78.74% L* (Fig. F79). The low values of reflectance found in the upper part of the hole are principally due to corallgal boundstones and in part due to the presence of coarse sand and pebbles in which reflectance measurements are more inaccurate. The higher values with a dispersed pattern from 7 to 22 m CSF-A correspond mainly to areas of lime pebbles with fragments of different corals. The presence of coralline algae and lime pebbles at 24 m CSF-A showed a nondispersive pattern for all color reflectance parameters. Data points at the base of the hole correspond to a disturbed area that was probably more homogeneous in color.

Thermal conductivity

For Hole M0047A, two measurements were performed with a thermal conductivity of 1.06 W/(m·K) at 18.4 m CSF-A and 0.98 W/(m·K) at 27.34 m CSF-A.

Paleomagnetism

Measurements of low-field and mass-specific magnetic susceptibility (χ) were performed on samples taken from the working half of the recovered core (Fig. F80). Low negative (diamagnetic) susceptibilities were measured throughout the core, ranging from -1.48×10^{-8} to -0.04×10^{-8} m³/kg with an arithmetic mean of -0.49×10^{-8} m³/kg. Five positive values at 3.29, 6.27, 12.24, 27.31, and 31.75 mbsf recorded susceptibilities of 0.46, 0.74, 0.08, 1.18, and 0.34×10^{-8} m³/kg, respectively, indicating the presence of paramagnetic and/or ferromagnetic minerals.

Chronology

Two calibrated radiocarbon ages (15 cal y BP, Core 325-M0047A-3R; 18 cal y BP, Core 7R) (Fig. F81) and one U-Th age (21 cal y BP, Core 11R) (see Table T10 in the "Methods" chapter) are consistent with their stratigraphic positions. The U-Th age is unaffected by corrections for initial ²³⁰Th, adding to the confidence in this age interpretation. Therefore, this hole recovered material from the Last Glacial Maximum and the early deglaciation to 15 cal y BP. There are three cores below the 20 cal y BP section, indicating that more Last Glacial Maximum material or even

older Pleistocene deposits may be present in the hole.

Hole M0048A

Operations

Site 12, Hole M0048A

The *Greatship Maya* came onto station over Hole M0048A at 0220 h on 12 March 2010 (Table T1). The seabed transponder was deployed, and an additional API pipe was run to take the pipe to just above the seabed by 0305 h. A downpipe camera survey was completed by 0325 h, and the first standard rotary corer core was recovered by 0405 h. Standard rotary corer coring continued until 0610 h, when the decision was made to halt operations after four runs because of winds in excess of 35 kt and heave >2.5 m. As a result, Hole M0048A was terminated at 7.1 mbsf with an average recovery of 9.7%.

The API pipe was tripped by 0805 h, and the seabed template was secured by 0850 h. The seabed transponder was then recovered and secured on deck by 0910 h.

Waiting on weather and port call, Townsville

The *Greatship Maya* departed Site 12 (Hole M0048A) at 0910 h on 12 March 2010 to transit to sheltered waters within Hydrographer's Passage in order to conduct a ship-to-ship transfer of equipment, including a bumper sub and drilling mud from the *PMG Pride*, which commenced at 1530 h. Because of the failure of previous HQ attempts using the seabed template suspended in the moonpool or water column as a guide for the HQ string and API "casing," a bumper sub was manufactured to facilitate further attempts at recovering HQ cores.

At 1645 h, the *Greatship Maya* departed Hydrographer's Passage to transit northward using the inner passage because of deteriorating weather conditions offshore. At 1510 h on 13 March 2010, the *Greatship Maya* dropped anchor at the Townsville Anchorage (Australia) to wait on weather. Preparations continued to be made in advance of Cyclone Ului; all containers, inside equipment, cables, winches, and banners were securely fastened while monitoring the weather every 6 h.

At 1916 h on 15 March, the *Greatship Maya* weighed anchor, coming alongside in Townsville at 2100 h. Following rebunkering and a GC Rieber marine crew change, the *Greatship Maya* departed Townsville at 2035 h on 16 March and arrived at the Townsville Anchorage at 2205 h to continue waiting on weather. At 1600 h on 17 March a pilot boat came

alongside with additional spares. The *Greatship Maya* continued to wait on weather at the Townsville Anchorage until 19 March.

Sedimentology and biological assemblages

Hole M0048A consists of one lithostratigraphic unit.

Unit 1: Sections 325-M0048A-1R-1 through 3R-CC: coralgall boundstone and lime sand with larger foraminifera

Unit 1, spanning Sections 325-M0048A-1R-1 through 3R-CC, is composed of fragments of coralgall boundstone in lime sand and mud. Some boundstone fragments are pieces of thin coralline algal framework (Fig. F82), whereas others consist of coral, coralgall boundstone, and bryozoans encrusted by blackened coralline algae. Some fragments are stained brown and likely to be material from the modern seafloor. Loose sediment includes examples of larger foraminifera, *Halimeda*, and mollusks. Larger foraminifera are rare fragmented or encrusted specimens of *Cycloclypeus*, *Amphistegina*, and *Alveolinella* in gravelly medium sands from interval 325-M0048A-1R-1, 0–5 cm, and a few well-preserved specimens of *Amphistegina* in muddy coarse sands from interval 3R-CC, 7–12 cm. The presence of modern seafloor crusts at the base of Section 325-M0048A-2R-1 suggests stratigraphic mixing of fragments while coring.

All corals are fragments and include *Leptoria*, *Leptoseris*, *Pachyseris speciosa*(?), *Porites*(?), *Montipora*(?), *Faviidae*, and solitary *Fungiidae*.

Physical properties

Hole M0048A was drilled to a depth of 7.10 m DSF-A. A total of 0.69 m of core was recovered (9.72% recovery). As with the other holes in this transect, petrophysical data from this hole are summarized in Table T2.

Density and porosity

Bulk density values from whole-core multisensor core logger measurements were taken on one section from Hole M0048A (Fig. F83). Values range from 2.02 to 2.16 g/cm³ and are relatively consistent downsection. Three discrete samples were measured for moisture and density in this hole. Bulk density values range from 1.79 to 2.17 g/cm³, whereas porosity measurements fall between 38% and 57%. Grain density presents a small variation with a range of 2.77 to 2.85 g/cm³ for all three measurements (Fig. F84).

P-wave velocity

P-wave velocity offshore measurements on whole cores were only taken on one core section, and values ranged from 1520 to 1581 m/s (Fig. F83). These values are similar to *P*-wave velocity for water and are probably a result of diminished core quality (see “Physical properties” in the “Methods” chapter). No discrete samples were measured on the *P*-wave logger for this hole.

Magnetic susceptibility

The one section (325-M0048A-1R-1) that was measured on the multisensor core logger yielded magnetic susceptibility data in the range of -0.08×10^{-5} to 1.15×10^{-5} SI.

Electrical resistivity

In Hole M0048A, resistivity ranges from 0.89 to 0.99 Ω m. Data are from one core section only, and it is therefore difficult to observe any downhole trends (Fig. F83).

Digital line scans and color reflectance

Only three small cores were recovered in Hole M0048A. All cores were digitally scanned and measured for color reflectance. L^* had a minimum of 47.26% and a maximum of 77.46% (Fig. F85). The three cores were composed of very heterogeneous unconsolidated material including lime pebbles, coral fragments, fine sand, and lime mud. Unsurprisingly, the sections showed in all cases a high dispersion of values in all three parameters of color reflectance (L^* , a^* , and b^*).

Thermal conductivity

The one thermal conductivity point taken for Hole M0048A gives a thermal conductivity value of 1.09 W/(m·K) at 3.09 m CSF-A.

Paleomagnetism

Measurements of low-field and mass-specific magnetic susceptibility (χ) were performed on samples taken from the working half of the recovered core (Fig. F86). Two positive susceptibility values were measured in samples located at 0.02 and 3.03 mbsf with values of 0.09×10^{-8} and 0.87×10^{-8} m³/kg. Low negative susceptibility was recorded in a sample located at 4.51 mbsf with a value of -2.02×10^{-8} m³/kg.

Chronology

This hole has only one calibrated radiocarbon age of 14 cal y BP from Core 325-M0048A-2R (Fig. F87). There are only two cores beneath this 14 cal y BP sec-

tion, indicating that this hole probably only contains material from the last deglaciation.

Transect HYD-02A summary

Sedimentology and biological assemblages

Few common patterns link lithologic successions in the eight holes along transect HYD-02A (Fig. F88). The following highlights describe some features along transect HYD-02A, focusing on shared features rather than on exceptions:

- In several holes, the upper sedimentary unit consists of unconsolidated to lithified modern or sub-recent seafloor sediment that is coarser grained in the shallower holes (M0042A and M0044A) and finer grained in the deeper ones (Holes M0040A and M0041A).
- Boundstones occur immediately below the modern sediments in all eight holes along the transect. Their thickness averages 9–10 m in the deepest two holes (M0040A and M0041A) and the shallowest hole (M0042A), and increases to 25 m in the two holes at intermediate depths (Holes M0047A and M0043A).
- In every hole that penetrated below the boundstone, there is a unit of unconsolidated material, usually lime sand, in which *Halimeda* is one of the main components. Recovered thicknesses of this material ranged from 5 to 10 m.
- The two holes (M0042A and M0043A) that penetrated below the unconsolidated interval encountered a packstone/grainstone unit, <1 m thick, that overlies unconsolidated sand in Hole M0043A and overlies alternating intervals of lithified grainstone to rudstone and unconsolidated sands in Hole M0042A. The lithified intervals in Hole M0042A contain clear evidence of subaerial exposure, including calcrete and possible root remains.

Boundstone lithologies contain variable proportions of coral, coralline algae, and microbialite that define several coralgal, coralgal-microbialite, and microbialite boundstones similar to those in the other Great Barrier Reef transects. The major corals in the boundstones are submassive to massive *Porites*, *Montipora*, branching Pocilloporidae, branching *Acropora*, massive *Isopora*, and submassive to massive Faviidae.

The common patterns of boundstone distribution in most of the holes are

- Coralgal boundstones, from 4 to 24 m thick, are the uppermost or only boundstone in six of the eight holes (excluding Holes M0040A and M0044A).

- Microbialite-rich boundstones (coralgal-microbialite or microbialite boundstones) lie beneath the coralgal boundstone or are the only boundstone lithology in Holes M0043A and M0042A.
- Microbialite boundstone, 4–7 m thick, occurs only in the deepest two holes (M0040A and M0041A).
- No simple relationship exists between the presence/absence of coralgal and coralgal-microbialite boundstones and the geographic location and/or water depth of holes along transect HYD-02A.

Table T3 documents all the larger foraminifera described in this transect in association with hole, run, and depth (below seafloor).

Physical properties

Recovery at transect HYD-02A sites was partial with an average of ~21%. However, recovery in Holes M0040A and M0041A reached ~50%. Cores were partially saturated and often disturbed, fractured, or contaminated. All of these factors act to degrade the quality of any physical property data collected. Borehole depths for this transect are as follows:

Hole M0040A = 126.07 mbsl, 21.50 m DSF-A.
 Hole M0041A = 126.58 mbsl, 22.10 m DSF-A.
 Hole M0042A = 50.78 mbsl, 46.40 m DSF-A.
 Hole M0043A = 102.93 mbsl, 35 m DSF-A.
 Hole M0044A = 105.25 mbsl, 11.00 m DSF-A.
 Hole M0045A = 105.25 mbsl, 14.60 m DSF-A.
 Hole M0046A = 117.49 mbsl, 20.40 m DSF-A.
 Hole M0047A = 99.12 mbsl, 33.20 m DSF-A.
 Hole M0048A = 104.57 mbsl, 7.10 m DSF-A.

Plugs and samples taken for discrete *P*-wave and moisture and density measurements were obtained from both consolidated and unconsolidated core material.

Density and porosity

Bulk density was measured at transect HYD-02A using gamma ray attenuation. Gamma ray attenuation on the multisensor core logger provided an estimate of bulk density (also referred to as gamma density) from whole cores. Discrete moisture and density measurements were also taken with a pycnometer on plugs and/or on rock fragments. This provides grain density, bulk density (in the case of plug samples), and porosity data. As in the previous transect, HYD-01C, one observes a classic linear relationship between the porosity (ϕ) and bulk density ($\rho = \rho_s[1 - \phi] + \rho_w\phi$) of discrete samples measured for all boreholes at transect HYD-02A (Fig. F89).

Average grain density (ρ_s) is 2.77 g/cm³. Grain density varies between 2.70 and 2.85 g/cm³ and may correspond to a value between the grain density of

calcite (2.71 g/cm³) and aragonite (2.93 g/cm³). Porosity values for all boreholes in this transect can be viewed in Figure F90. Porosity in the transect ranges between 16% and 72%. Similar trends in porosity can be picked out in Holes M0047A and M0043A with a stepwise decrease in porosity between 0 and 12 m CSF-A followed by an increase at ~15 m CSF-A and gradual decrease to ~25 m CSF-A. Holes M0040A and M0041A have almost identical trends in porosity, with 25% porosity (~0–10 m CSF-A) increasing to 53% at the bottom of the drilled holes.

P-wave velocity

A crossplot of velocity versus porosity (both from discrete samples) for all sites shows primarily an inverse relationship (Fig. F91) between *P*-wave velocity and porosity. Whole-core multisensor core logger data ranges from 1508.59 to 1895.75 m/s. As expected, much lower, possibly erroneous (see “Physical properties” in the “Methods” chapter) *P*-wave velocity values have been recorded by the multisensor core logger for coralgal boundstone units, unlike the discrete measurements on core plugs, which are probably more reliable.

Magnetic susceptibility

Magnetic susceptibility data are very difficult to interpret for this transect because of limited core recovery in all holes across transect HYD-02A. However, values are generally similar across the holes, with the majority of readings being in the -1×10^{-5} to 1×10^{-5} SI range, which is delineated by short intervals of magnetic susceptibility highs.

Electrical resistivity

Over the entire transect, resistivity is highly variable, with the lowest values (0.56 Ω m) measured in Hole M0040A and highest values (44.84 Ω m) recorded in Hole M0044A. Because of the relatively poor core quality (as mentioned above) and undersaturated cores, very little confidence can be placed in these data.

Color reflectance

In transect HYD-02A, Holes M0048A, M0047A, M0043A, M0044A, and M0046A are located at similar water depths and can be correlated (with <5 m separation between the drilled holes). Holes M0047A and M0043A exhibit similar trends, but Hole M0047A presents smaller dispersion in the values of reflectance per section. This is probably due to the presence of massive corals in Hole M0047A. Hole M0046A was corrected for depth because of its location on a pinnacle. This was taken into account

when plotting it against the other boreholes in order to make direct comparisons across the transect. Hole M0046A shows a similar trend in data points to the shallower holes. However, there is a smoother distribution of the reflectance measurements. Holes M0048A and M0044A have similar values; however, because of the lack of measurements with depth in Hole M0048A, no trend can be identified. Recovery in Hole M0045A was so low that color reflectance was not measured.

Holes M0040A and M0041A are located very close to each other in the same water depth. Both boreholes exhibit less dispersion in color reflectance measurements than other boreholes from this transect. Data from these boreholes show a consistent pattern of ~50% L^* at 2.5 m CSF-A, a slight increase at 6–8 m CSF-A, and a decrease in reflectance below that, re-tuning to ~50% at 21 m CSF-A. Color reflectance measurements for all transect HYD-02A boreholes are represented in Figure F92. Boreholes are plotted from shallower to deeper water (left to right) at the same depth scale. For boreholes found at similar depths, similar trends are present in the color reflectance data, which suggests a possible correlation between them.

Paleomagnetism

Transect HYD-02A comprises nine holes located at five sites in the southern part of Hydrographer's Passage. Recovered materials were dominated by corals and calcareous sediments. The materials show mainly low and/or negative values of low-field and mass-normalized magnetic susceptibility. The arithmetic means of the measurements taken suggest that they are related mainly to diamagnetic materials. Further studies may detect minimal fractions of ferromagnetic material and further define the magnetic properties and geomagnetic behavior of the records obtained thus far.

The lower magnetic susceptibility values related to diamagnetic material are difficult to correlate to a common geological or paleomagnetic feature. However, high magnetic susceptibility values for samples located in the uppermost 1–2 m or between 2 and 5 mbsf are common to the majority the sites in this transect, are most evident in the deep Site 10 location (Holes M0040A and M0041A), and are mainly associated with lithologic variations. Variations between 17 and 20 mbsf and 27 and 30 mbsf can be attributed to the occurrence of sandy layers, which may represent an important variation in the growth regime of the Great Barrier Reef, potentially marking significant paleoclimatic changes.

At Site 10 (Holes M0040A and M0041A), strong magnetic susceptibility spikes at 14–15 and 16–17 mbsf

were recorded. Magnetic susceptibility for these layers is strong enough to suggest alternative hypotheses beyond a simple variation in the concentration of magnetic minerals as a result of a paleoclimatic pulse. However, further rock magnetic studies are required to define the nature and processes that produced these susceptibility variations. Environmental magnetic studies will define the climatic origin of these layers and provide further information on the volume, composition, and grain size of the magnetic component retained in these layers.

Drilling contamination appears to have occurred in the uppermost ~10–30 cm of some cores from Holes M0040A and M0041A. The strong signal may be caused by rust from the pipe. Alternatively, the high values of susceptibility may be due to sulfide pieces that were not washed out of the hole during drilling and accumulated at the top of each core.

Geochemistry

A total of 20 interstitial water samples from transect HYD-02A were obtained from Holes M0040A (4), M0041A (6), M0042A (2), M0043A (4), M0046A (2), and M0047A (2). Samples were analyzed for cation and anion concentrations (Table T4). Parameters including pH, alkalinity, and concentrations of ammonium were measured during the offshore phase of the expedition, whereas major cations and anions were measured during the Onshore Science Party. All geochemical constituents were determined to be within the normal ranges for marine sediments. Because of the scarcity of interstitial water samples in this transect, interpretations relating to vertical variations could not be made.

Chronology

The shallowest hole on transect HYD-02A (Fig. F88), Hole M0042A (Site 2), was drilled into a 50 m feature and returned ages of 13–10 cal y BP from 65 to 51 meters below seafloor (mbsl) (Cores 325-M0042A-1R and 10R), thus recording the middle of the last deglaciation. Deeper in Hole M0042A, an age of 169 cal y BP was recovered from 86 mbsl (Core 325-M0042A-24R), indicating the potential for recovering pre-Last Glacial Maximum (LGM) material in deeper cores from this hole. Sites 7–12 drilled a range of features from 98 to 108 mbsl. Where dated, the tops of holes at these sites return ages of 15–14 cal y BP (15 cal y BP, Core 325-M0043A-2R, 106 mbsl; 14 cal y BP, Core 325-M0044A-2R, 109 mbsl; 15 cal y BP, Core 325-M0047A-3R, 102 mbsl; 14 cal y BP, Core 325-M0048A-2R, 101 mbsl), and the lower portions of the two holes at Site 12 that have greater penetration (Holes M0043A and M0047A) returned ages of 20 and 21 cal y BP from 129 and 127 mbsl (Cores 325-

M0043A-18R and 325-M0047A-11R), respectively. Therefore, at these sites, the early portion of the deglaciation was recovered, whereas the LGM has been captured in the deeper cores at Site 12. The deepest site on transect HYD-02A, Site 10 (Holes M0040A and M0041A), was drilled into a feature at 127 mbsl. Ages of 17–10 cal y BP have been returned from the tops of the two holes at this site (Cores 325-M0040A-2R, 4R, and 325-M0041A-2R), indicative of accumulation during the last deglaciation. However, the lower portion of Hole M0040A returned an age of 25 cal y BP (Core 325-M0049A-8R) from 138 mbsl, indicating that Site 10 also recovered material representative of the LGM.

Downhole measurements

Downhole geophysical logs provide continuous information on a broad range of formation properties. In this transect, this continuous data set provides important data where core recovery is limited.

Borehole geophysical instruments

The wireline sondes deployed at HYD-02A were as follows:

- Optical Borehole Televiewer (OBI40),
- Acoustic Borehole Televiewer (ABI40),
- Spectral Natural Gamma Probe (ASGR),
- Induction Conductivity Probe (DIL45)—with medium investigation depth (ILM, 0.57 m) and deep investigation depth (ILD, 0.83 m),
- Full Waveform Sonic Probe (SONIC),
- Magnetic susceptibility probe (EM51), and
- Caliper probe (CAL3)—borehole diameter.

Preliminary results

Wireline logging operations were performed in one API hole (M0042A) on transect HYD-02A. The priority imaging tools (ABI40 and OBI40) were also run to see if good image data could be obtained in an API hole. The standard maximum hole diameter for successful image data acquisition is 15 cm, and API holes tend to have a minimum diameter of ~20 cm, so images were not successfully collected.

Four main logging units were identified from the downhole data from Hole M0042A:

1. The uppermost Unit I is characterized by low total gamma ray (TGR) counts (through-pipe and open hole), high conductivity, and very low magnetic susceptibility. Borehole diameter is extremely large in Unit I (>40 cm in places), which may be a consequence of the API bottom-hole assembly moving and swabbing the top of the

open hole. Four main lithostratigraphic are associated with Unit I: lime sand and algal bindstone, coralgal boundstone, coralgal-microbialite boundstone, and unconsolidated sediment (lime granules and pebbles).

2. Unit II is associated with a downsection sequence of grainstone to unconsolidated sediment (lime granules and pebbles) to grainstone with rhodoliths units. These lithologic variations are most mirrored by the conductivity data, which exhibit some minor fluctuations downhole. TGR has intermediate values, whereas magnetic susceptibility is extremely low and constant. The borehole diameter is in gauge in this unit.
3. Unit III is characterized by increasing values of TGR downhole and relatively high conductivity and stable borehole diameter figures. Lithostratigraphic units associated with this logging unit are (top-down) grainstone with rhodoliths, unconsolidated sediment (lime granules and pebbles), and gray rudstone and rudstone with brown staining.
4. Unit IV represents a zone of reduced TGR counts. A decline in conductivity is present at the very top of Unit IV, but overall values gradually increase to the base of the hole. Magnetic susceptibility remains very low and only fluctuates slightly, and the caliper registers the hole to be in gauge. Only one lithostratigraphic (rudstone with brown staining) is associated with this logging unit.

References

- Bronk Ramsey, C., 2009. Bayesian analysis of radiocarbon dates. *Radiocarbon*, 51(1):337–360. <http://digitalcommons.arizona.edu/restrictedobjectviewer?o=http://radiocarbon.library.arizona.edu/Volume51/Number1/0b094122-5128-4777-9edd-b4dad8f3864d>
- Reimer, P.J., Baillie, M.G.L., Bard, E., Bayliss, A., Beck, J.W., Blackwell, P.G., Bronk, R.C., Buck, C.E., Burr, G.S., Edwards, R.L., Friedrich, M., Grootes, P.M., Guilderson, T.P., Hajdas, I., Heaton, T.J., Hogg, A.G., Hughen, K.A., Kaiser, K.F., Kromer, B., McCormac, F.G., Manning, S.W., Reimer, R.W., Richards, D.A., Southon, J.R., Talamo, S., Turney, C.S.M., van der Plicht, J., and Weyhenmeyer, C.E., 2009. Intcal09 and Marine09 radiocarbon age calibration curves, 0–50,000 years cal BP. *Radiocarbon*, 51(4):1111–1150. <http://digitalcommons.arizona.edu/restrictedobjectviewer?o=http://radiocarbon.library.arizona.edu/Volume51/Number4/49691745-6a68-4e2c-a26f-08f0a16c1a53>

Publication: 16 July 2011
MS 325-104

Figure F1. Contour plot showing transect HYD-02A (Hydrographer’s Passage), Expedition 325. Sites 1–12 and Holes M0040A–M0048A are indicated. See Figure F2 in the “Expedition 325 summary” chapter for general location. EPSP = Environmental Protection and Safety Panel.

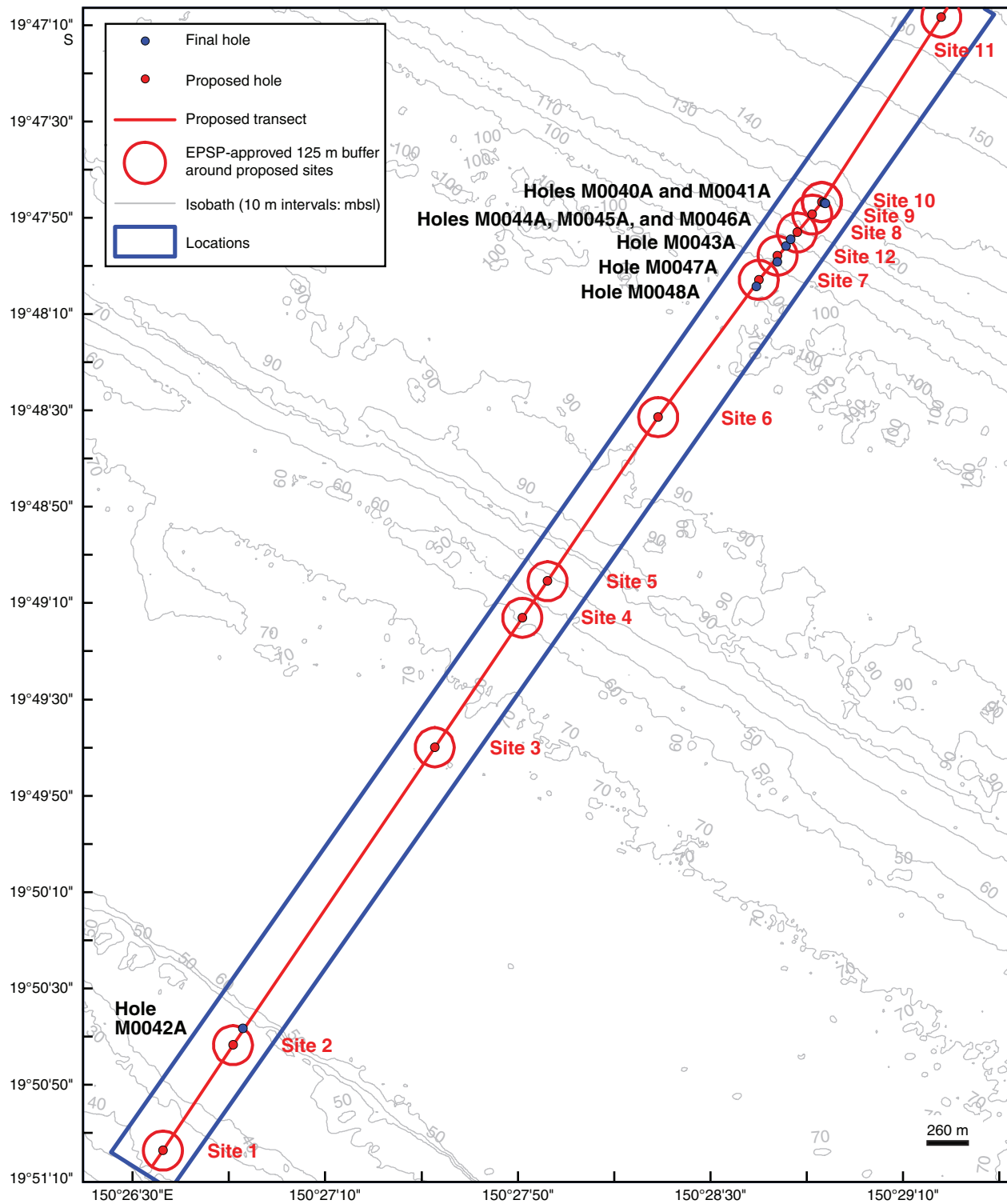


Figure F2. High-resolution line scan image of packstone/rudstone containing corals, coralline algae, echinoid spines, *Halimeda*, mollusk shells, serpulids, and traces of *Tubipora musica* with thick crusts of coralline algae (interval 325-M0040A-7R-1, 9–39 cm).

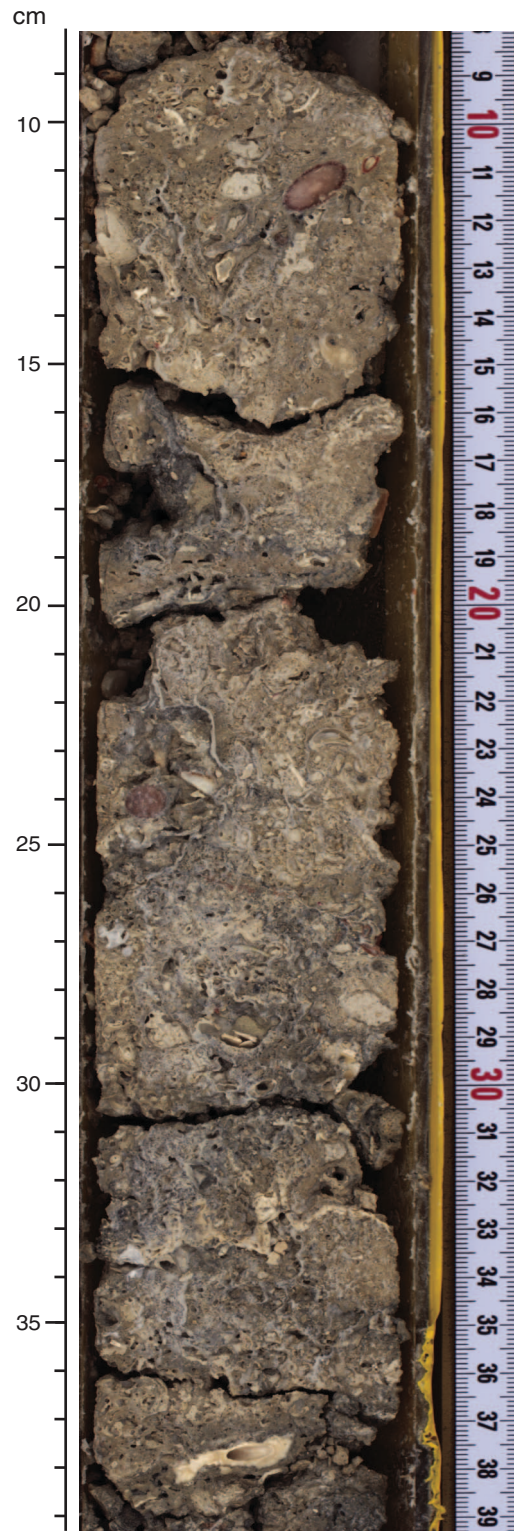


Figure F3. High-resolution line scan image of a microbialite-coralgal boundstone with mollusks, *Halimeda*, foraminifera, and small pieces of Acroporidae, Poritidae, and Agariciidae (interval 325-M0040A-9R-1, 1–14 cm).



Figure F4. High-resolution line scan image of a bioclastic rudstone to rudstone with coral, coralline algae, mollusks, foraminifera, and *Halimeda* (interval 325-M0040A-9R-1, 14–36 cm).



Figure F5. High-resolution line scan image of thick microbialites with cavities partially filled with consolidated or unconsolidated fine-grained bioclastic packstone (interval 325-M0040A-5R-1, 42–52 cm).

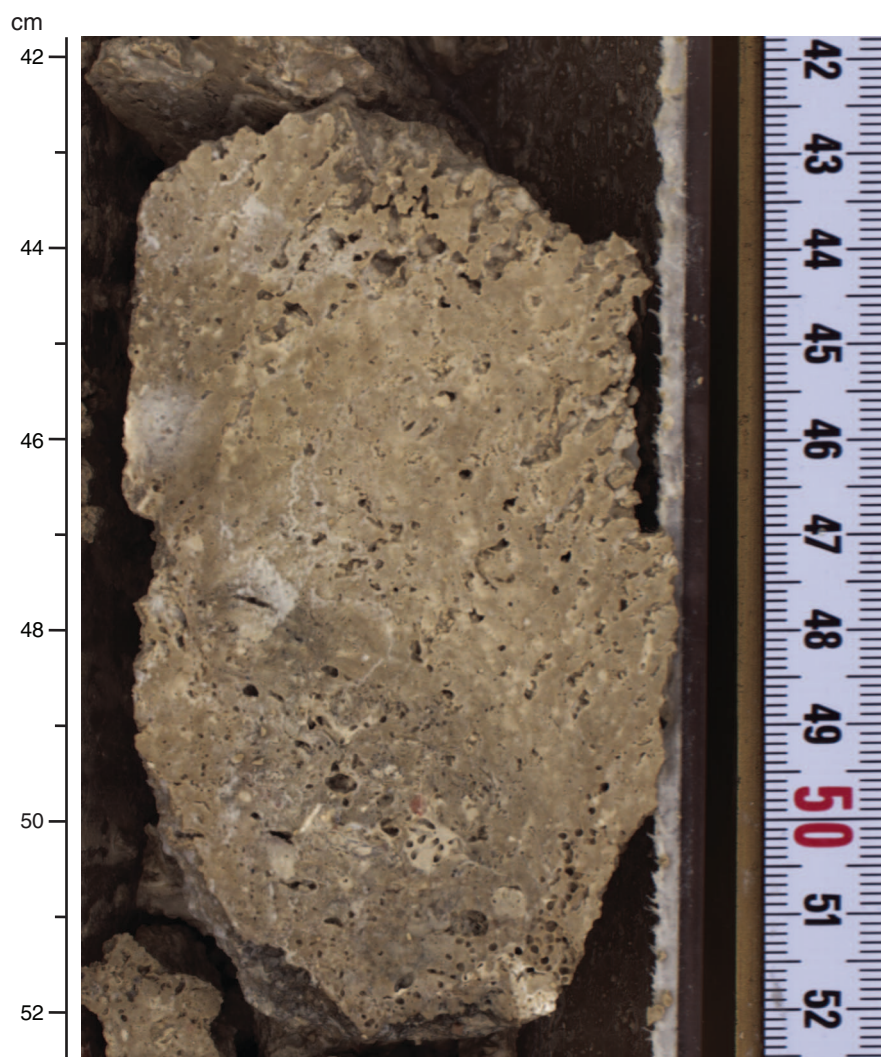


Figure F6. High-resolution line scan image of a coralgal-microbialite boundstone with packstone intercalations (internal sediments) (interval 325-M0040A-8R-1, 12–40 cm). The coral framework is composed of fine branching Acroporidae (12–15 cm), encrusting Agariciidae (22.5–24 cm), *Tubipora musica* (27 cm), and encrusting Agariciidae (in situ?; 34–37 cm).



Figure F7. High-resolution line scan image of a submassive *Porites* (in situ?) (interval 325-M0040A-8R-1, 127–130 cm).



Figure F8. Summary diagram showing data collected on whole cores using the multisensor core logger (MSCL), Hole M0040A.

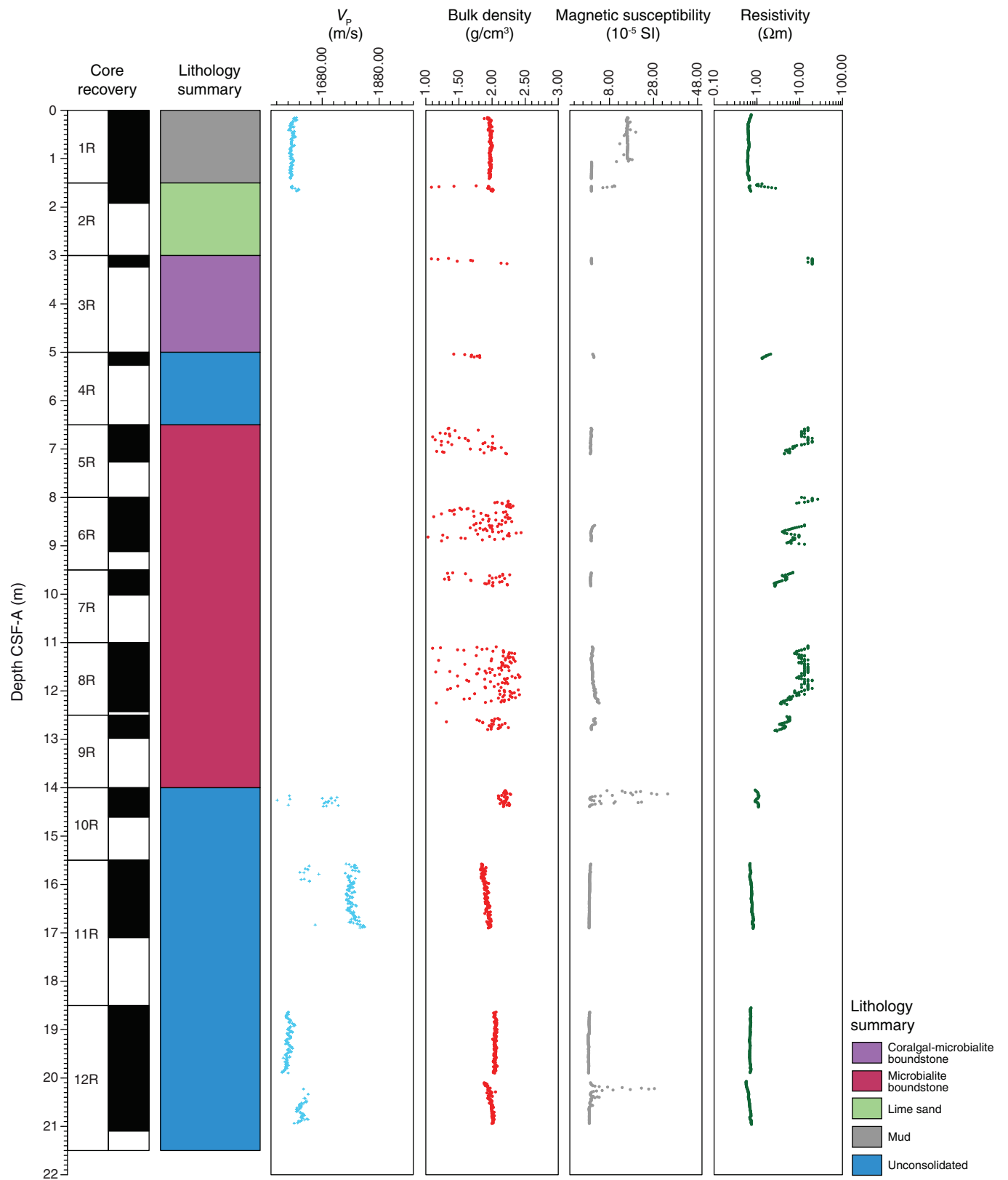


Figure F9. Petrophysical measurements obtained from discrete samples with a pycnometer, Hole M0040A. Bulk density measured on whole cores with the MSCL is shown in red on the bulk density plot.

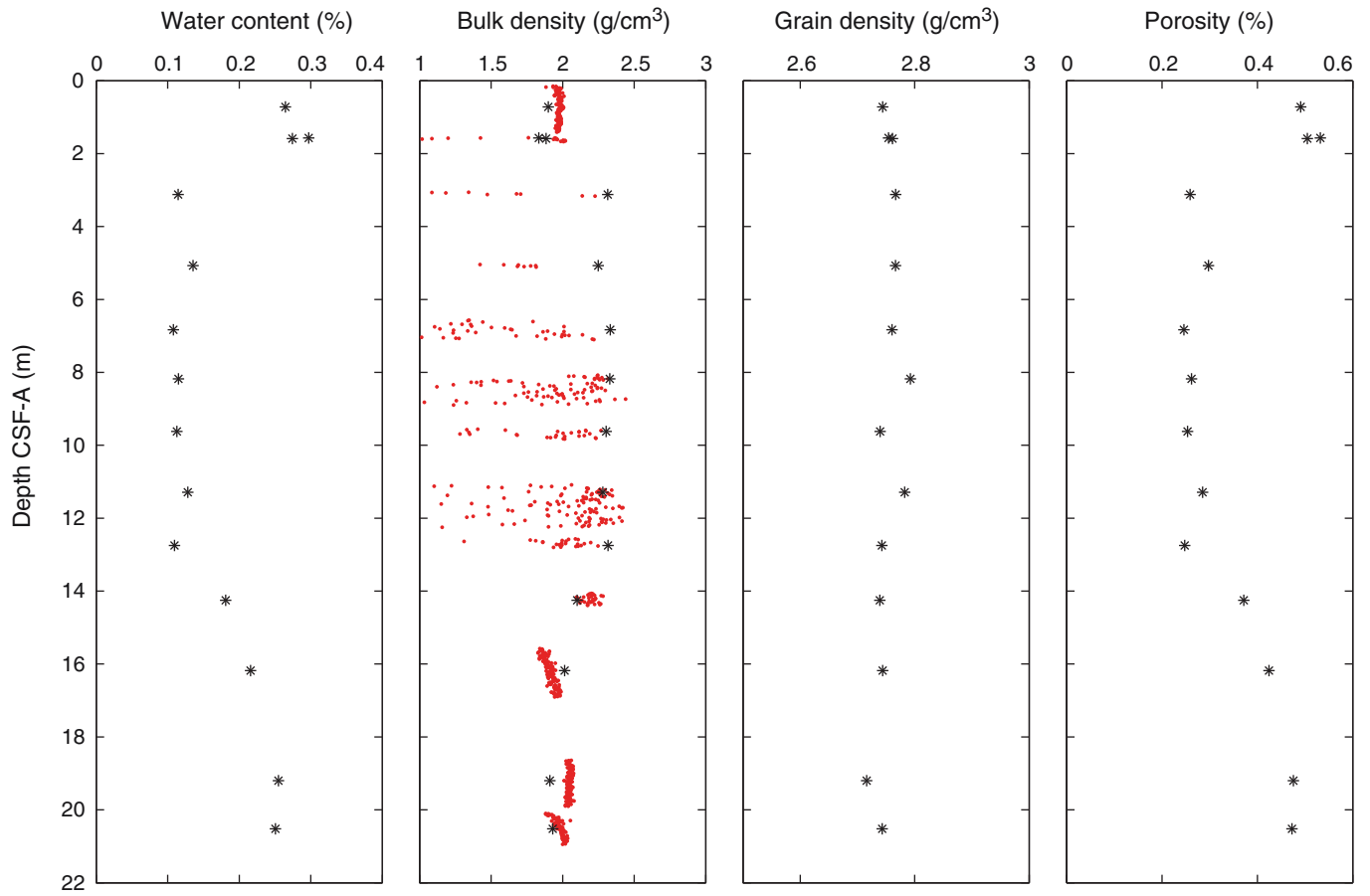


Figure F10. *P*-wave velocity data, Hole M0040A. **A.** Plot of initial, dry, and resaturated *P*-wave velocity measurements on discrete samples vs. depth. Three measurements were taken at each depth and are denoted by a dot. Average values are plotted as an open triangle. **B.** Plot showing discrete *P*-wave velocity vs. discrete bulk density.

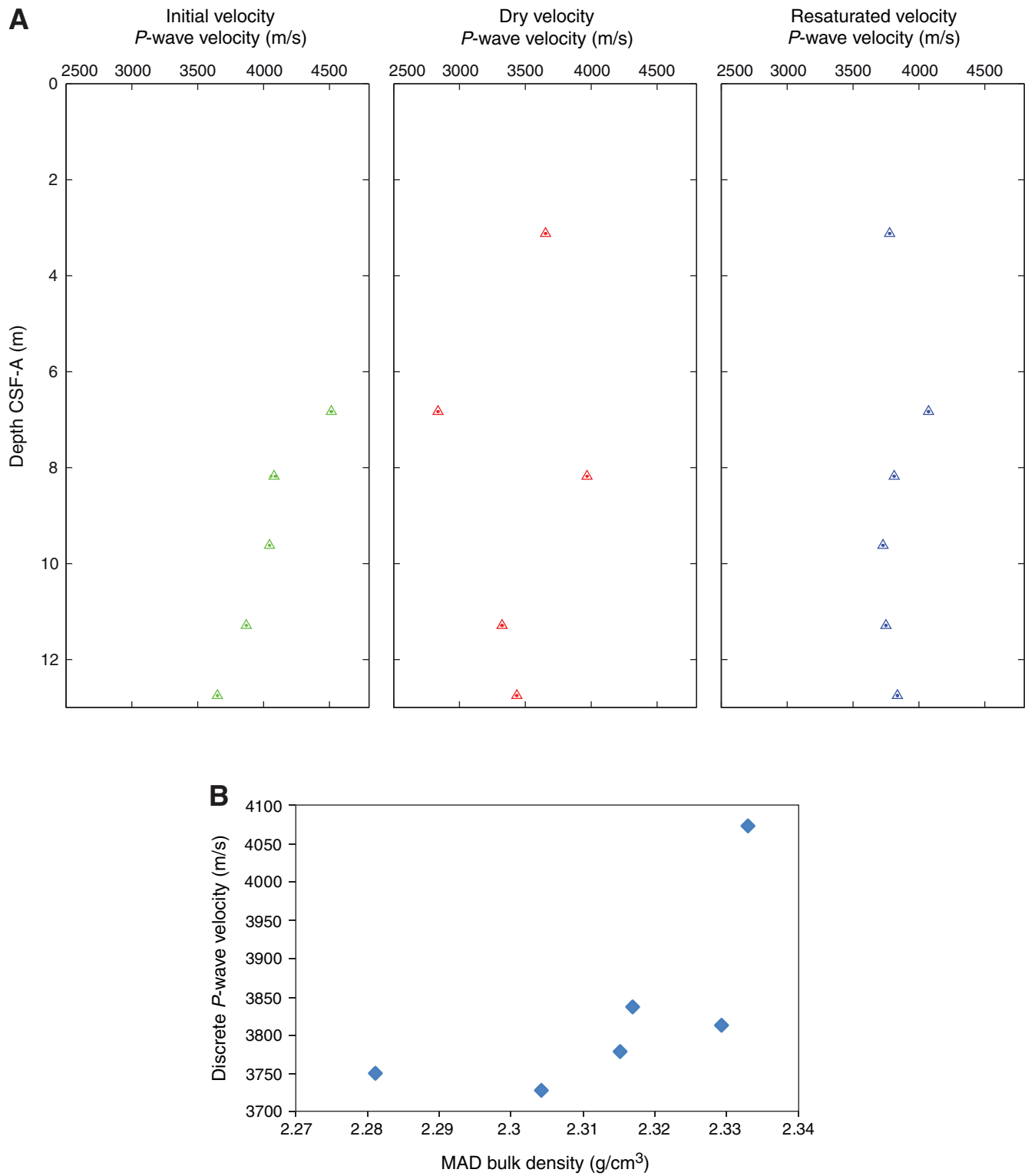


Figure F11. Values of reflectance (L^*), green to red (a^*), and blue to yellow (b^*) indexes, along with ratio a^*/b^* for Hole M0040A.

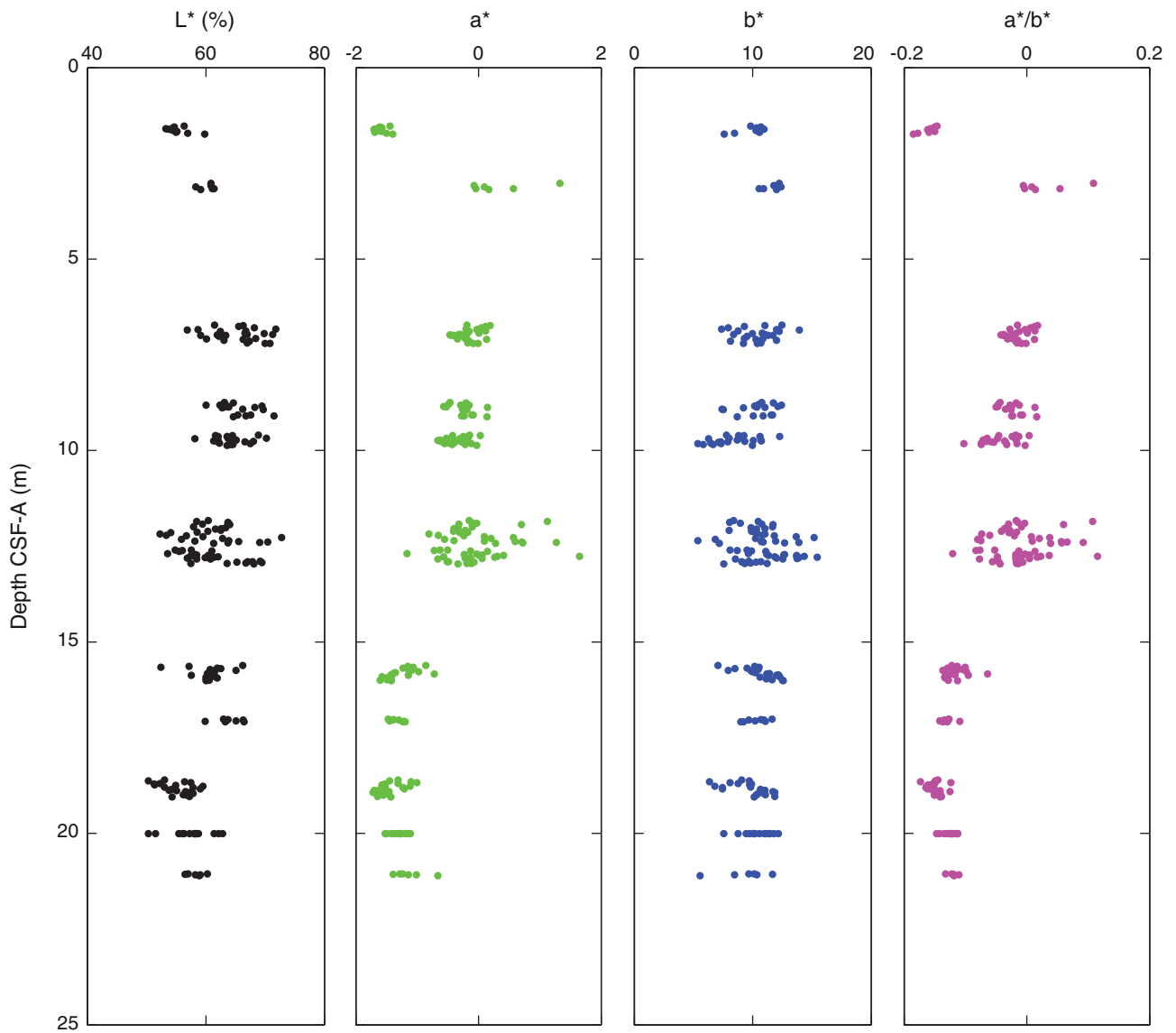


Figure F12. Plot of thermal conductivity vs. depth, Hole M0040A. Error bars indicate the standard deviation.

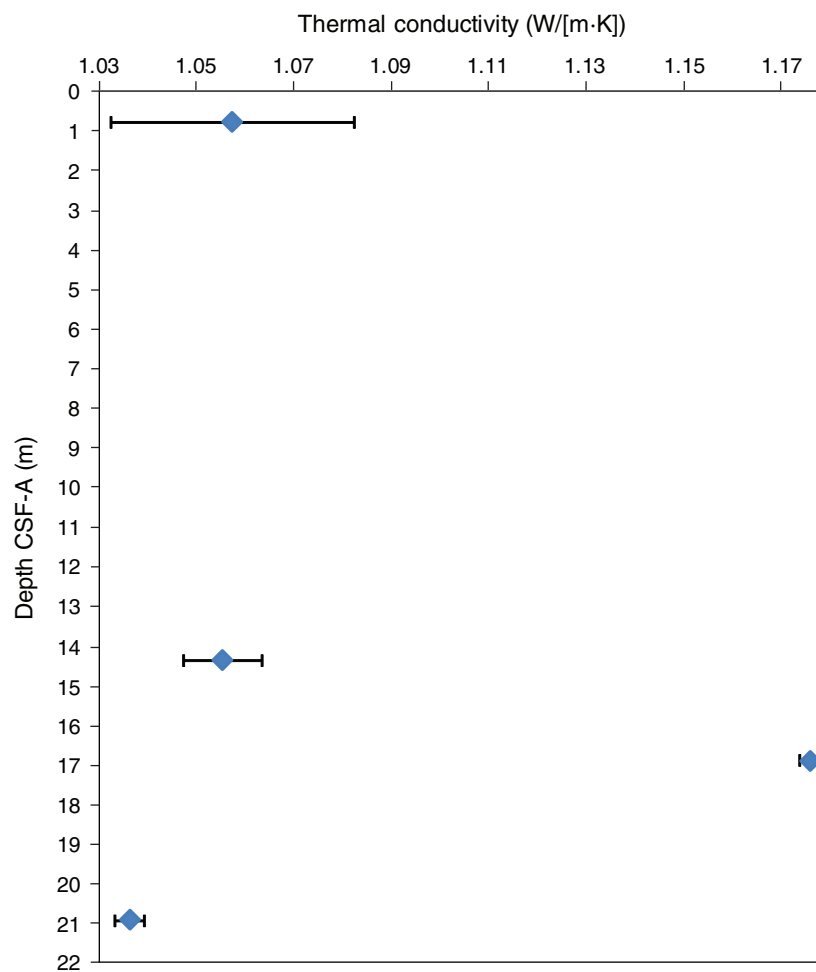


Figure F13. Magnetic susceptibility record for Hole M0040A. Water depth = 126.07 m (LAT).

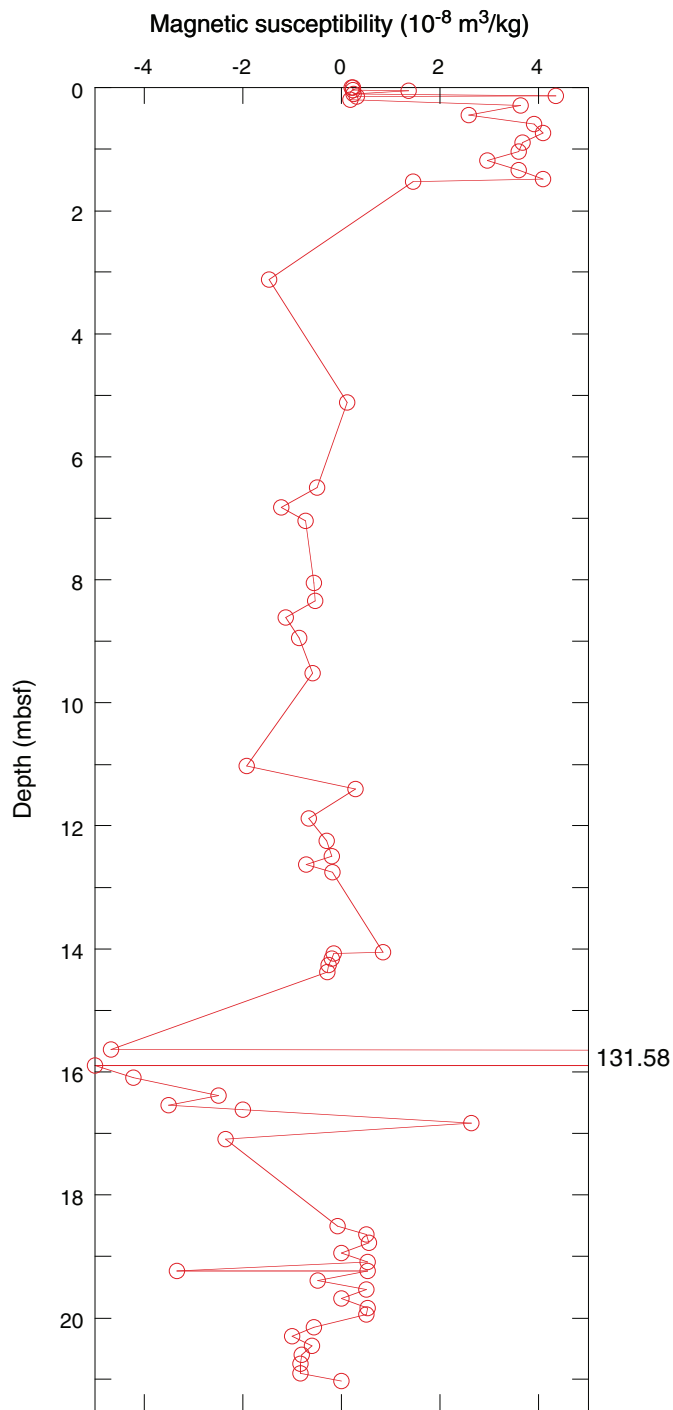


Figure F14. Preliminary chronology for Hole M0040A. Radiocarbon data are presented as graphs with the uncalibrated radiocarbon age and uncertainty shown as the red normal distribution on the ordinate axis and the probability distribution of the calibrated age shown in gray on the abscissa. The marine09 calibration curve is shown in blue. Horizontal bars indicate portions of the age distribution that are significant at the 95.4% confidence interval and the mean age (white circle ± 1 standard deviation) used for the purposes of preliminary dating. All ages are presented as thousands of calendar years BP (1950 AD). See Table T10 in the “Methods” chapter. (See Bronk Ramsey [2009], as well as Bronk Ramsey [2010] at c14.arch.ox.ac.uk/oxcal.html.)

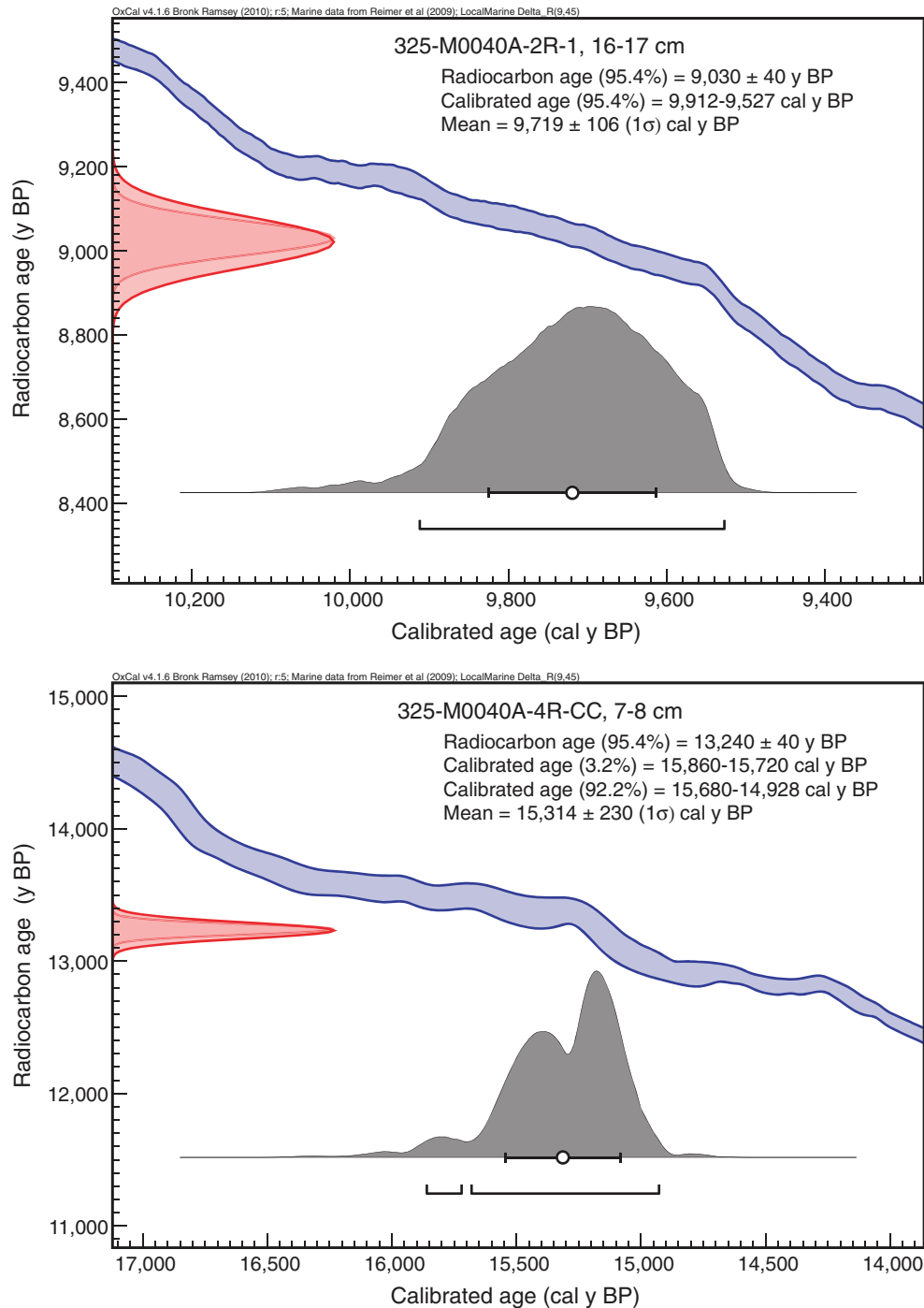


Figure F15. High-resolution line scan image of coralgall boundstone fragments with massive Poritidae, fragments of Poritidae and Acroporidae(?), and thick coralline algae, fragments of mollusks, and *Halimeda* (interval 325-M0041A-2R-1, 42–64 cm).

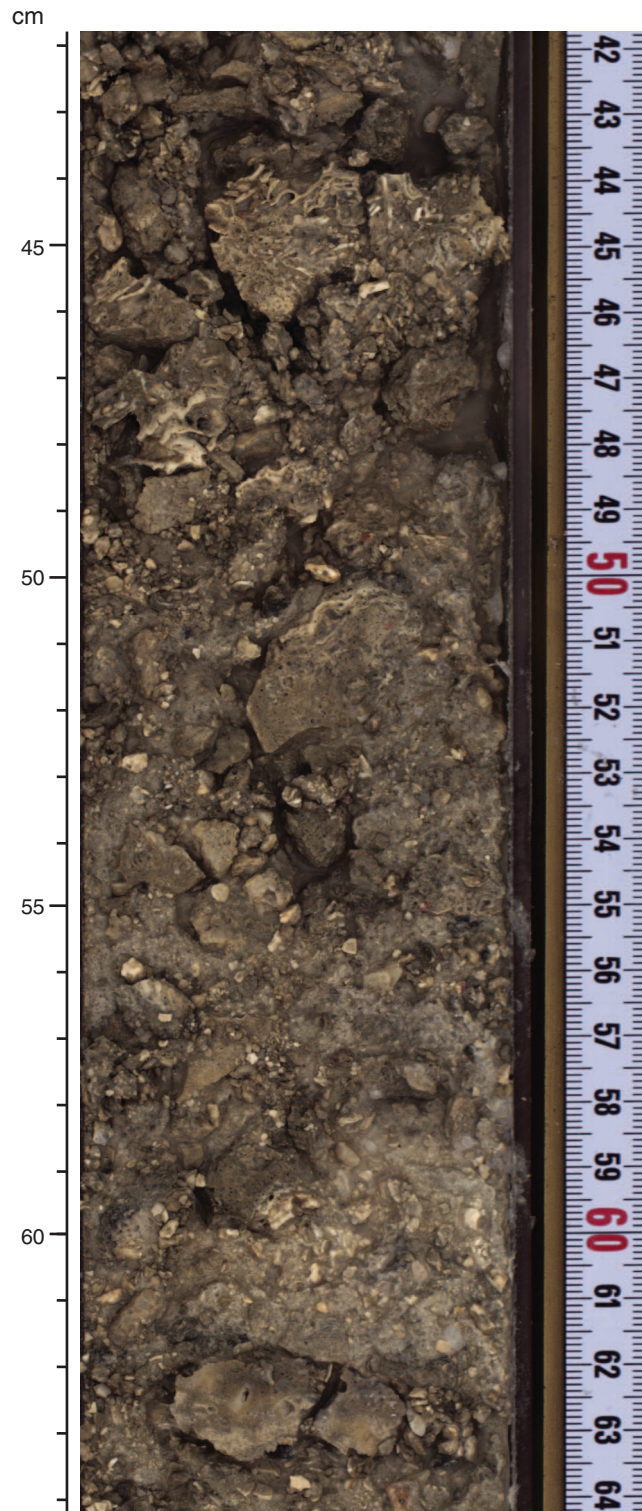


Figure F16. High-resolution line scan image of a microbialite boundstone with corals (encrusting Agariciidae), pockets of bioclastic packstone, and some columnar laminated microbialites (interval 325-M0041A-6R-1, 13–31 cm).

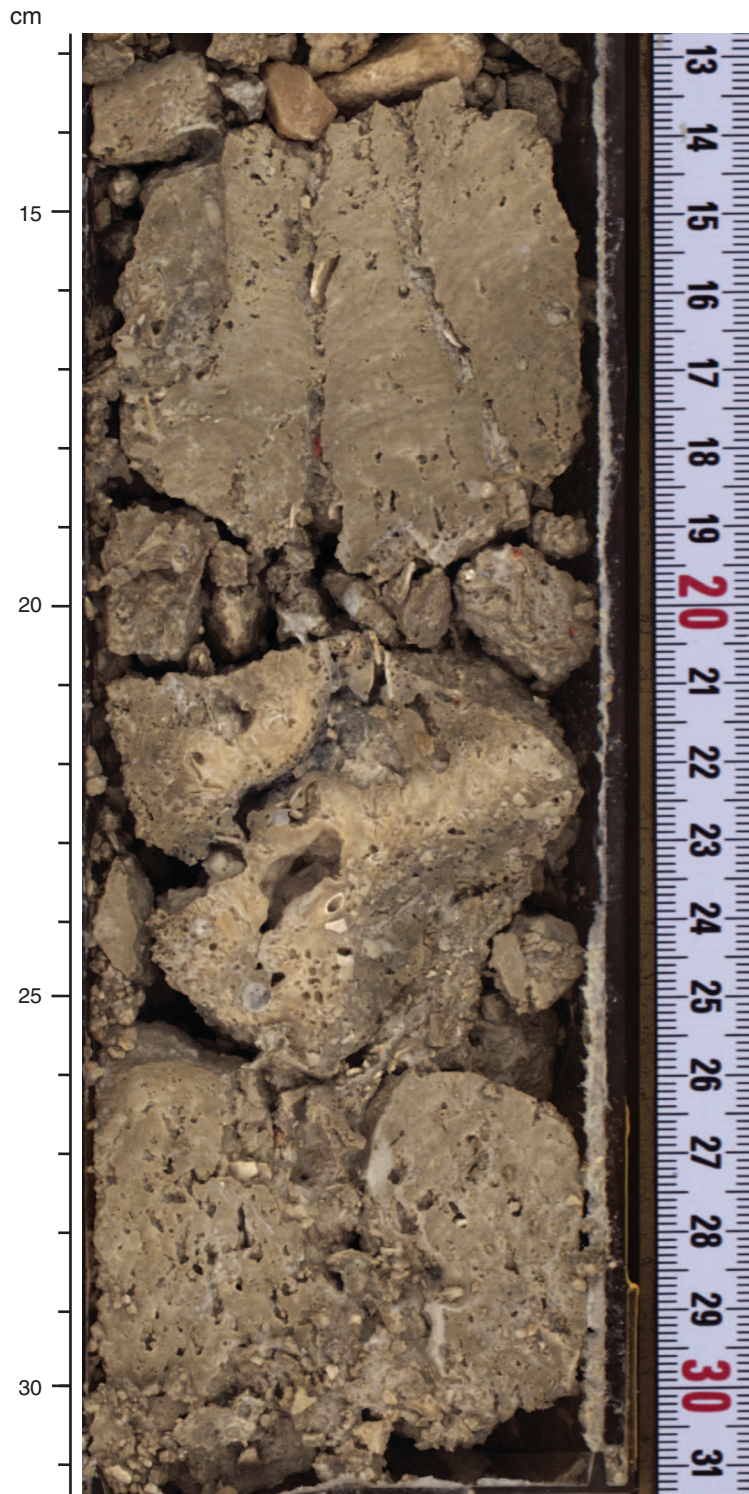


Figure F17. High-resolution line scan image of medium-coarse lime sand with coral granules and pebbles (interval 325-M0041A-8R-1, 10–30 cm). Bioclasts include benthic foraminifera, mollusks, *Halimeda*, and fragments of massive Faviidae and platy *Porites*(?).

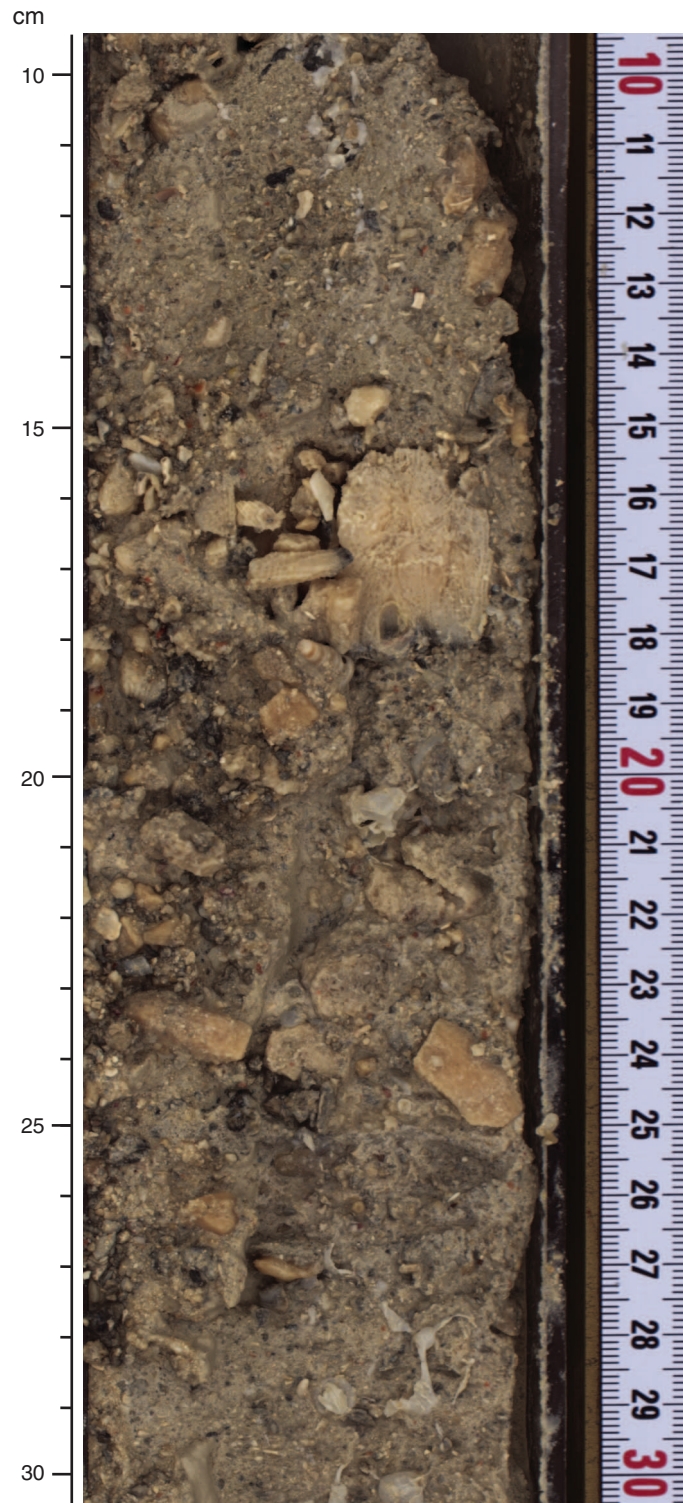


Figure F18. High-resolution line scan image of fine to medium lime sand with granules and pebbles of benthic foraminifera, mollusks, and *Halimeda* (interval 325-M0041A-11R-1, 35–60 cm).

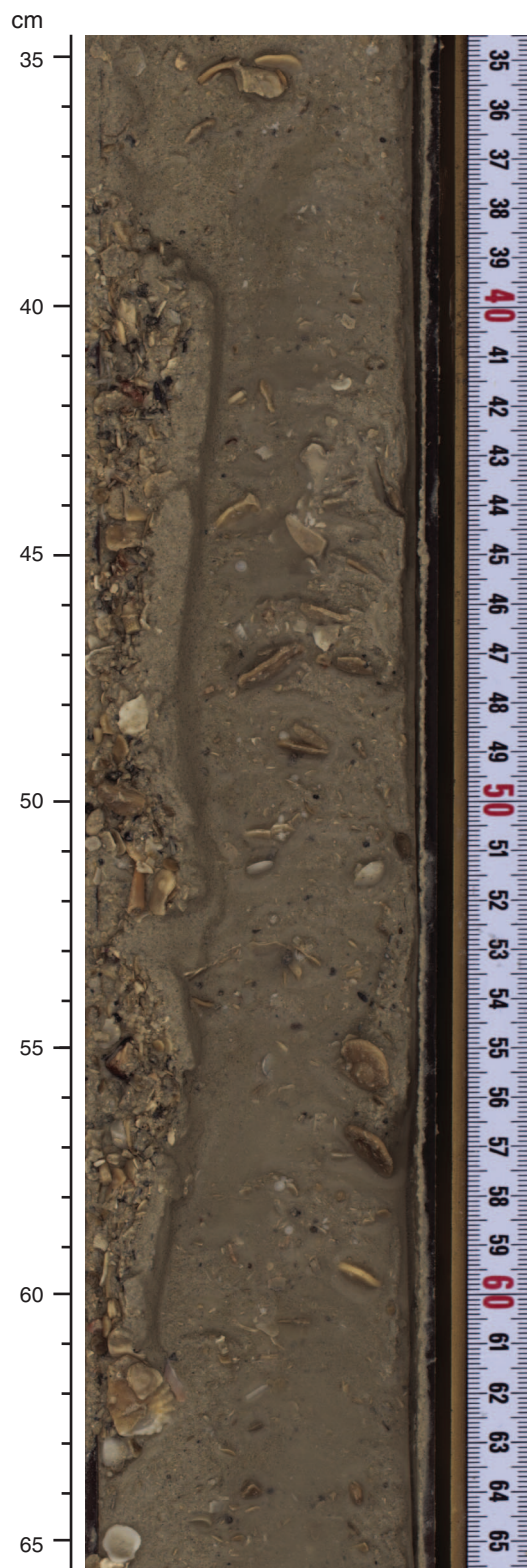


Figure F19. Summary diagram showing data collected on whole cores using the multisensor core logger (MSCL), Hole M0041A.

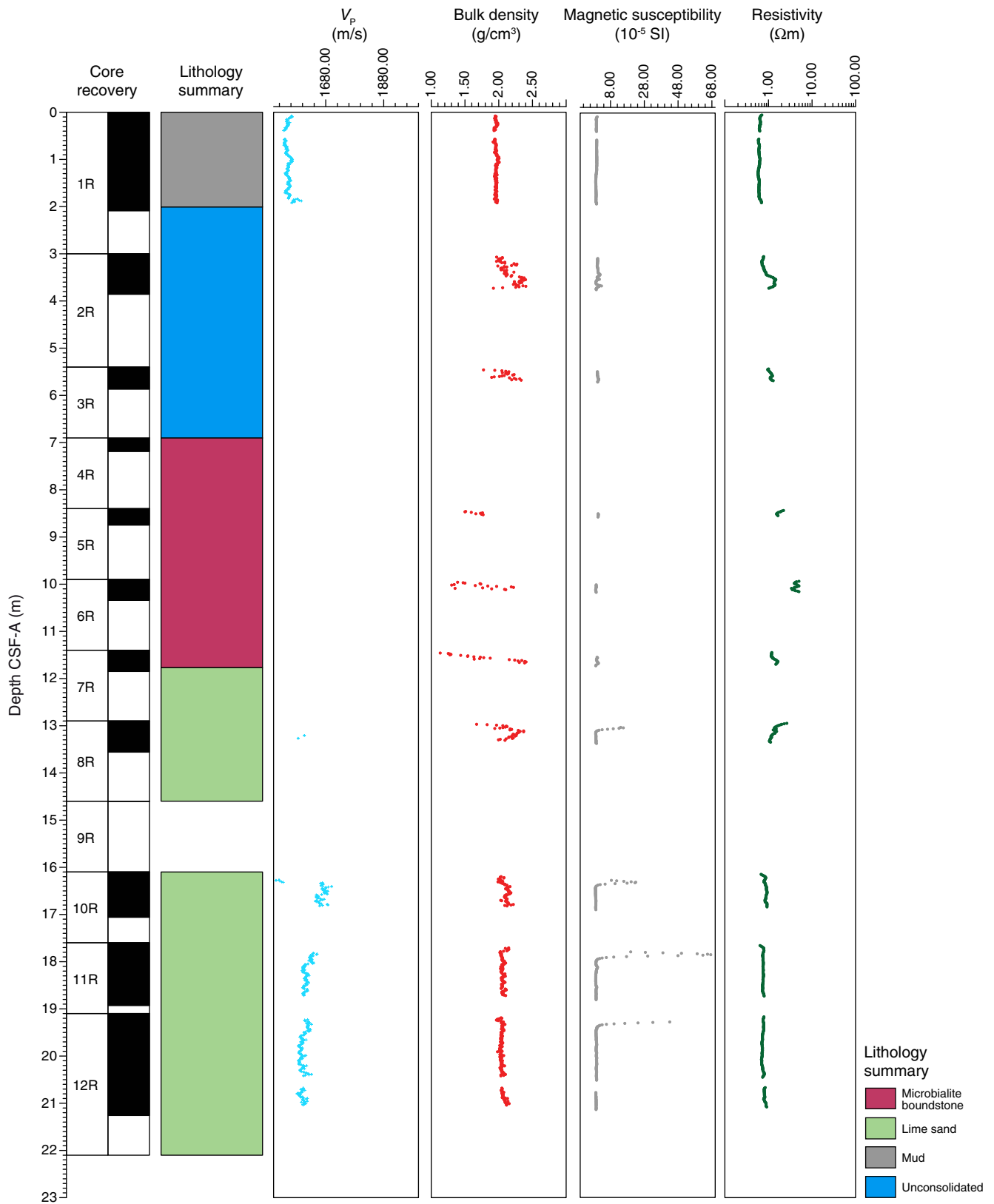


Figure F20. Petrophysical measurements obtained from discrete samples with a pycnometer, Hole M0041A. Bulk density measured on whole cores with the MSCL is shown in red on the bulk density plot.

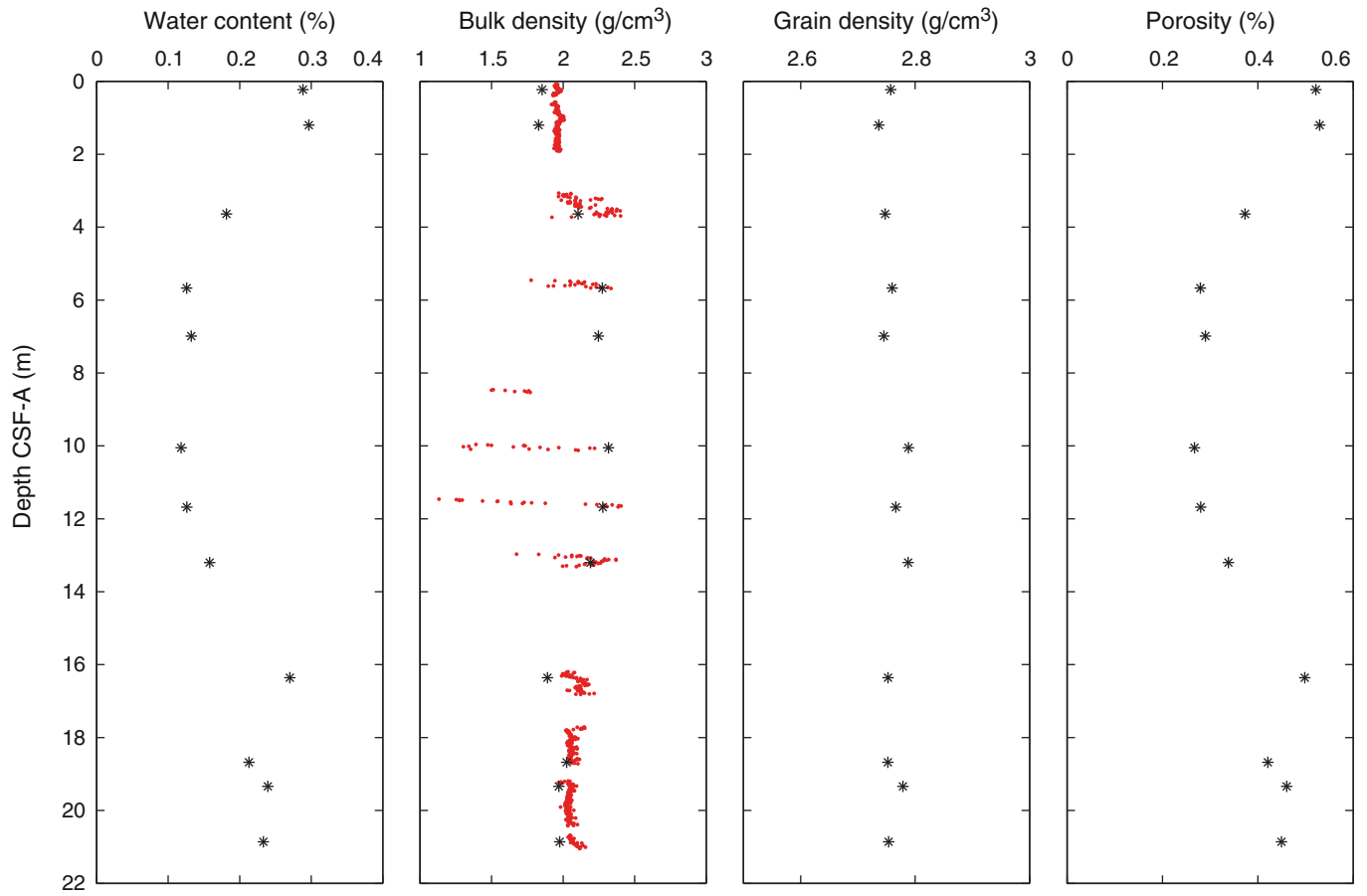


Figure F21. Values of reflectance (L^*), green to red (a^*), and blue to yellow (b^*) indexes, along with ratio a^*/b^* for Hole M0041A.

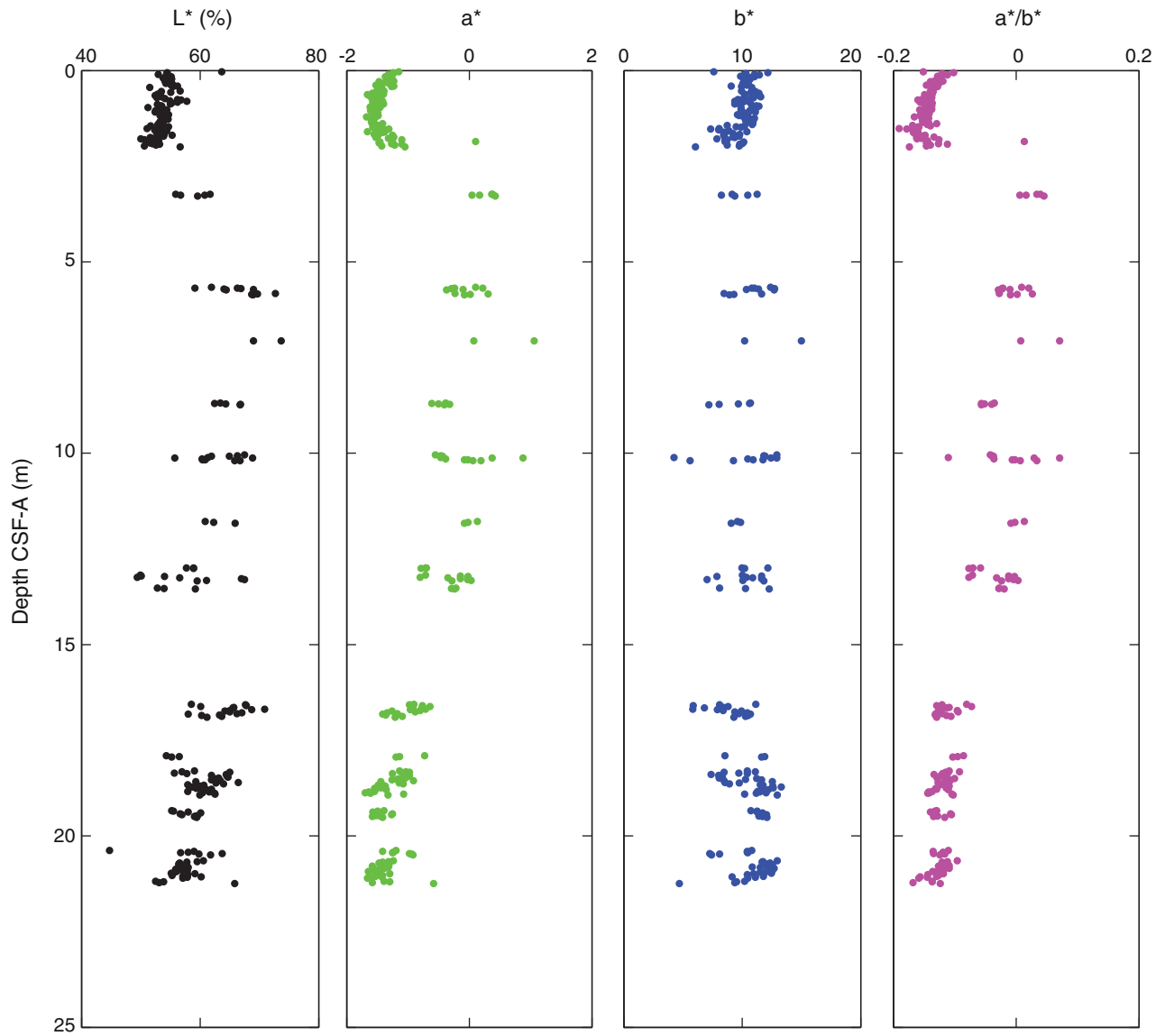


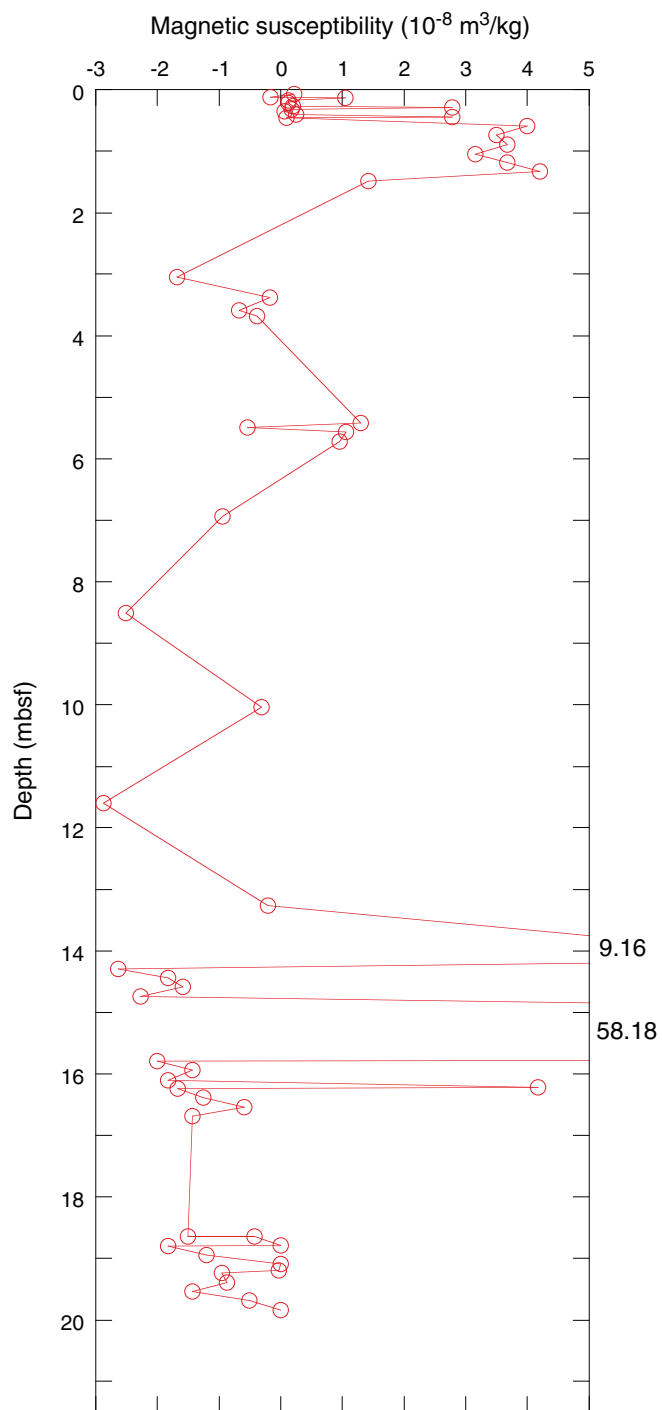
Figure F22. Magnetic susceptibility record for Hole M0041A. Water depth = 126.58 m (LAT).

Figure F23. A–C. Downhole U-channel variations (Section 325-M0041A-12R-1). A. NRM intensity, with intensity after demagnetization at 20 mT and 40 mT. (Continued on next three pages.)

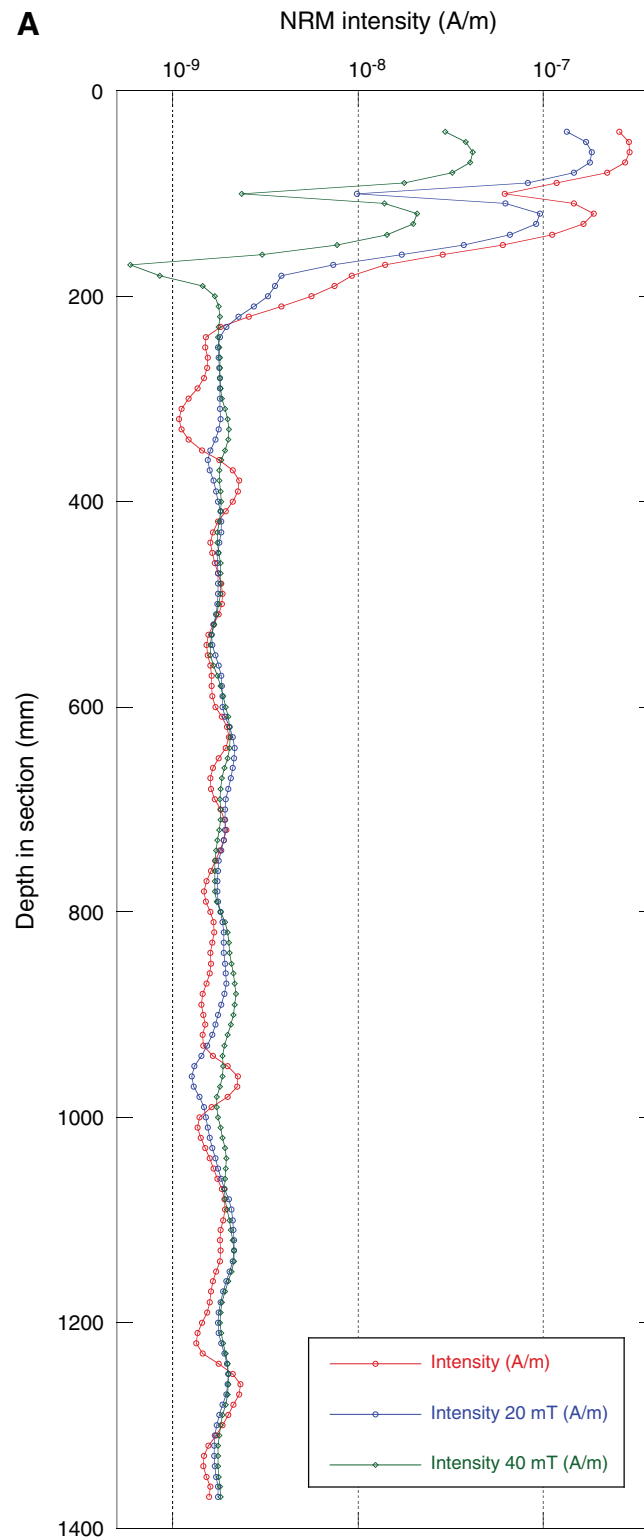


Figure F23 (continued). B. Inclination. (Continued on next page.)

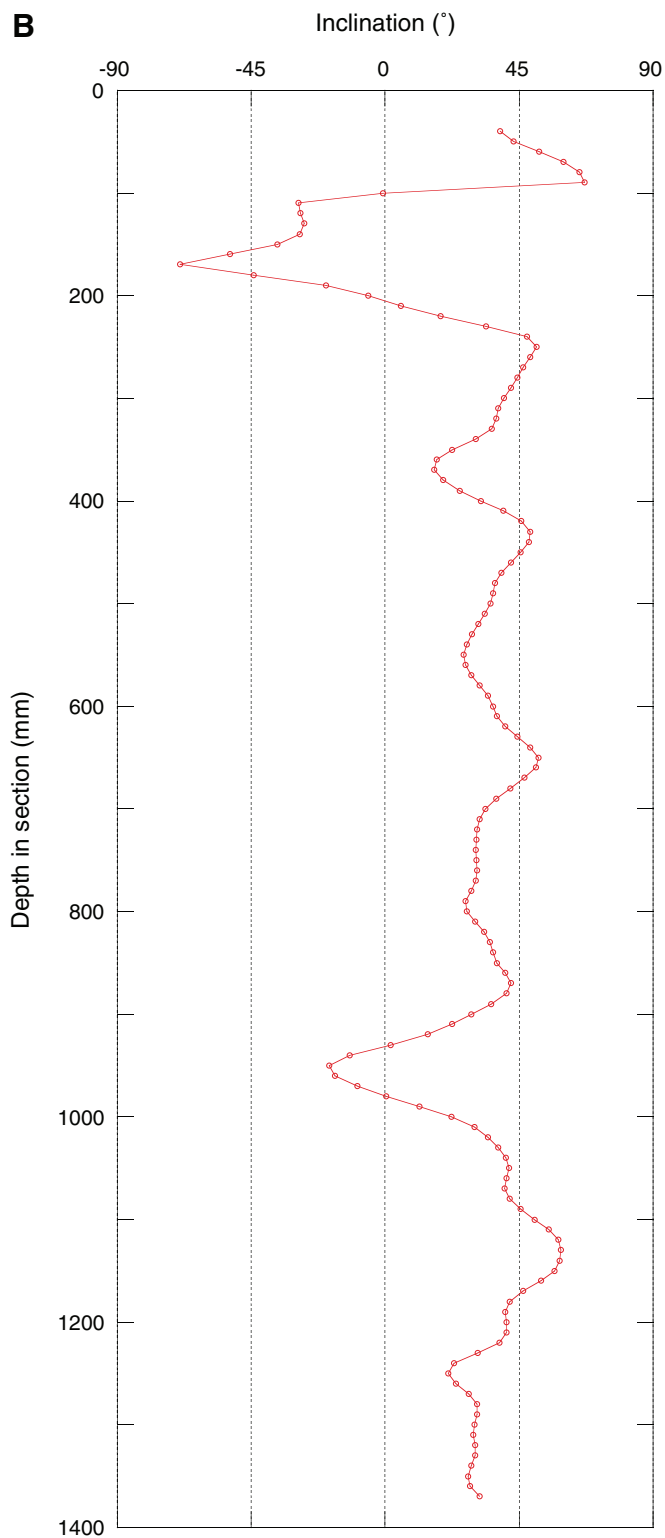


Figure F23 (continued). C. Declination. (Continued on next page.)

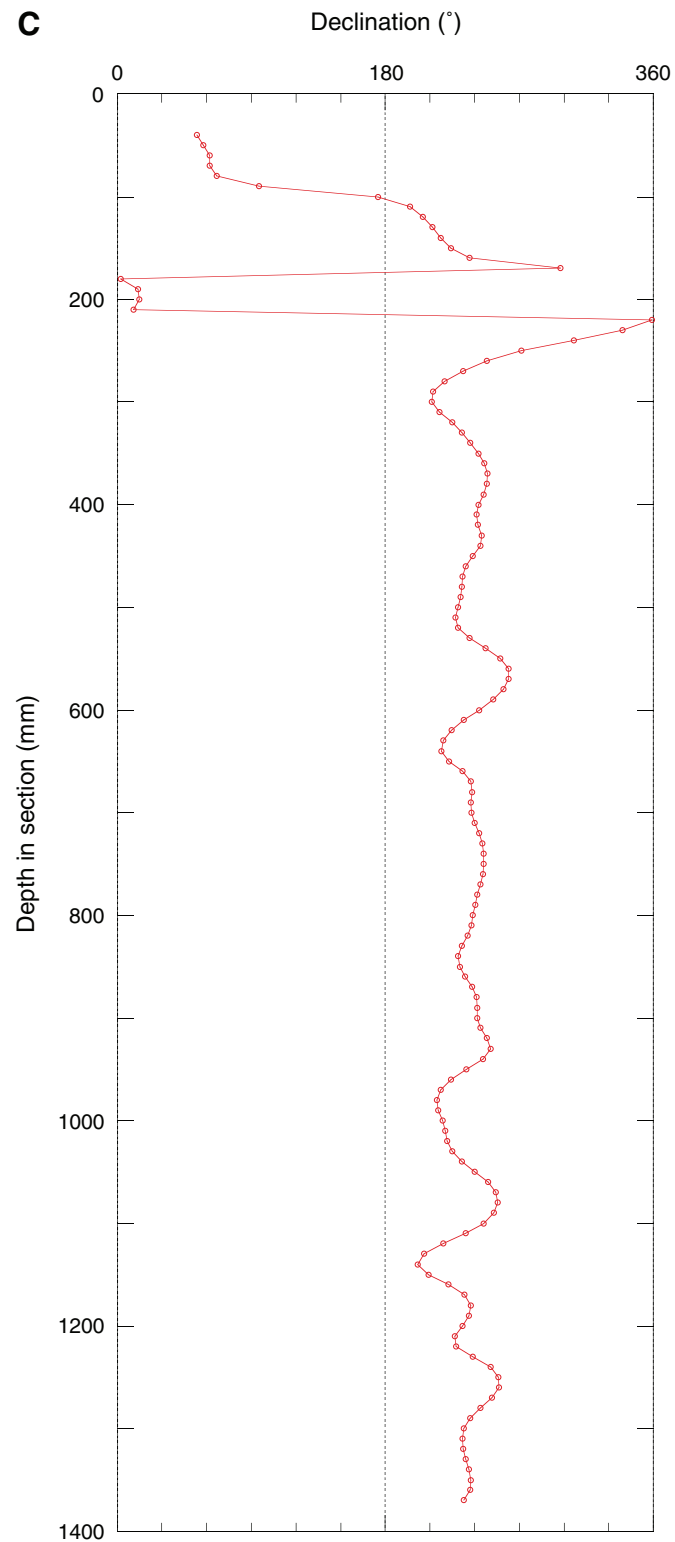


Figure F23 (continued). D. Anhyysteretic Remanent Magnetization (ARM) for the same U-channel. 4 cm measurements have been removed at the beginning and end of the U-channel to avoid the influence of edge effects.

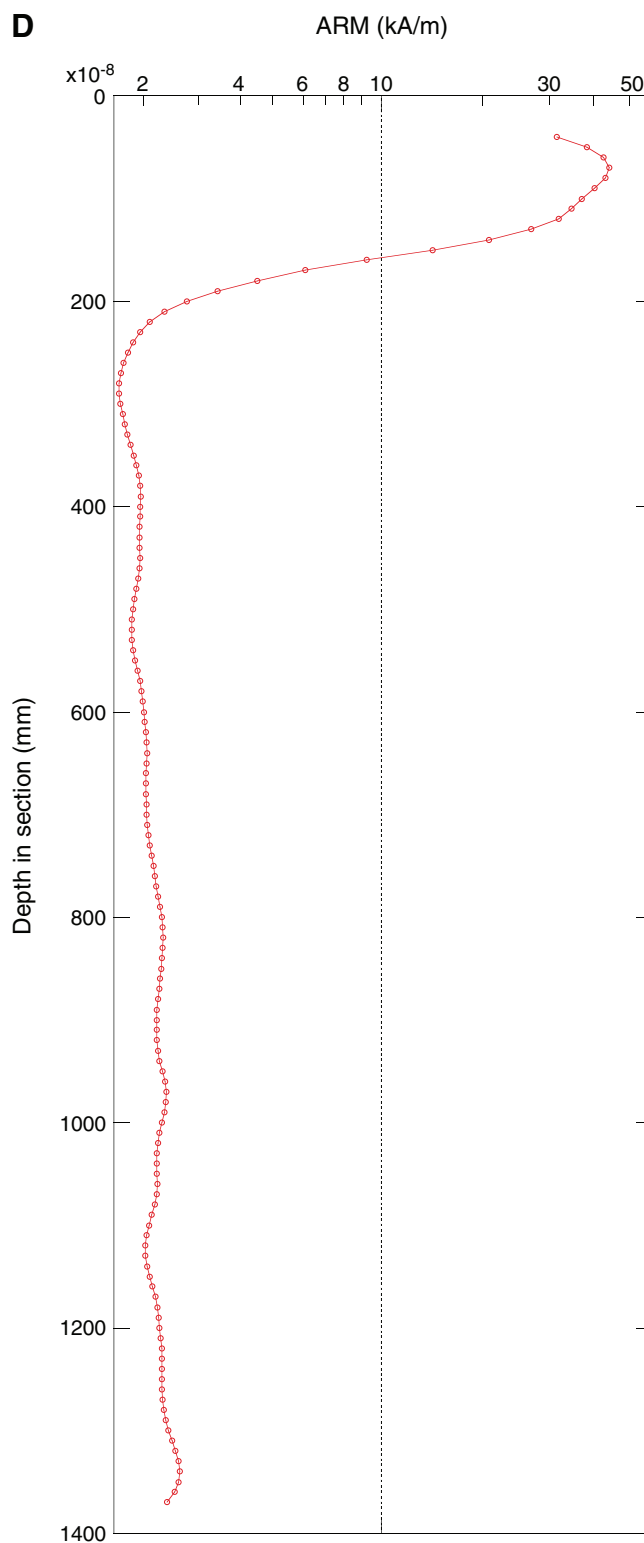


Figure F24. Orthogonal plots of the vector decay on AF demagnetization for four specimens located along the sampled U-channel. The example at 15 cm shows a low remagnetization easily removed at 5 mT and then a simple univectorial decay toward the origin with stable geomagnetic behavior. The examples at 21, 72 and 131 cm show no decay toward the origin but instead toward the southern hemisphere (reverse magnetization) with increased intensities. This characteristic depends from the fact that the AF is not able to demagnetize the material. An alternative explanation can be related to the presence of a strong drilling overprinting which remagnetized the weak magnetic component. NRM = natural remanent magnetization. A. Sample 325-M0041A-12R-1, 15 cm. (Continued on next three pages.)

A Sample 325-M0041A-12R-1, 15 cm

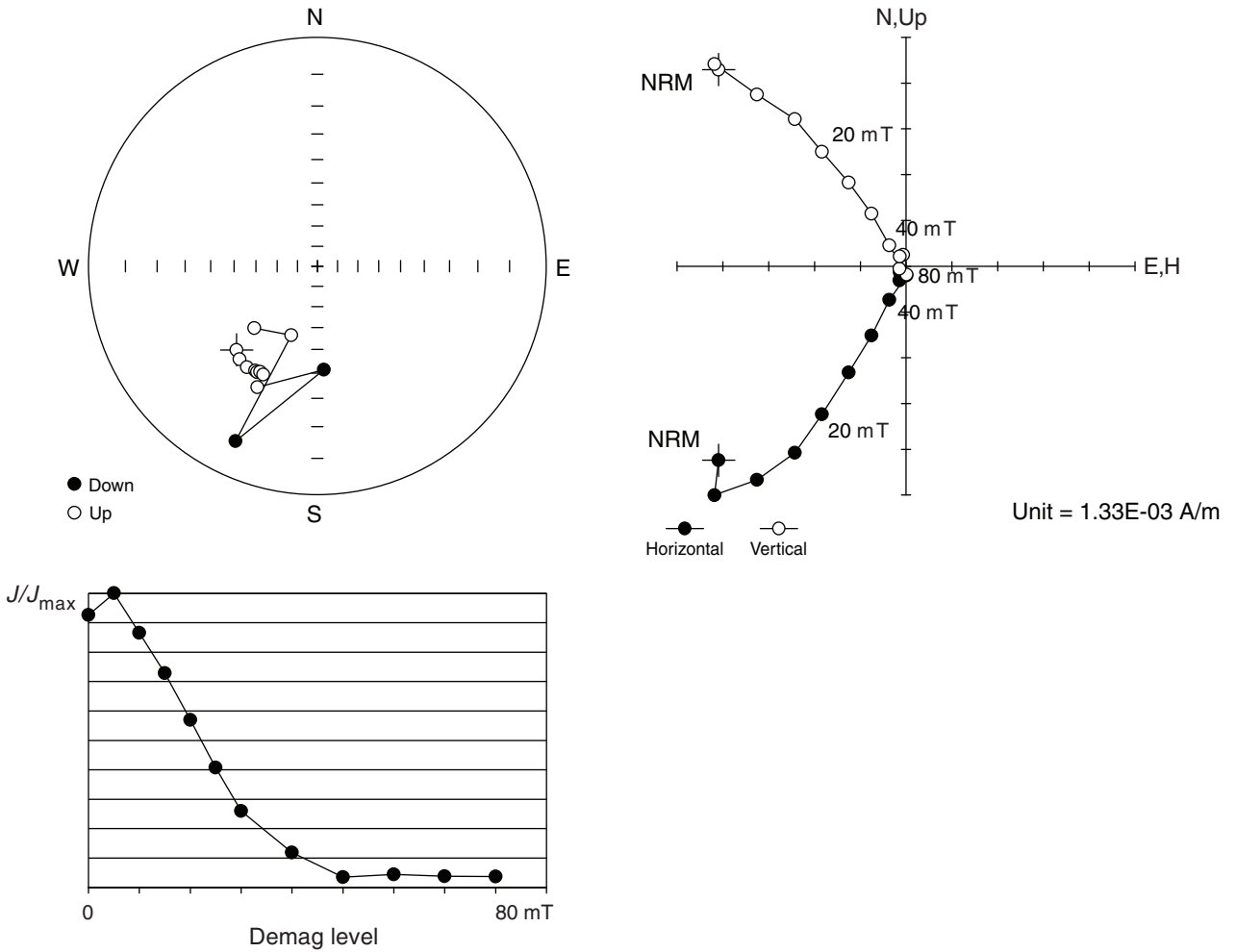


Figure F24 (continued). B. Sample 325-M0041A-12R-1, 21 cm. (Continued on next page.)

B Sample 325-M0041A-12R-1, 21 cm

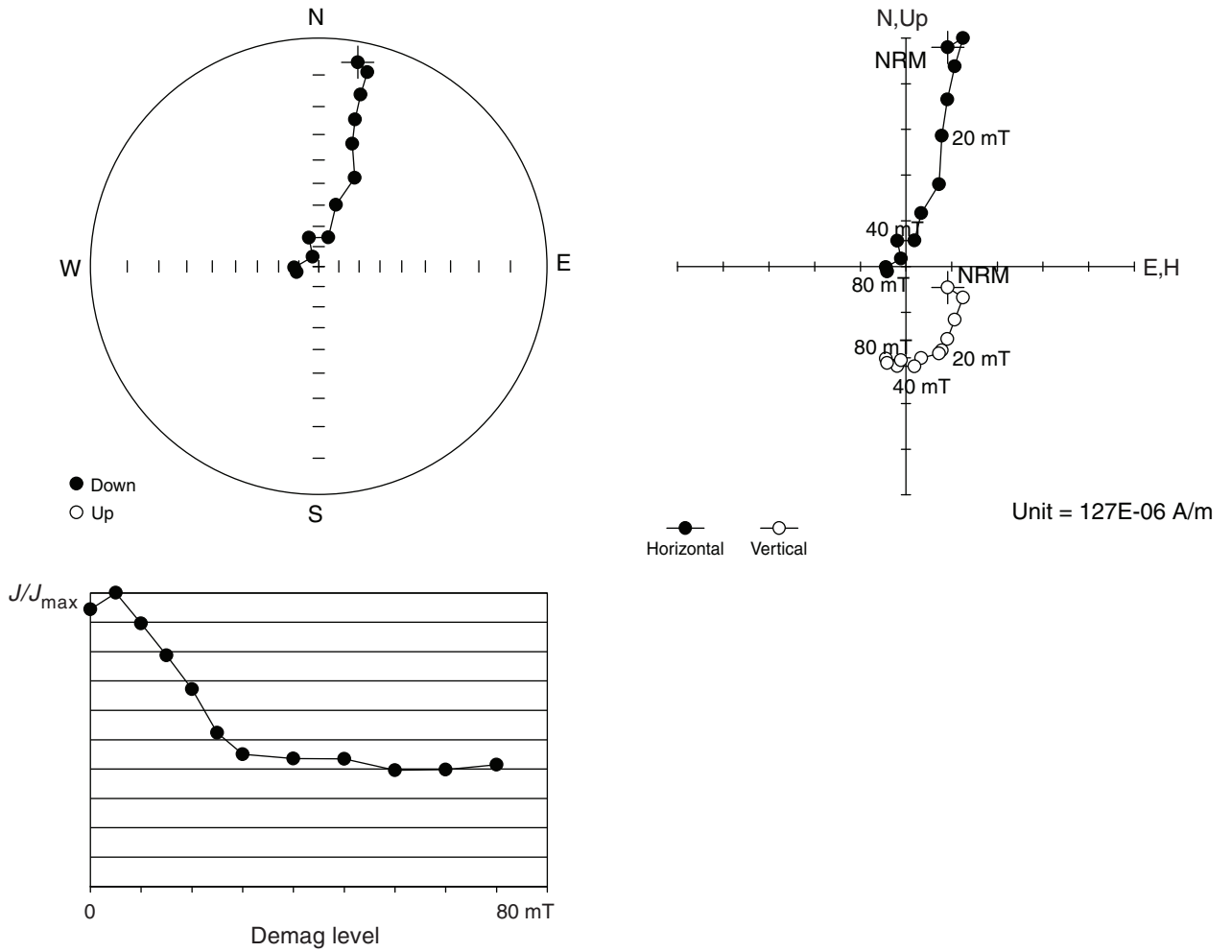


Figure F24 (continued). C. Sample 325-M0041A-12R-1, 72 cm. (Continued on next page.)

C Sample 325-M0041A-12R-1, 72 cm

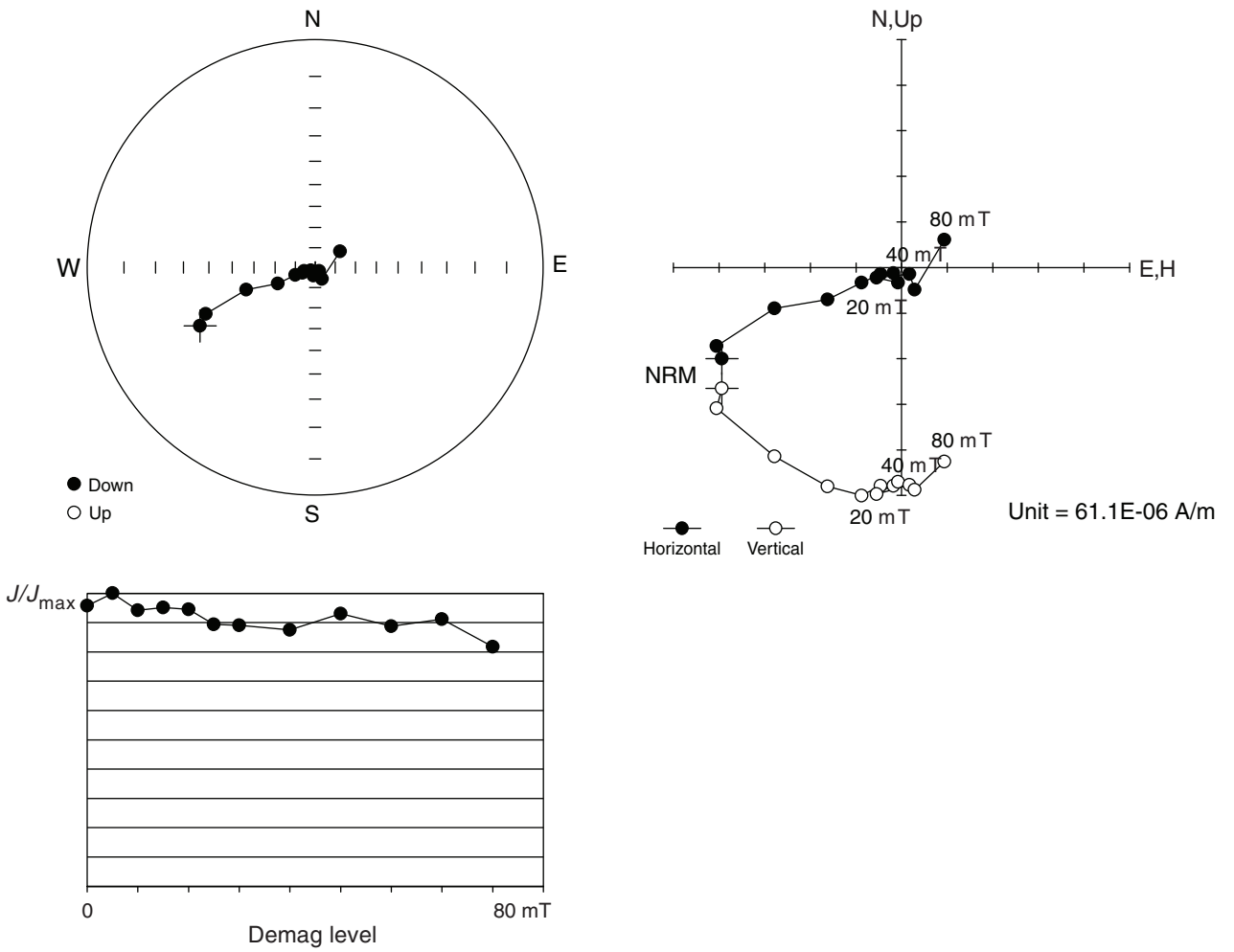


Figure F24 (continued). D. Sample 325-M0041A-12R-1, 131 cm.

D Sample 325-M0041A-12R-1, 131 cm

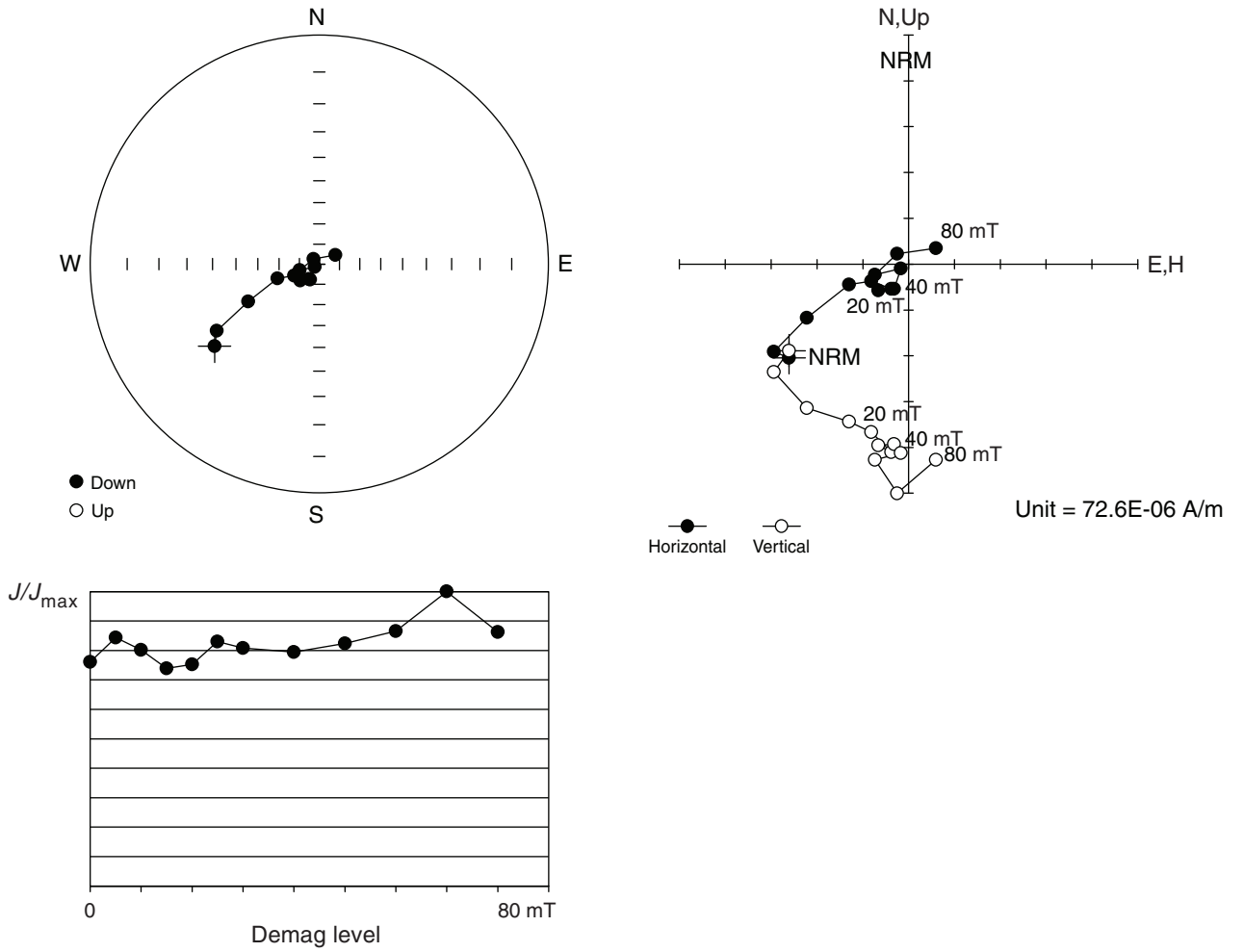


Figure F25. Preliminary chronology for Hole M0041A. Radiocarbon data are presented as graphs with the uncalibrated radiocarbon age and uncertainty shown as the red normal distribution on the ordinate axis and the probability distribution of the calibrated age shown in gray on the abscissa. The marine09 calibration curve is shown in blue. Horizontal bars indicate portions of the age distribution that are significant at the 95.4% confidence interval and the mean age (white circle ± 1 standard deviation) used for the purposes of preliminary dating. All ages are presented as thousands of calendar years BP (1950 AD). See Table T10 in the “Methods” chapter. (See Bronk Ramsey [2009], as well as Bronk Ramsey [2010] at c14.arch.ox.ac.uk/oxcal.html.)

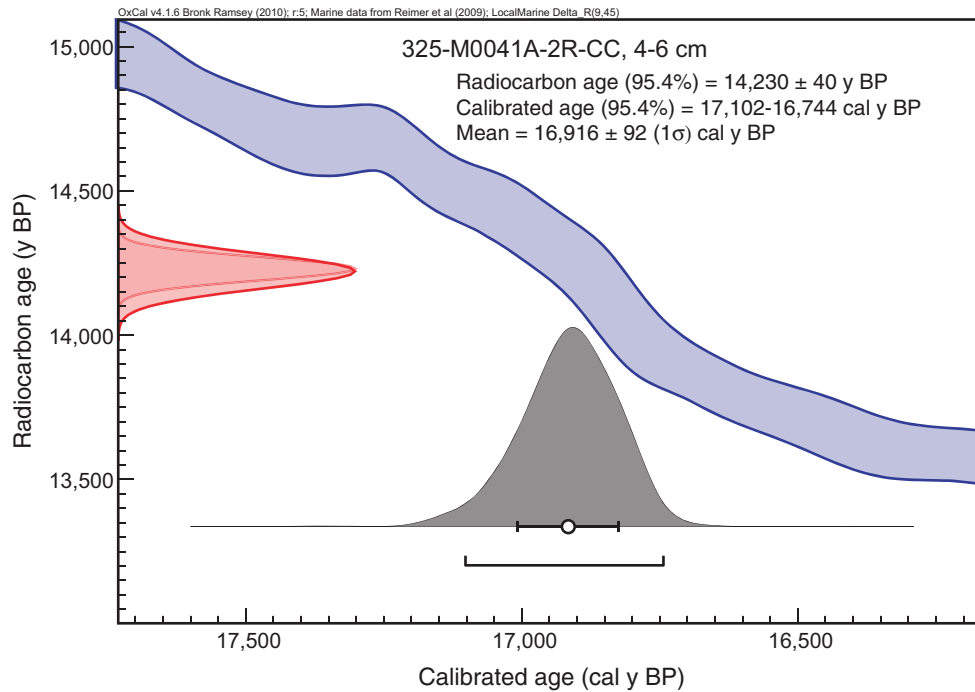


Figure F26. High-resolution line scan image of corallal boundstone fragments with minor microbialites and internal sediment (broken during coring) (interval 325-M0042A-2R-1, 5–13 cm). A coralline algal crust caps the top of the interval, encrusting a submassive *Porites* or *Montipora*. The “reddish” surface may indicate subaerial exposure and a break in reef growth.

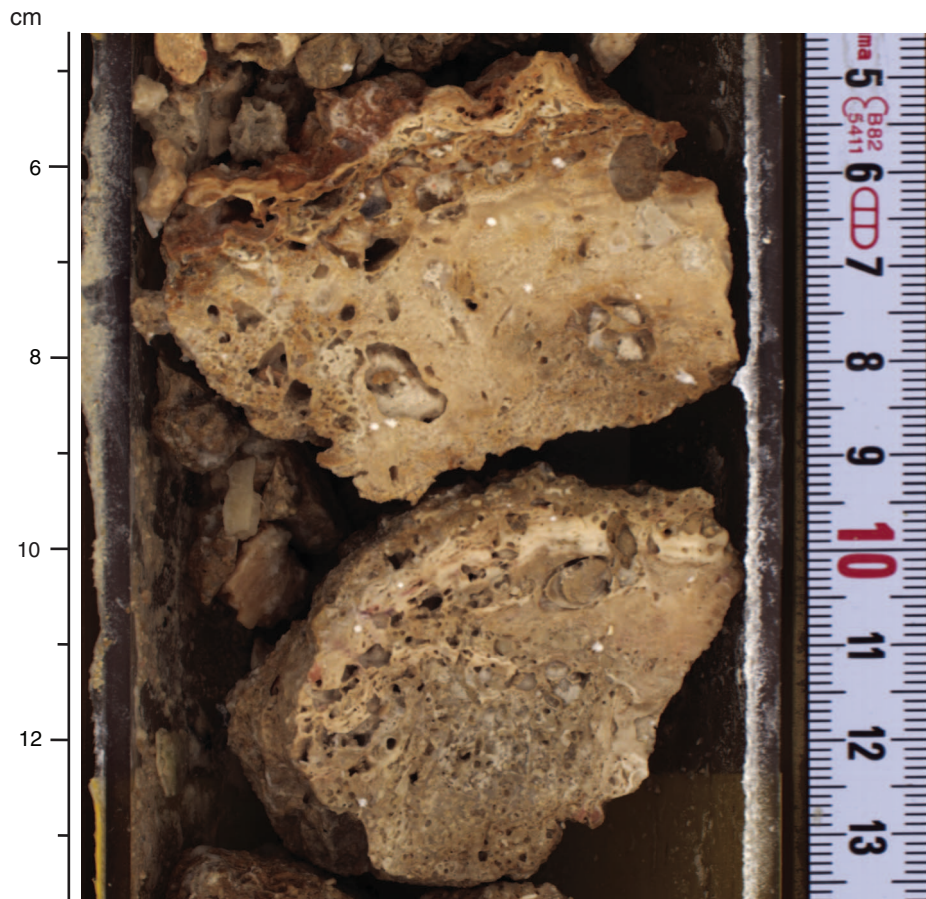


Figure F27. High-resolution line scan image of a massive *Acropora* with a thick coralline algal crust and thick microbialite (interval 325-M0042A-4R-1, 63–82 cm).



Figure F28. High-resolution line scan image of a medium to robustly branching *Acropora* (in situ) (interval 325-M0042A-4R-1, 0–21 cm). The coral framework is bored, and its surface encrusted by coralline algae.

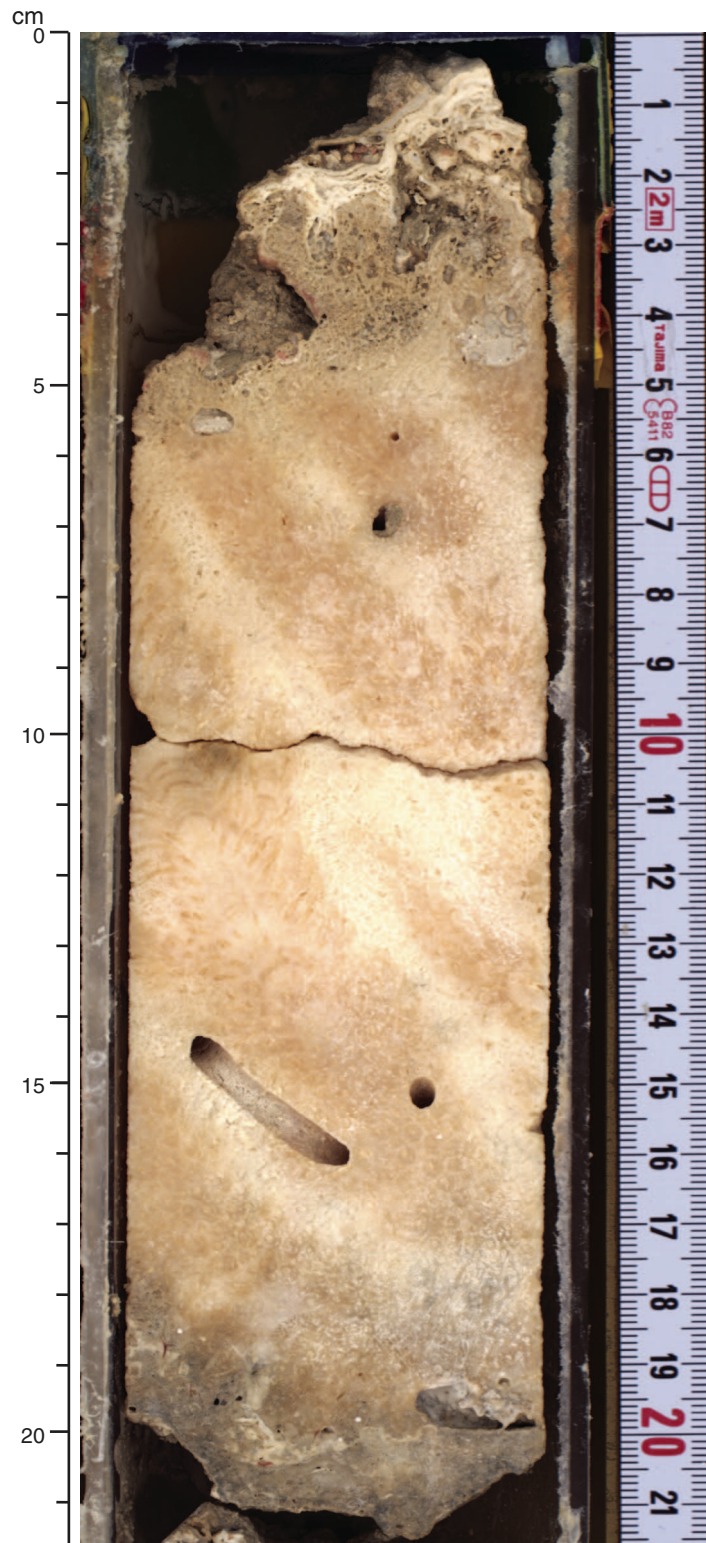


Figure F29. High-resolution line scan image of the transition between a massive *Isopora* boundstone (top) and a grainstone to rudstone rich in larger foraminifera, *Halimeda*, mollusk fragments, and a few pieces of fine branching *Seriatopora* (interval 325-M0042A-11R-1, 13–33 cm).

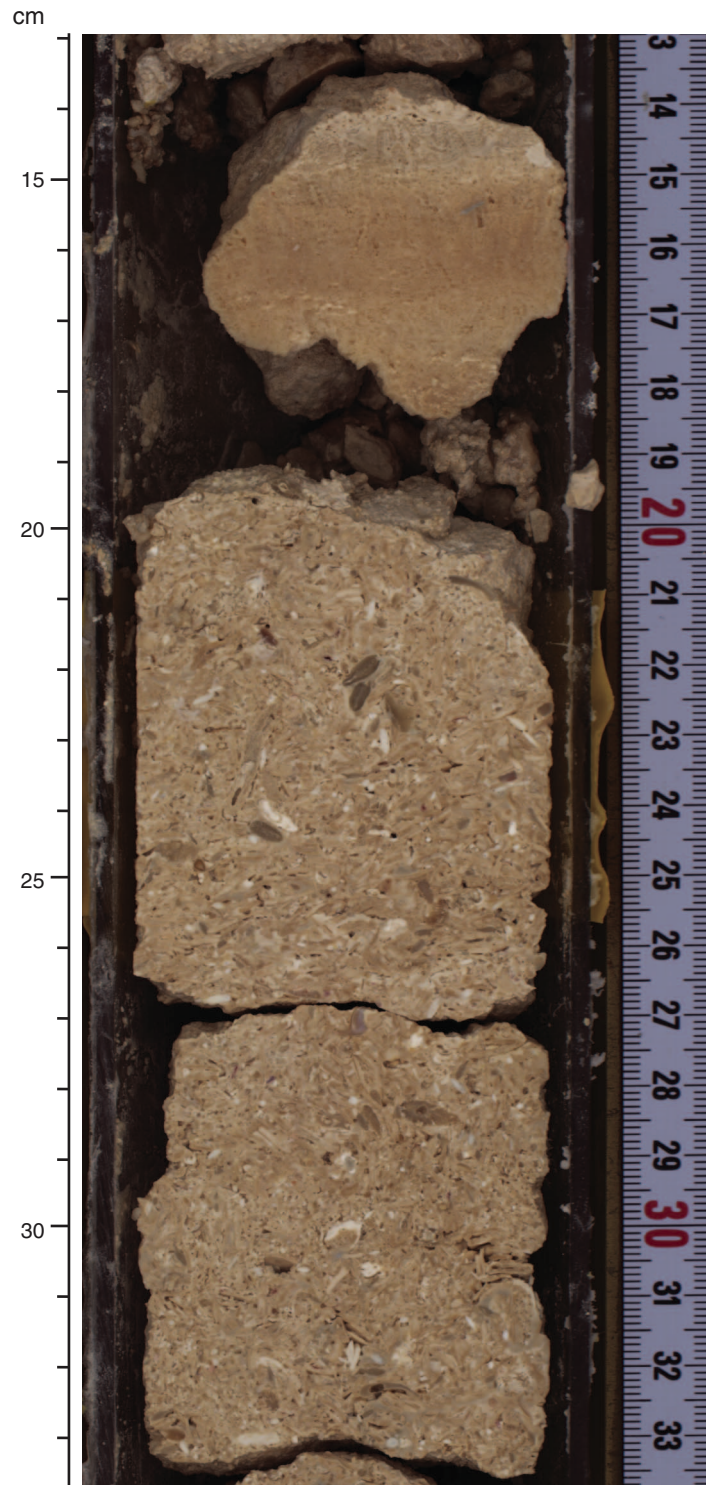


Figure F30. High-resolution line scan image of a rudstone with larger foraminifera, dissolved *Halimeda*, and fine branching *Acropora*(?) (interval 325-M0042A-21R-1, 13–16 cm). Original aragonitic components are partly dissolved.



Figure F31. High-resolution line scan image of a grainstone to rudstone with rhodoliths, dissolved coral fragments, bivalves, *Halimeda*, and larger foraminifera (interval 325-M0042A-23R-1, 9–39 cm). The brown staining at the top may indicate a paleosol.

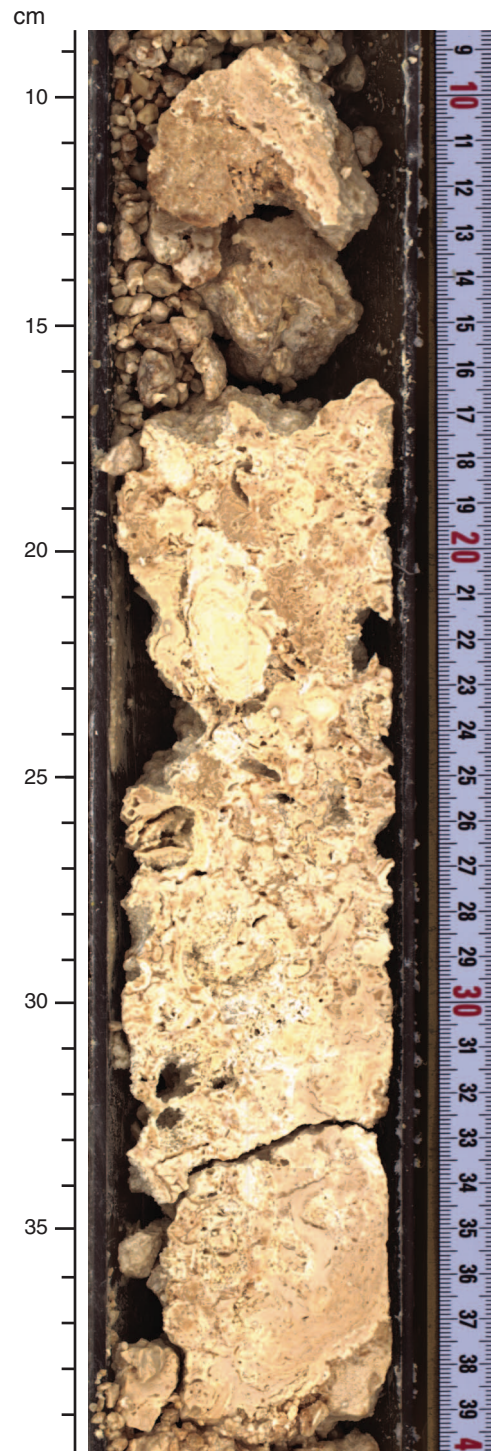


Figure F32. High-resolution line scan image of a grainstone to rudstone with large (>7 cm) rhodoliths, dissolved coral fragments, bivalves, *Halimeda*, and larger foraminifera, with dissolution of aragonite components and brown staining (interval 325-M0042A-24R-1, 7–16 cm).



Figure F33. High-resolution line scan image of a grainstone to rudstone with rhodoliths, dissolved coral fragments, bivalves, *Halimeda*, and larger foraminifera (interval 325-M0042A-25R-1, 31–37 cm).



Figure F34. High-resolution line scan image of a rudstone with partially dissolved *Halimeda* segments, coralline algae, larger foraminifera, and mollusks (interval 325-M0042A-27R-CC, 6–13 cm).



Figure F35. High-resolution line scan image of a grainstone to rudstone with rhodoliths, dissolved coral fragments, bivalves, *Halimeda*, and larger foraminifera (interval 325-M0042A-25R-1, 0–13 cm). The brown staining at the top may indicate a paleosol.

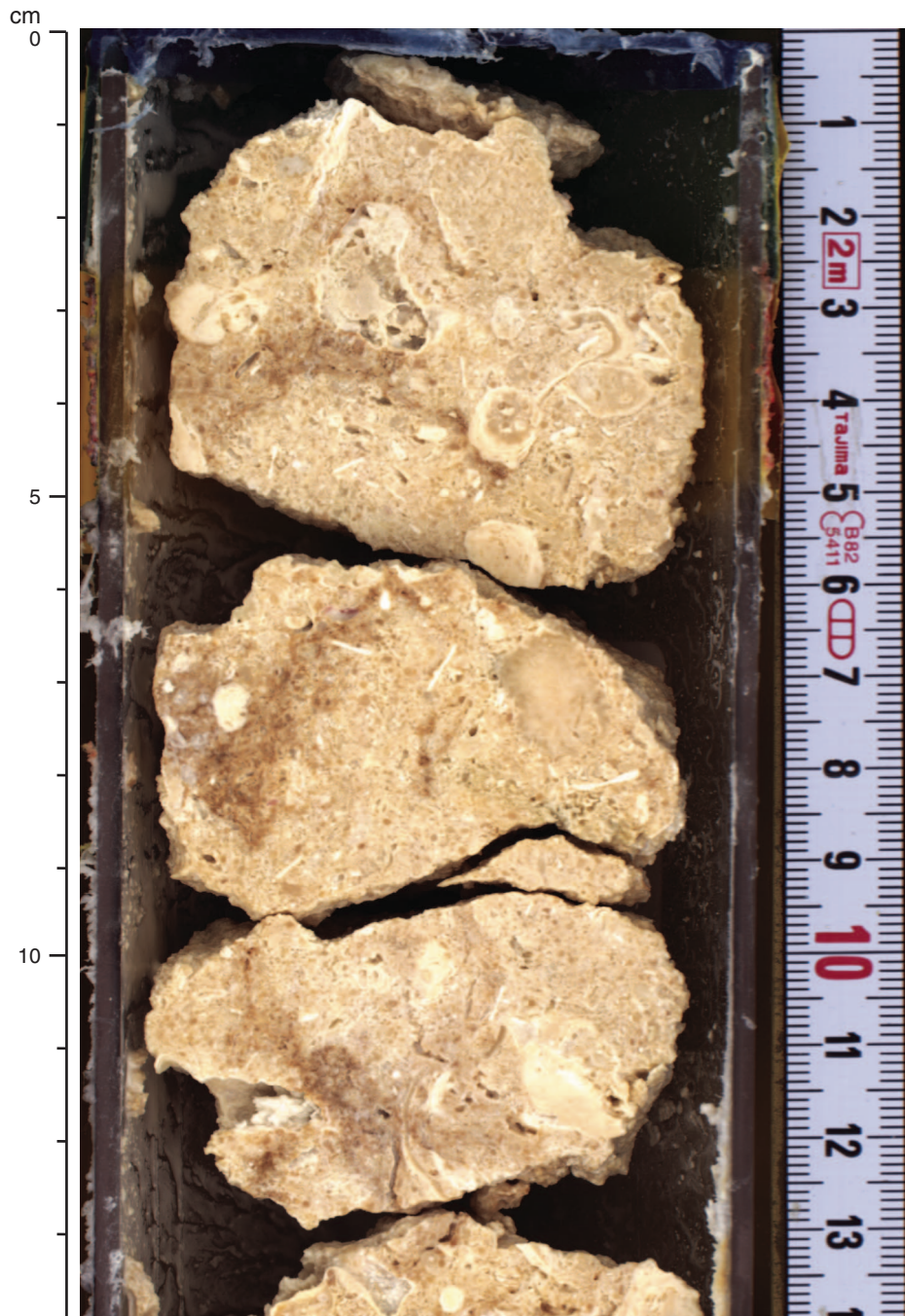


Figure F36. High-resolution line scan image of a grainstone to rudstone with rhodoliths, dissolved coral fragments, bivalves, *Halimeda*, and larger foraminifera (interval 325-M0042A-25R-1, 53–59 cm). The brown staining at the top may indicate a paleosol. There is also a possible root trace in the lower right of the image.



Figure F37. High-resolution line scan image of a rudstone with large coral fragments (massive *Acroporidae* or *Poritidae*(?)), partially dissolved coralline algae, and *Halimeda* (interval 325-M0042A-28R-CC, 0–16 cm).



Figure F38. Summary diagram showing data collected on whole cores using the multisensor core logger (MSCL), Hole M0042A.

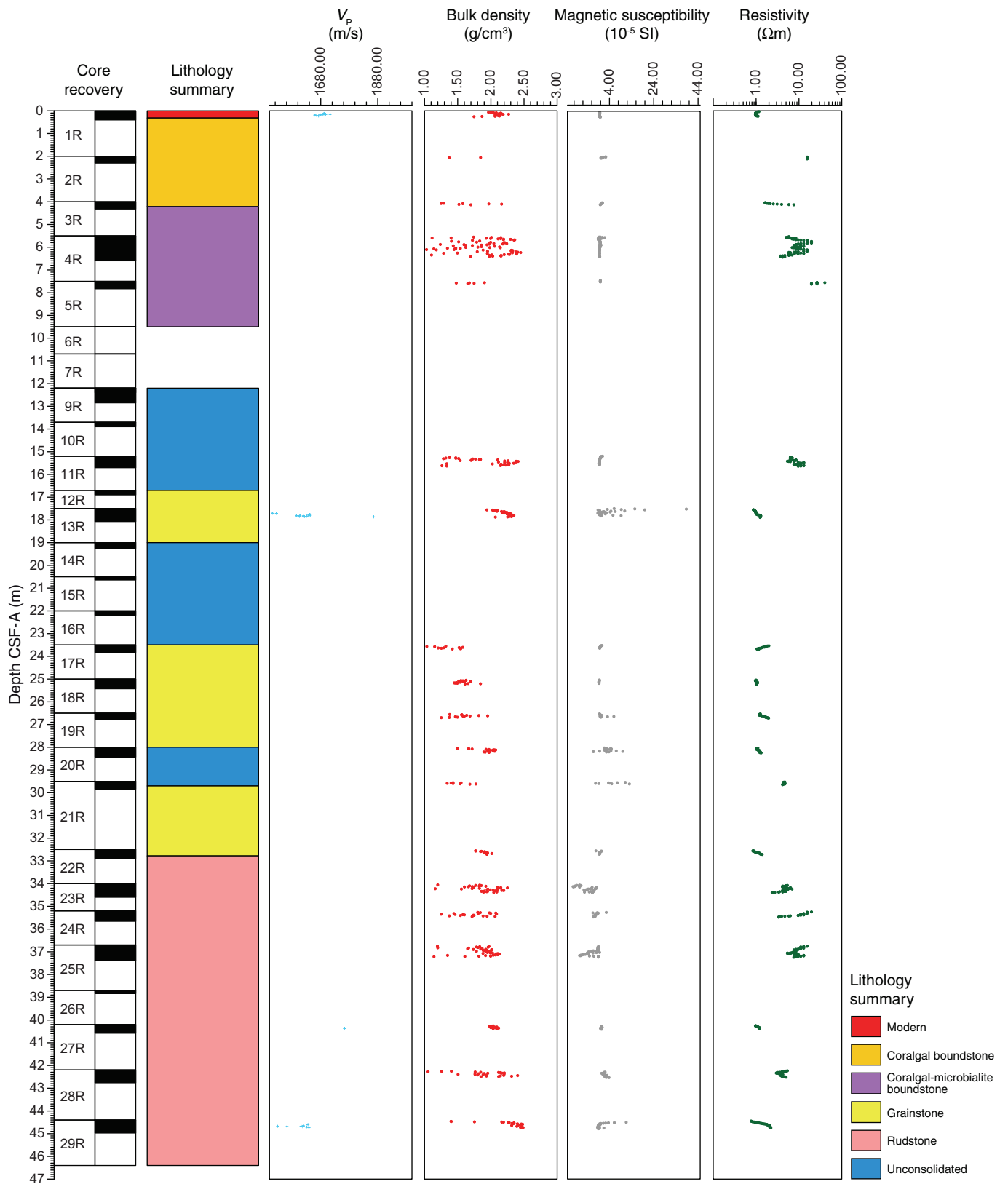


Figure F39. Petrophysical measurements obtained from discrete samples with a pycnometer, Hole M0042A. Bulk density measured on whole cores with the MSCL is shown in red on the bulk density plot.

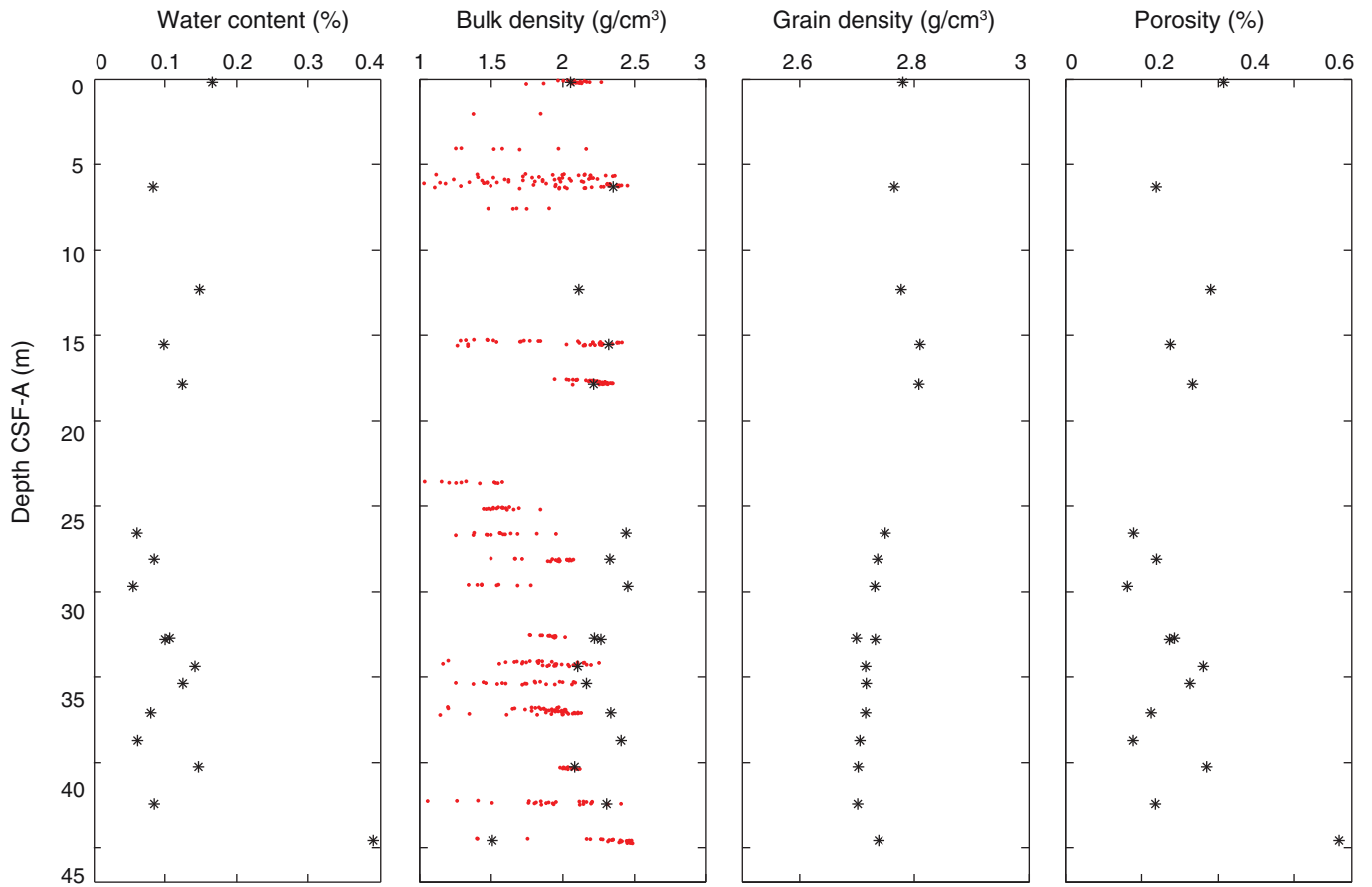


Figure F40. *P*-wave velocity data, Hole M0042A. **A.** Plot of initial, dry, and resaturated *P*-wave velocity measurements on discrete samples vs. depth. Three measurements were taken at each depth and are denoted by a dot. Average values are plotted as an open triangle. **B.** Plot showing discrete *P*-wave velocity vs. discrete bulk density.

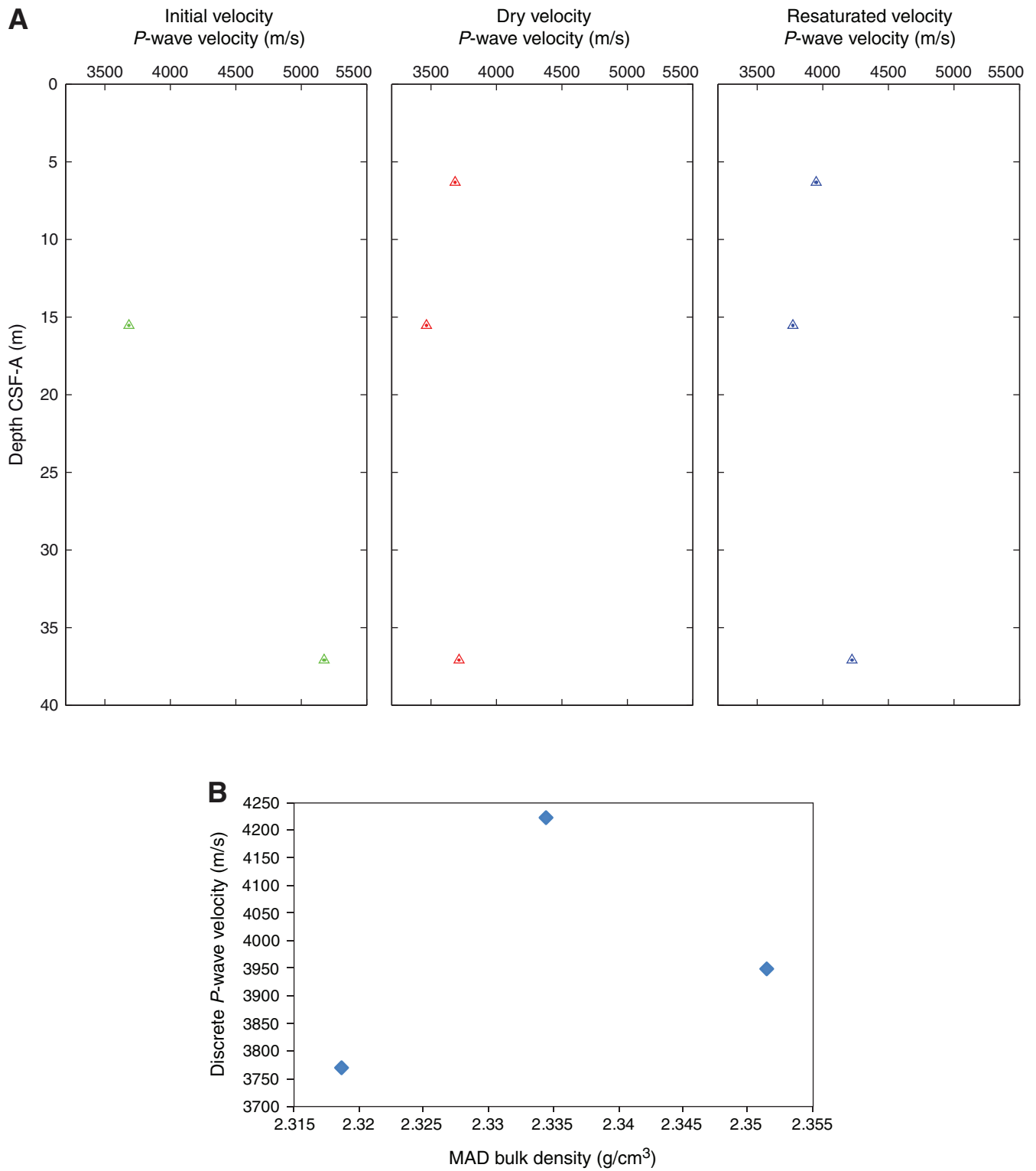


Figure F41. Values of reflectance (L^*), green to red (a^*), and blue to yellow (b^*) indexes, along with ratio a^*/b^* for Hole M0042A.

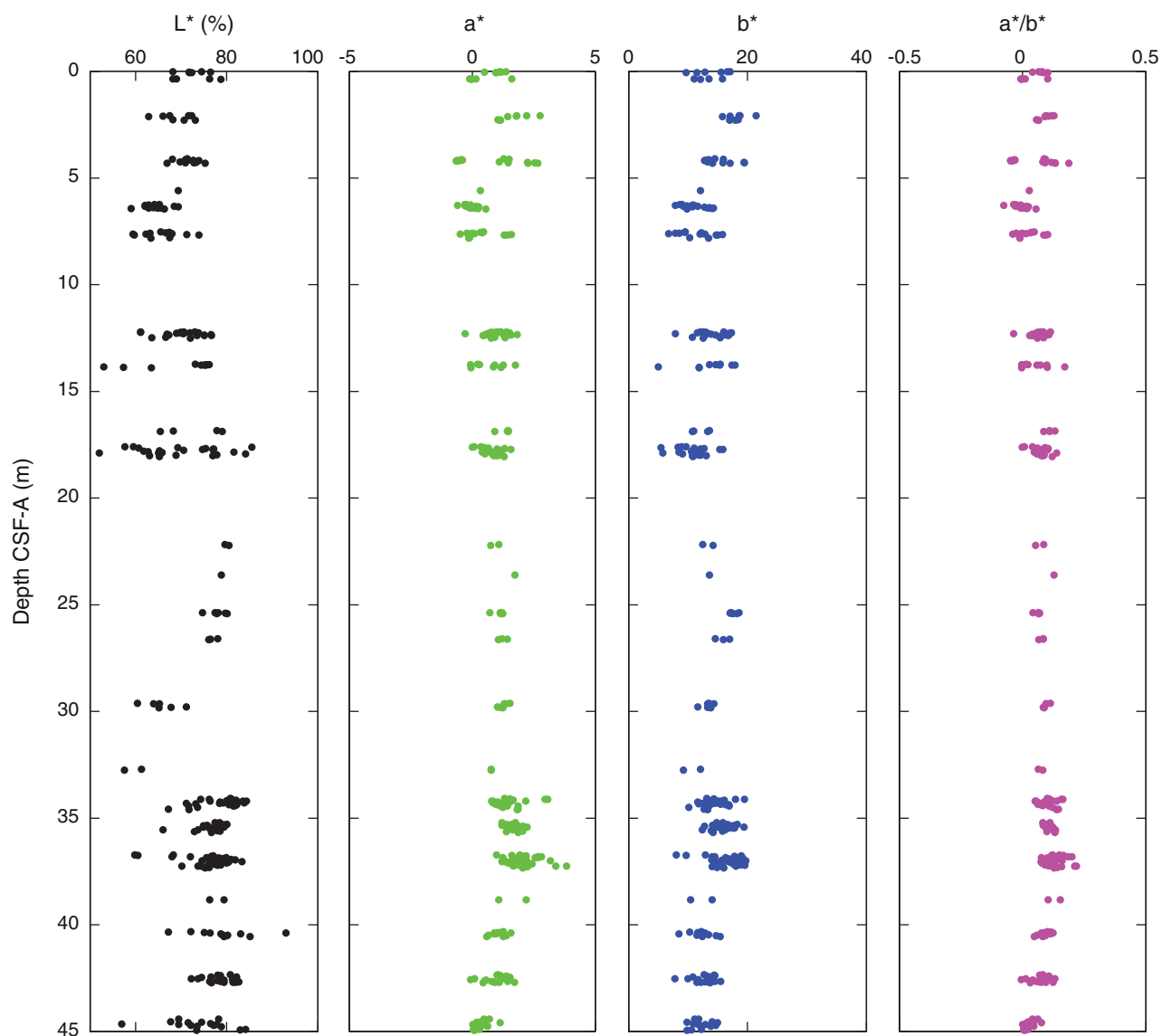


Figure F42. Magnetic susceptibility record for Hole M0042A. Water depth = 50.78 m (LAT).

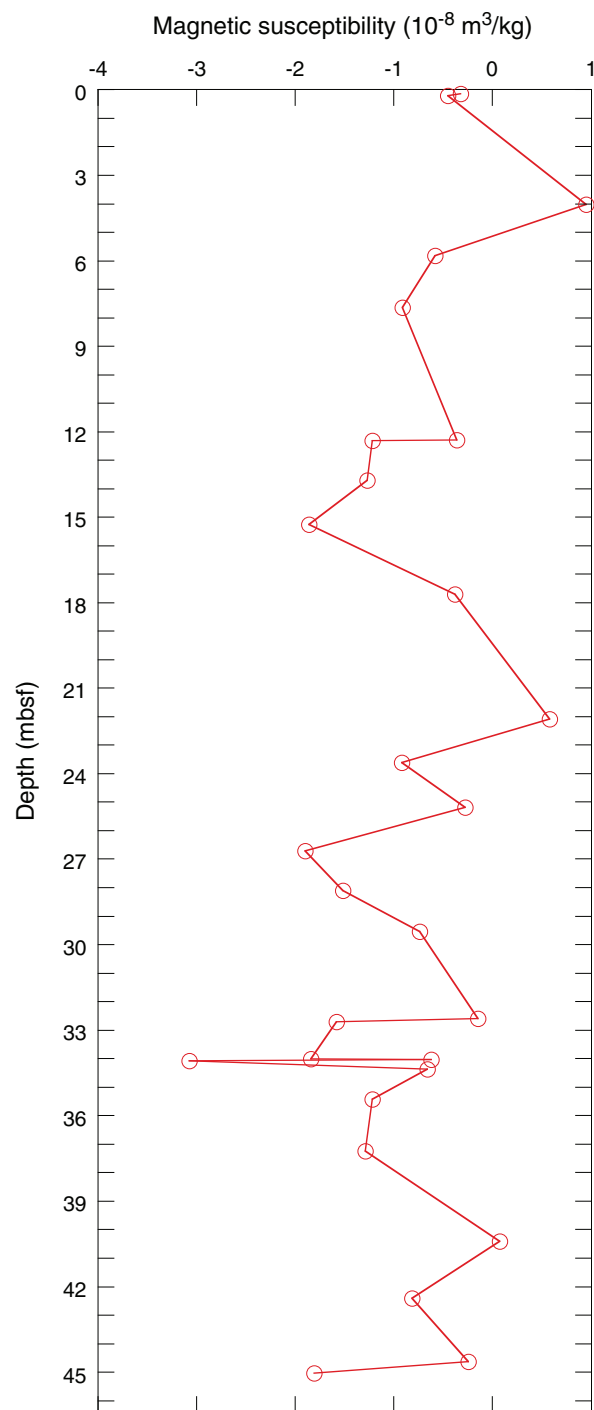


Figure F43. Preliminary chronology for Hole M0042A. Radiocarbon data are presented as graphs with the uncalibrated radiocarbon age and uncertainty shown as the red normal distribution on the ordinate axis and the probability distribution of the calibrated age shown in gray on the abscissa. The marine09 calibration curve is shown in blue. Horizontal bars indicate portions of the age distribution that are significant at the 95.4% confidence interval and the mean age (white circle ± 1 standard deviation) used for the purposes of preliminary dating. All ages are presented as thousands of calendar years BP (1950 AD). See Table T10 in the “Methods” chapter. (See Bronk Ramsey [2009], as well as Bronk Ramsey [2010] at c14.arch.ox.ac.uk/oxcal.html.)

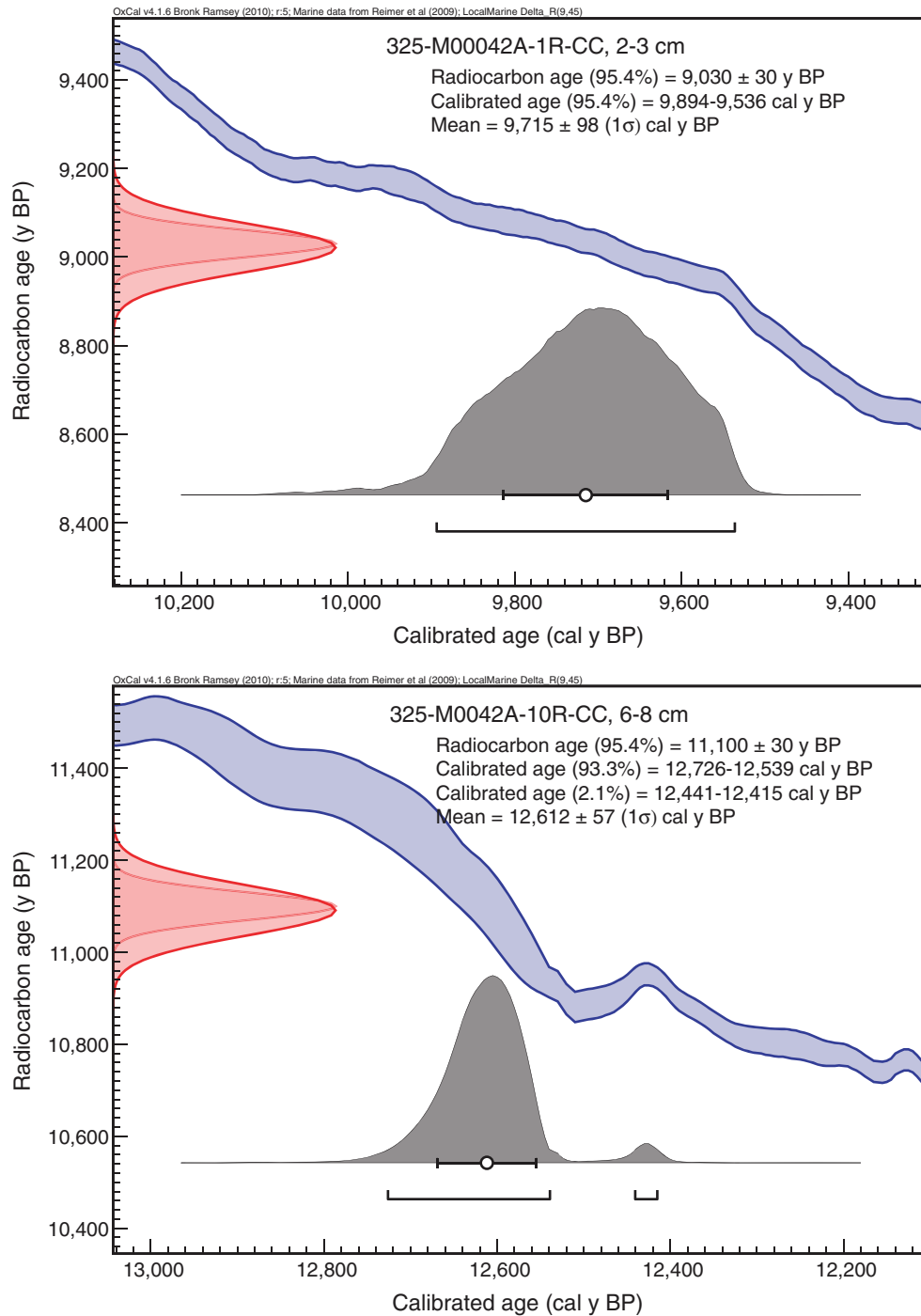


Figure F44. A. Composite showing all through-pipe logging data collected in Hole M0042A. TGR = total gamma ray (raw), TP = through-pipe. (This figure is also available in an **oversized format**.) (Continued on next four pages.)

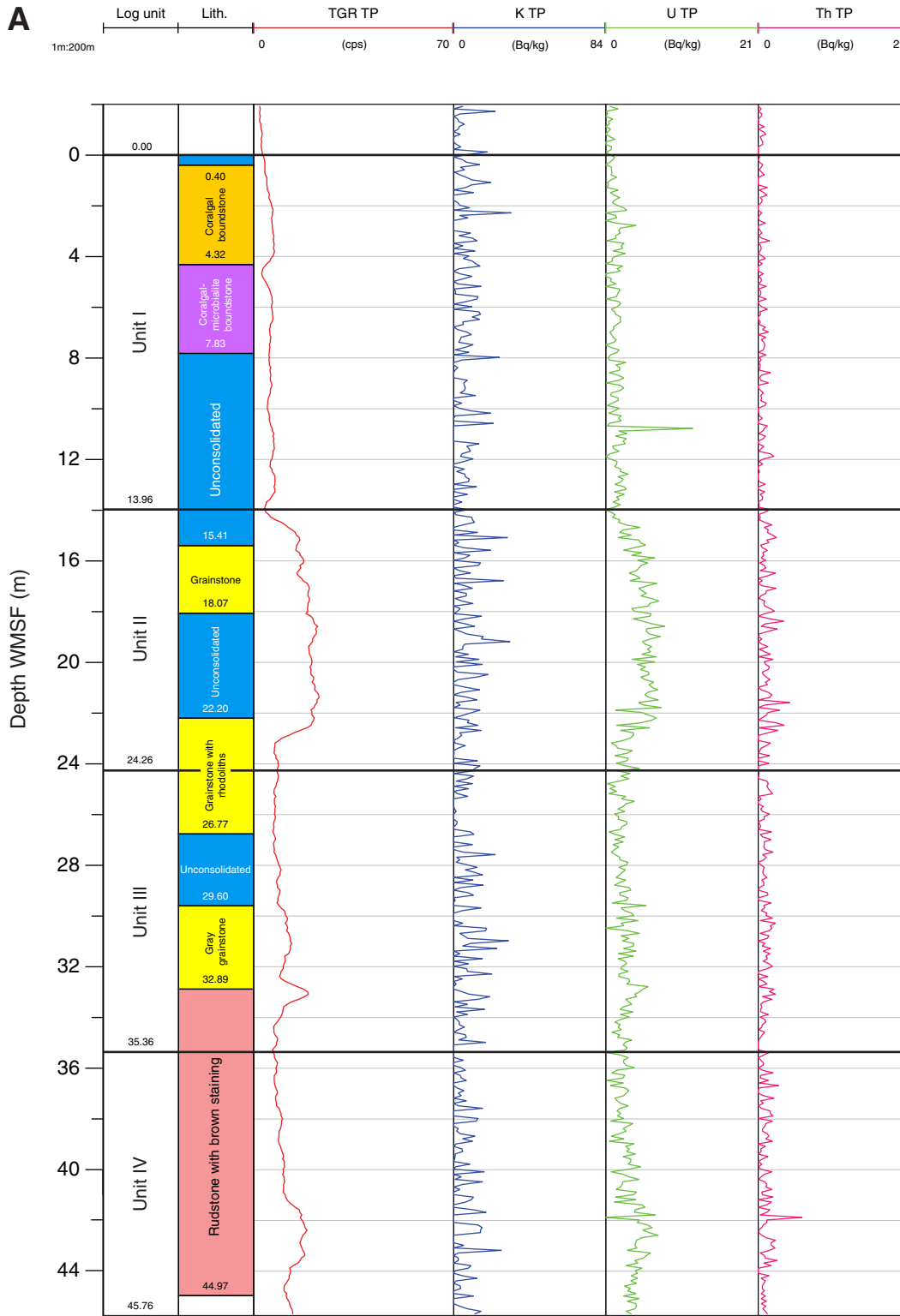


Figure F44 (continued). B. Composite showing conductivity and acoustic image logging data for Hole M0042A. ILD = deep conductivity, ILM = medium conductivity. (Continued on next page.)

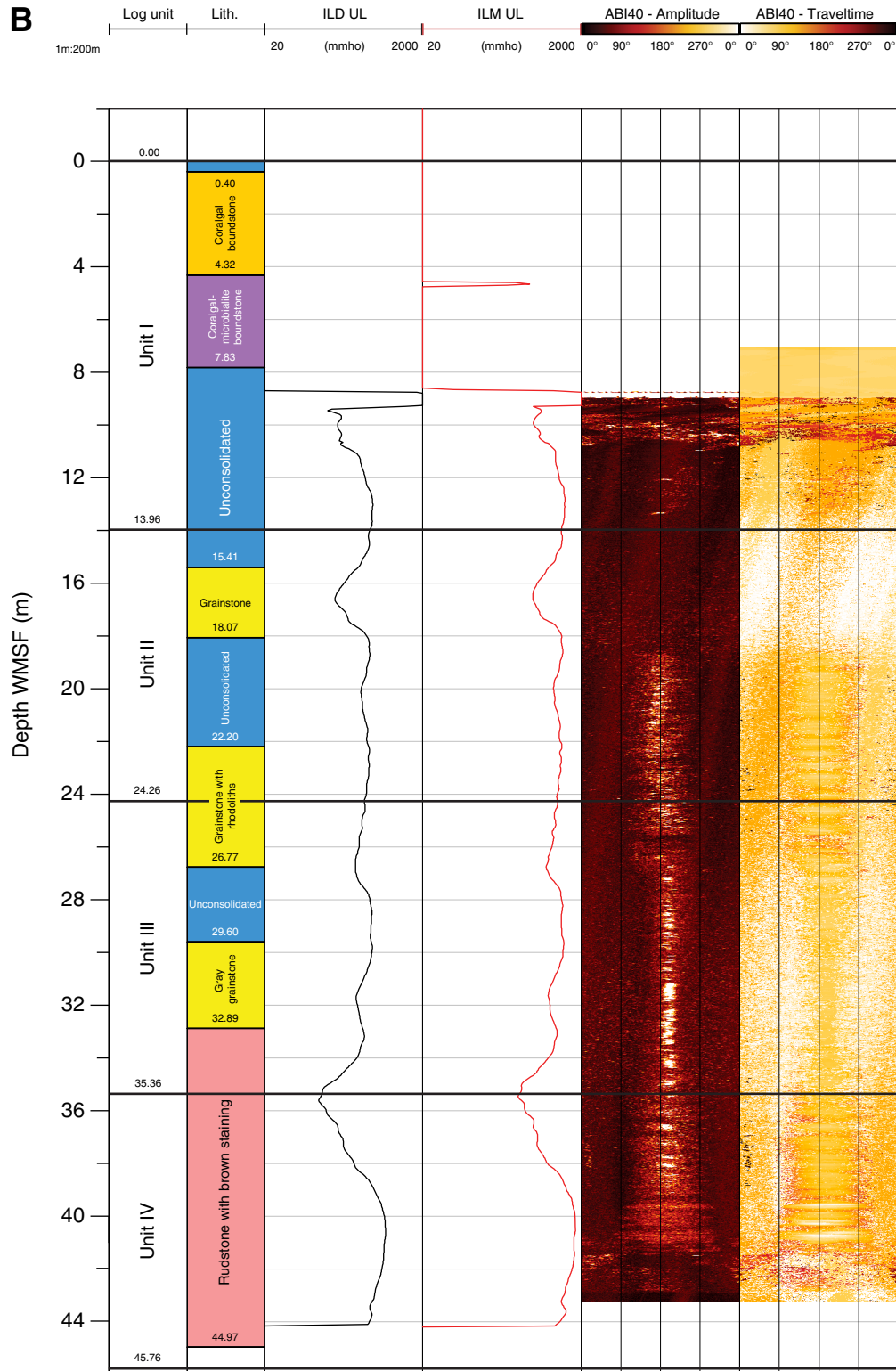


Figure F44 (continued). C. Composite showing open hole gamma logging data from Hole M0042A. TGR = total gamma ray (raw), OH = open hole. (Continued on next page.)

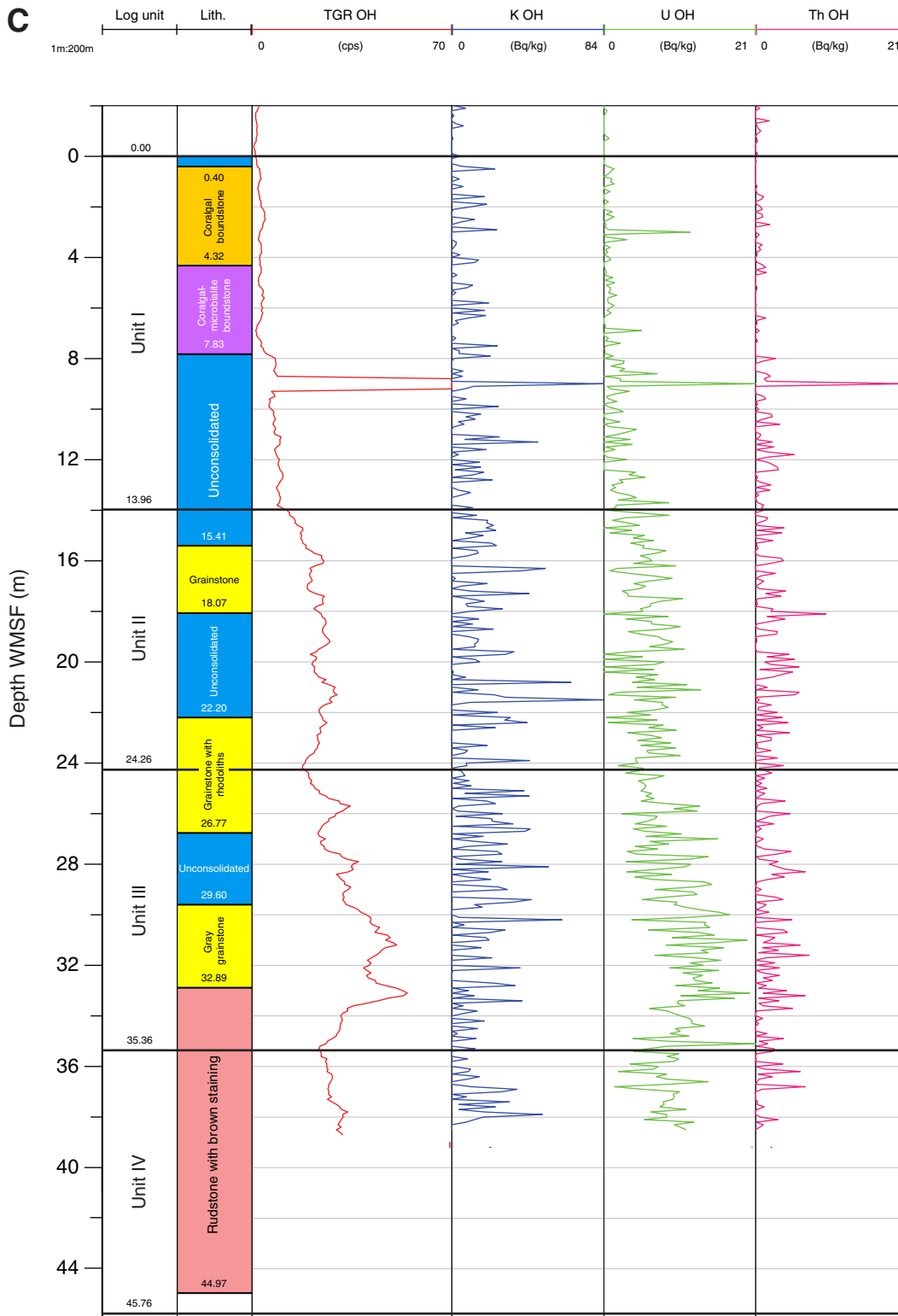


Figure F44 (continued). D. Composite showing EM51 and sonic logging data for Hole M0042A. IL = induction log, MSUS = magnetic susceptibility, RX1 = sonic waveforms for receiver 1, RX2 = sonic waveforms for receiver 2, V_p = P -wave velocity. (Continued on next page.)

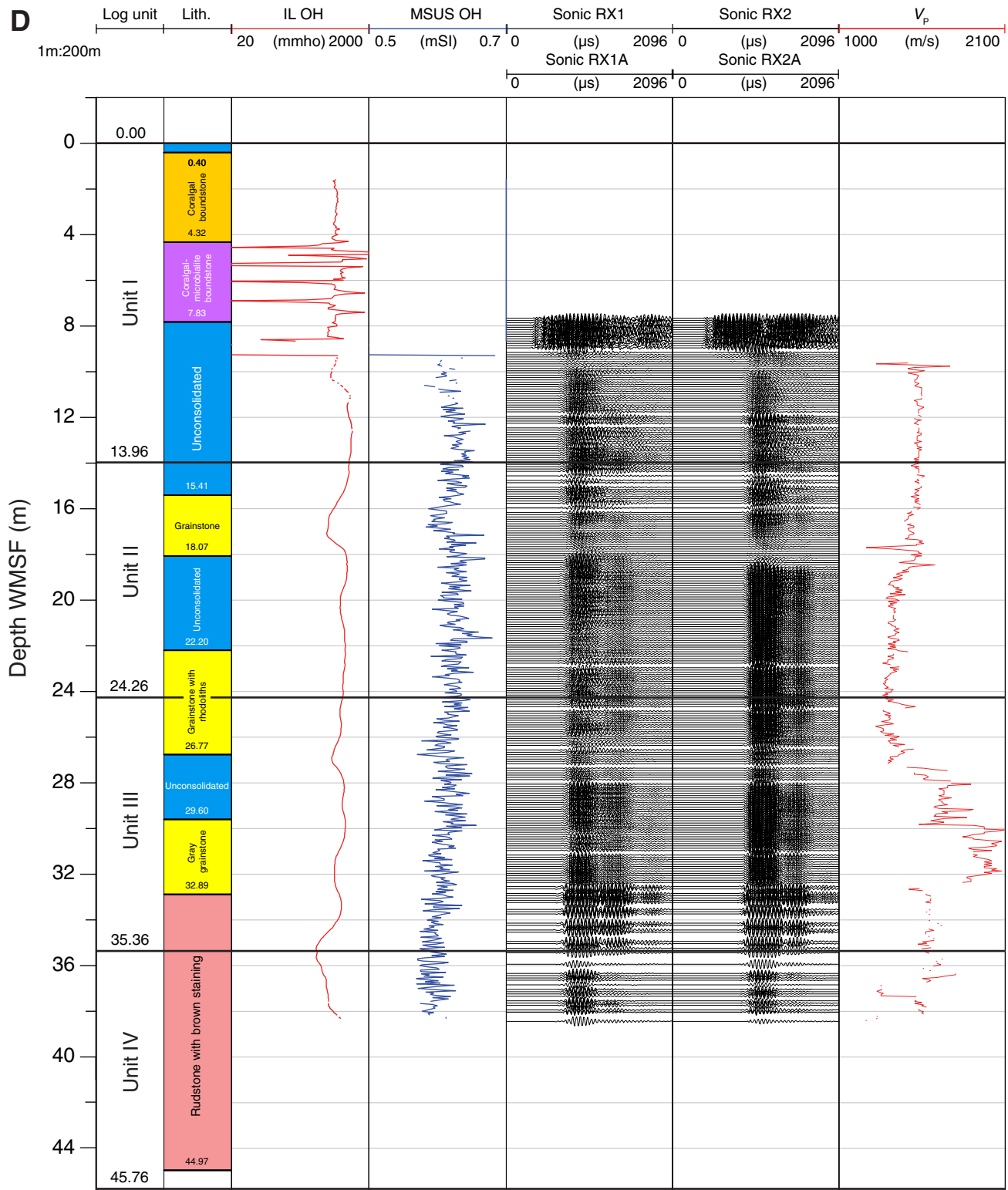


Figure F44 (continued). E. Composite showing optical image and borehole diameter logging data for Hole M0042A.

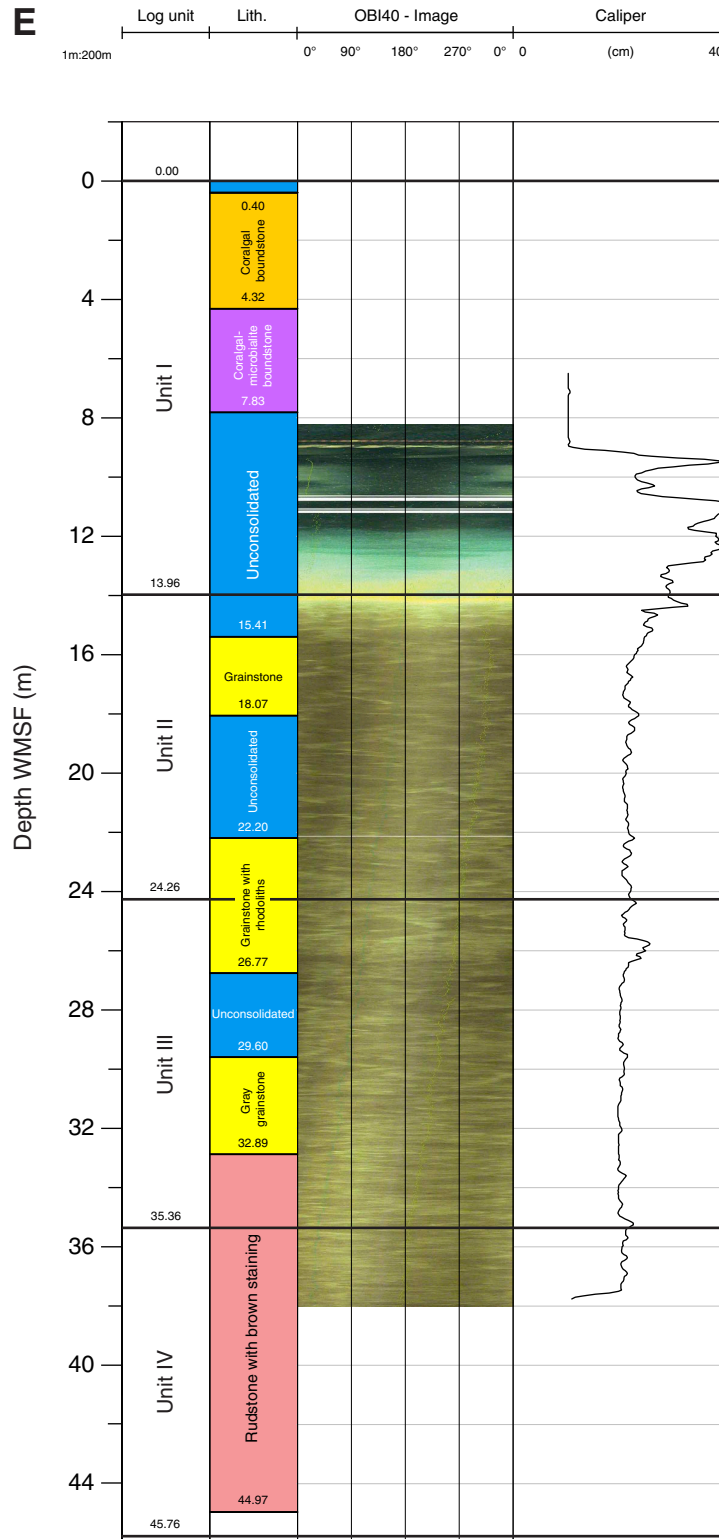


Figure F45. High-resolution line scan image of a broken coralgall boundstone with thin algal crusts (interval 325-M0043A-2R-1, 27–41 cm). Bioclasts include benthic foraminifera, *Halimeda*, and mollusks. Corals include submassive *Porites* and massive Faviidae.

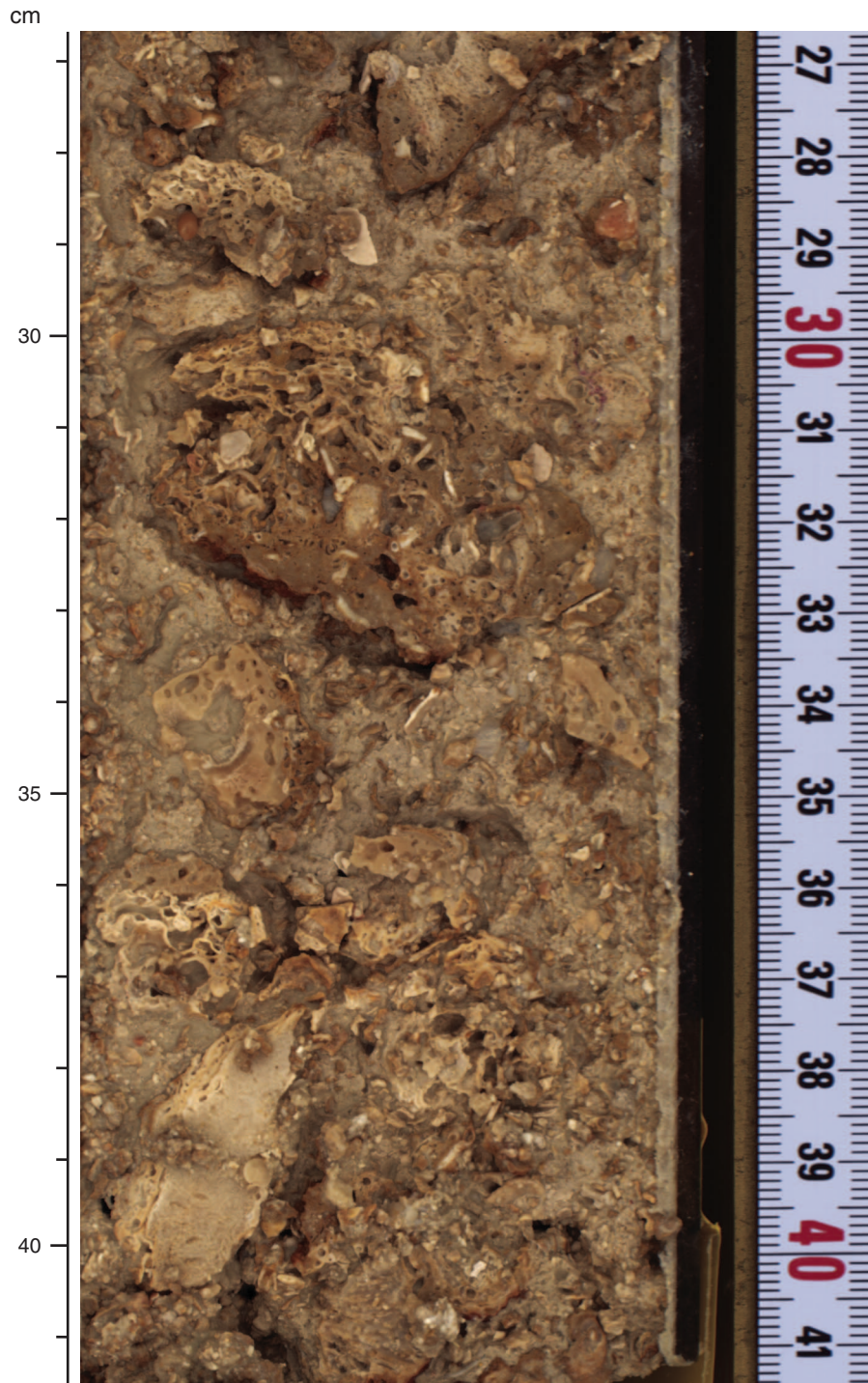


Figure F46. High-resolution line scan image of a coralline algal boundstone with bioclasts, including gastropod shells (interval 325-M0043A-1R-1, 9–16 cm).



Figure F47. High-resolution line scan image of a massive Faviidae encrusted by thick coralline algae and microbialites (interval 325-M0043A-11R-1, 32–38 cm).



Figure F48. High-resolution line scan image of a coralg-al-microbialite boundstone with fine branching *Seriatopora* and massive Acroporidae, encrusted by laminated microbialites (interval 325-M0043A-10R-1, 41–52 cm).

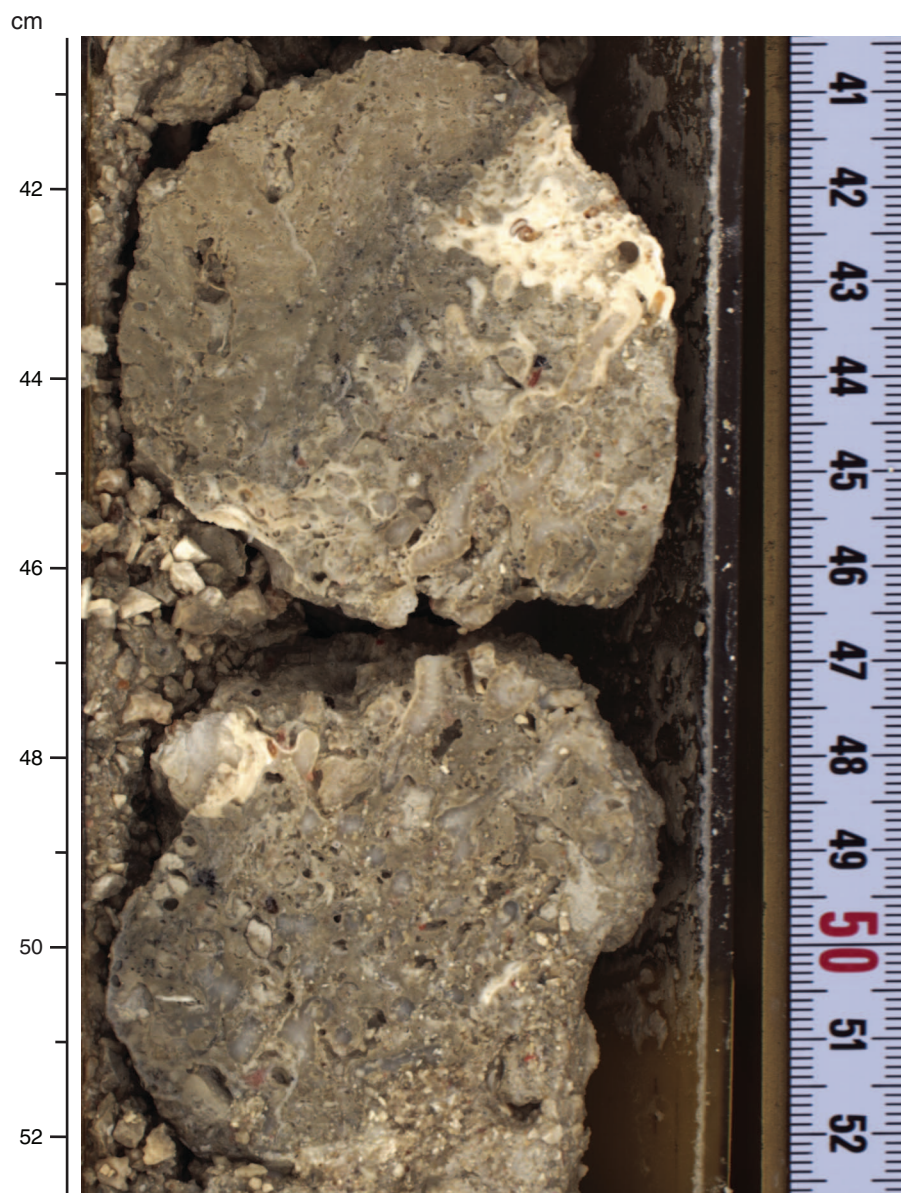


Figure F49. High-resolution line scan image of laminated microbialites (interval 325-M0043A-14R-1, 12–20 cm).

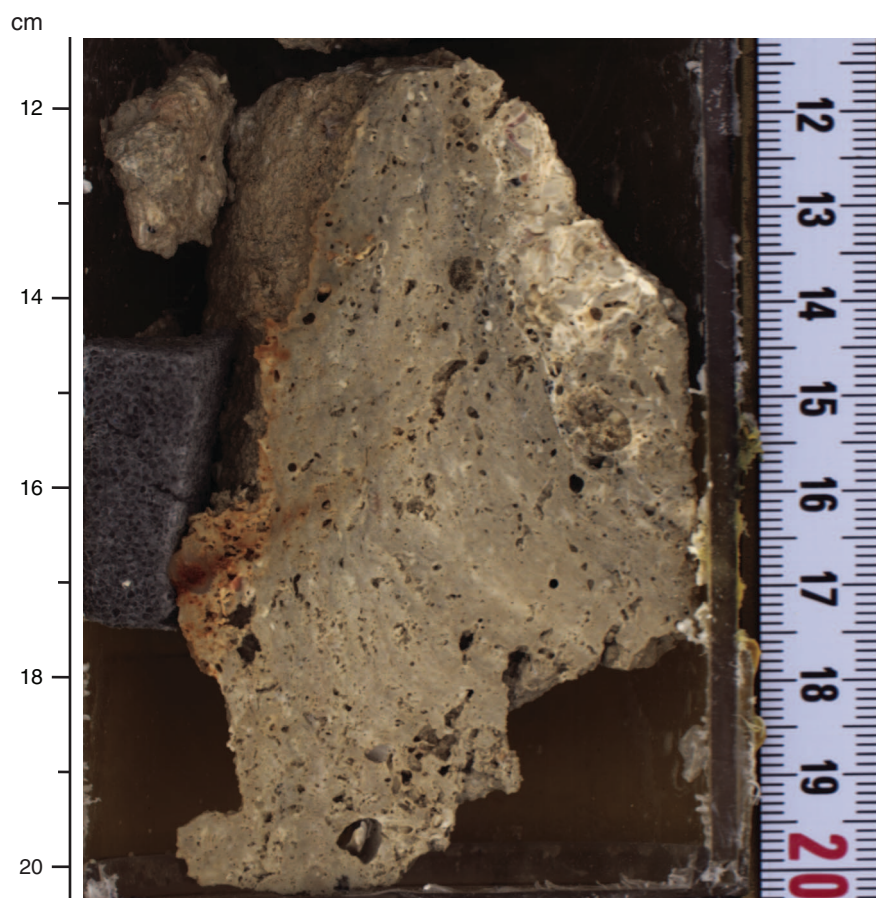


Figure F50. High-resolution line scan image of a medium branching *Acropora* (interval 325-M0043A-3R-CC, 2–8 cm).



Figure F51. High-resolution line scan image of a medium branching *Acropora* (interval 325-M0043A-8R-1, 1–6 cm).



Figure F52. High-resolution line scan image of a blackened boundstone with thin foliose coralline algae and worm tubes overlying a dark packstone with larger foraminifera, *Halimeda*, mollusks, and coral fragments (interval 325-M0043A-22R-CC, 0–14 cm).

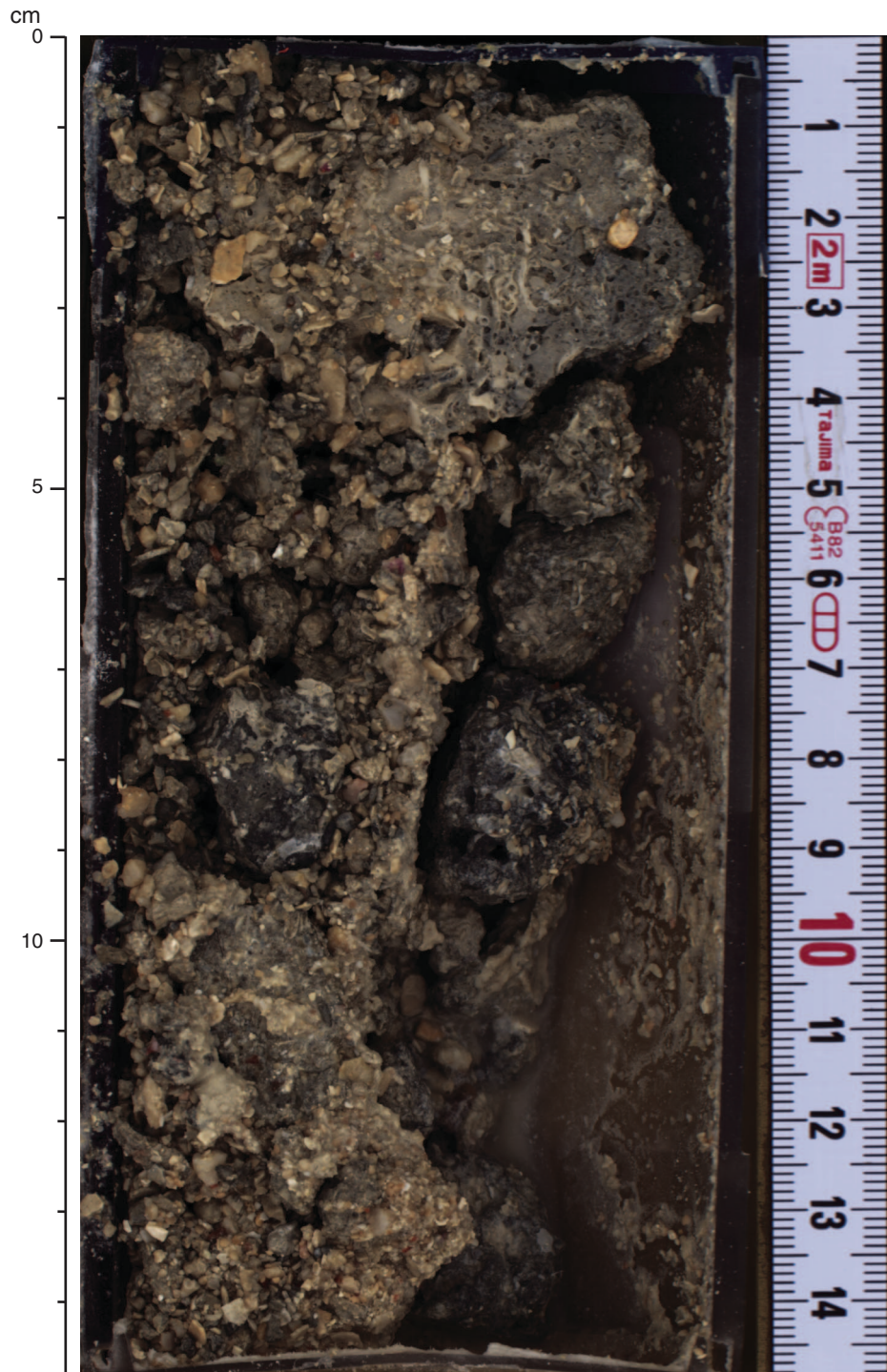


Figure F53. Summary diagram showing data collected on whole cores using the multisensor core logger (MSCL), Hole M0043A.

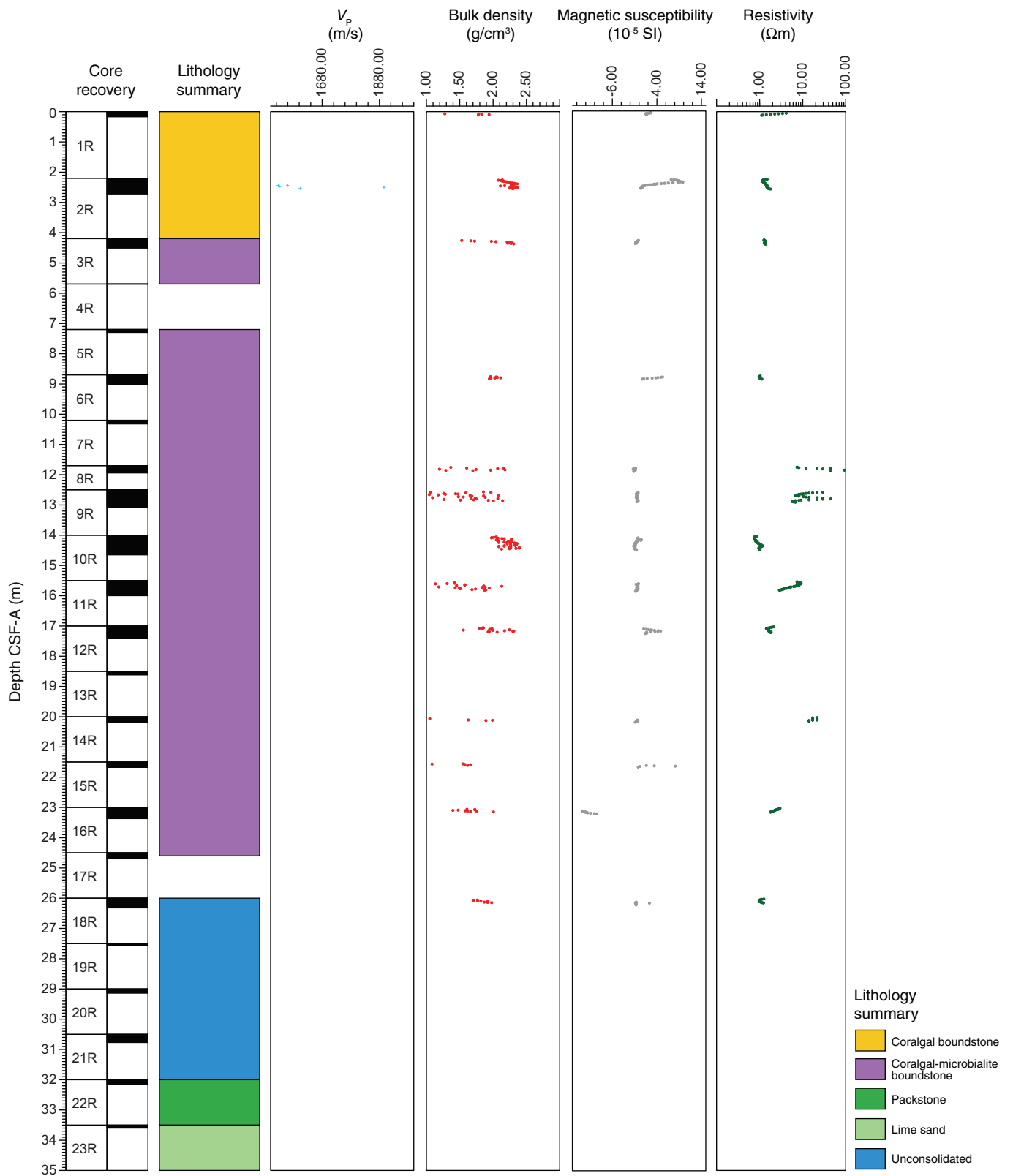


Figure F54. Petrophysical measurements obtained from discrete samples with a pycnometer, Hole M0043A. Bulk density measured on whole cores with the MSCL is shown in red on the bulk density plot.

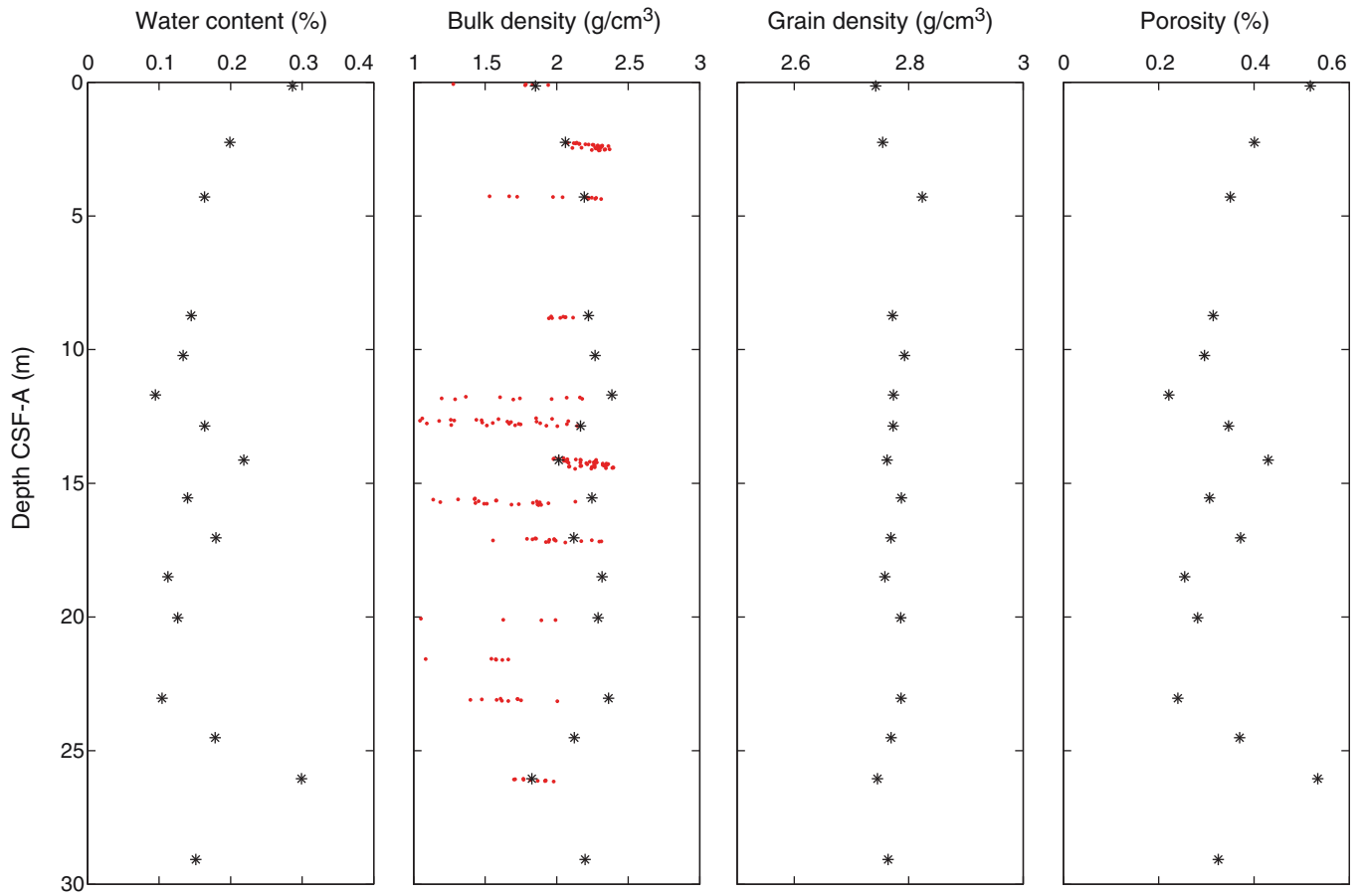


Figure F55. Values of reflectance (L^*), green to red (a^*), and blue to yellow (b^*) indexes, along with ratio a^*/b^* for Hole M0043A.

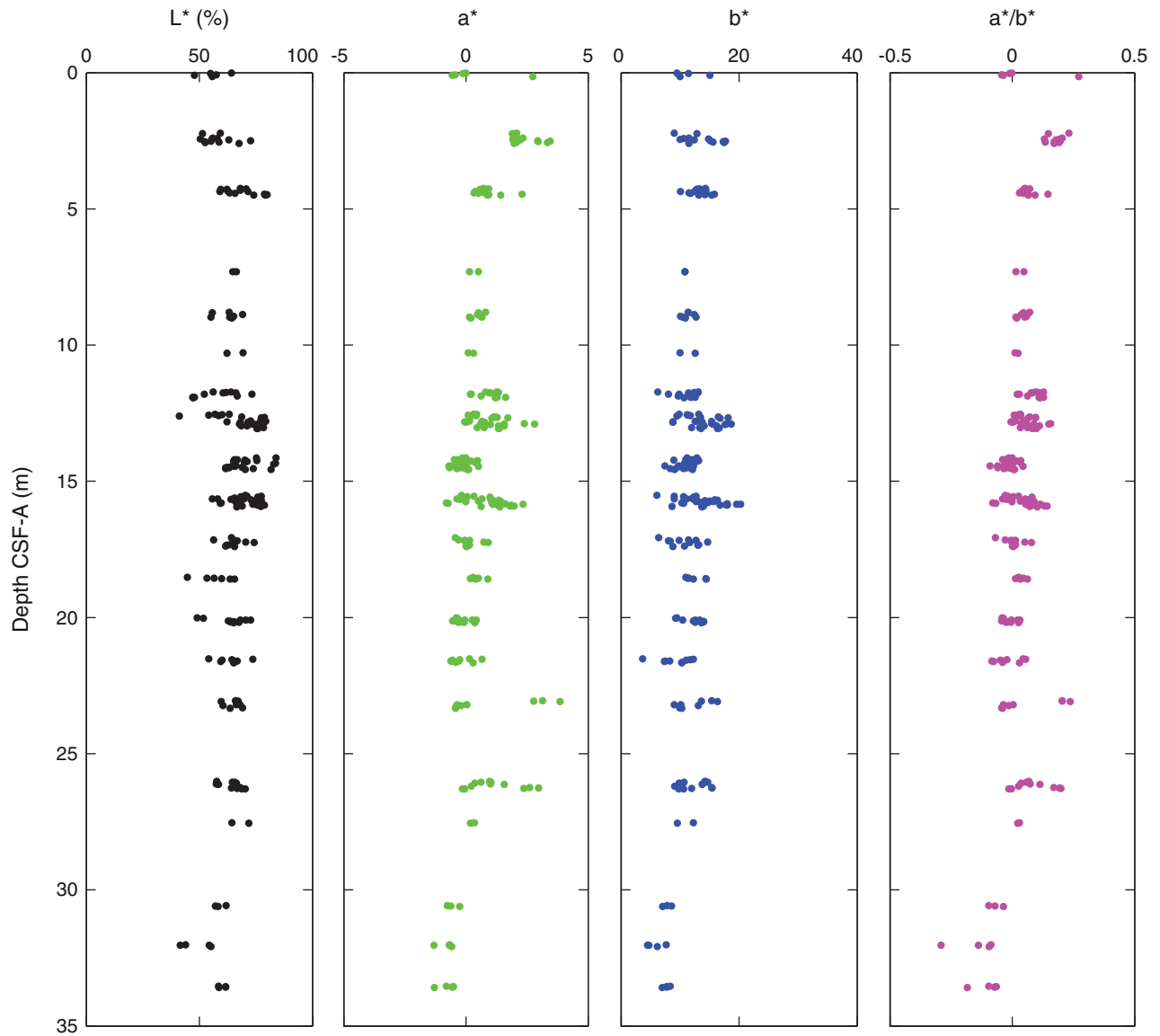


Figure F56. Magnetic susceptibility record for Hole M0043A. Water depth = 102.93 m (LAT).

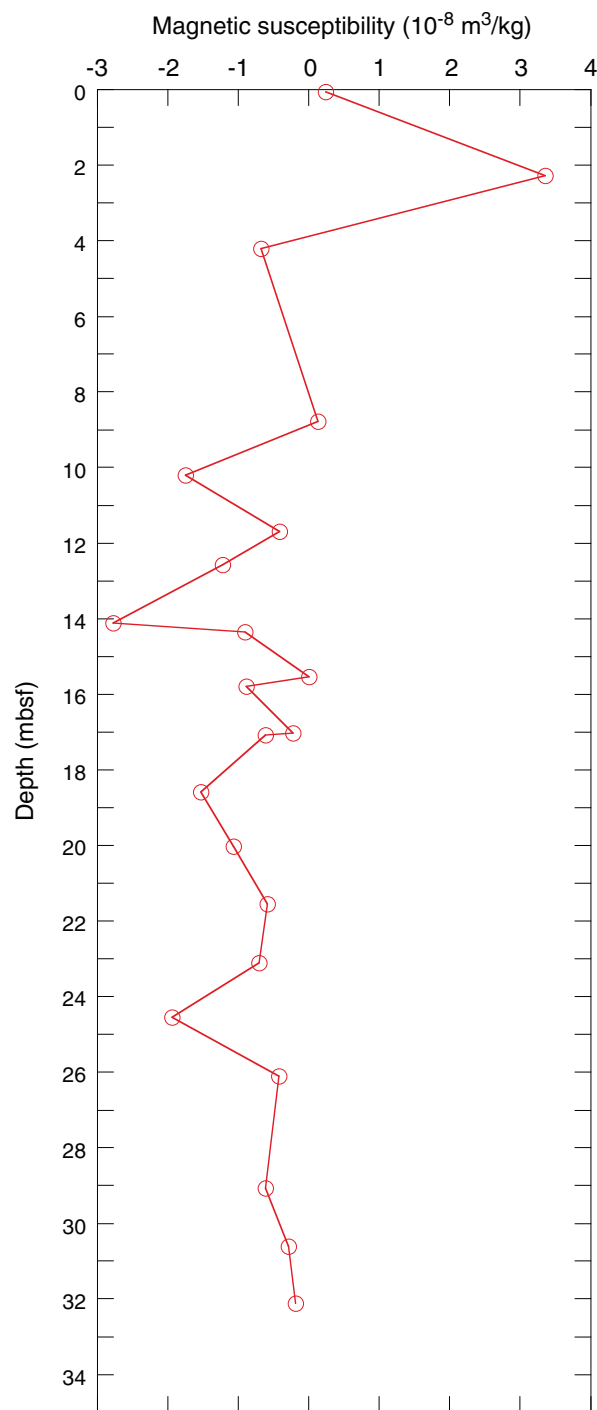


Figure F57. Preliminary chronology for Hole M0043A. Radiocarbon data are presented as graphs with the uncalibrated radiocarbon age and uncertainty shown as the red normal distribution on the ordinate axis and the probability distribution of the calibrated age shown in gray on the abscissa. The marine09 calibration curve is shown in blue. Horizontal bars indicate portions of the age distribution that are significant at the 95.4% confidence interval and the mean age (white circle ± 1 standard deviation) used for the purposes of preliminary dating. All ages are presented as thousands of calendar years BP (1950 AD). See Table T10 in the “Methods” chapter. (See Bronk Ramsey [2009], as well as Bronk Ramsey [2010] at c14.arch.ox.ac.uk/oxcal.html.)

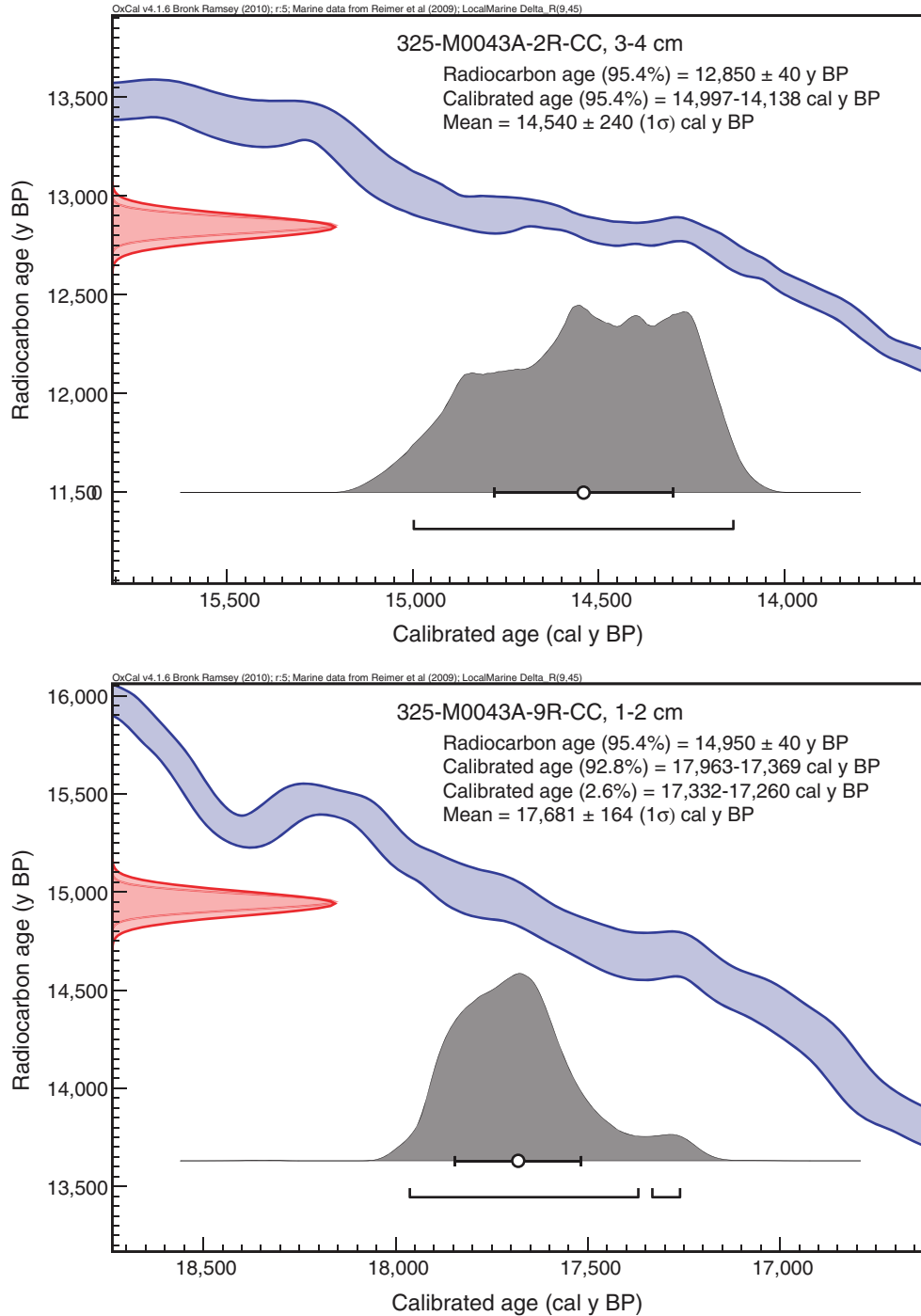


Figure F58. High-resolution line scan image of a bioclastic packstone with corals, bryozoans, encrusting foraminifera, coralline algae, and mollusks with a brown/dark gray crust (interval 325-M0044A-1R-1, 2–18 cm).

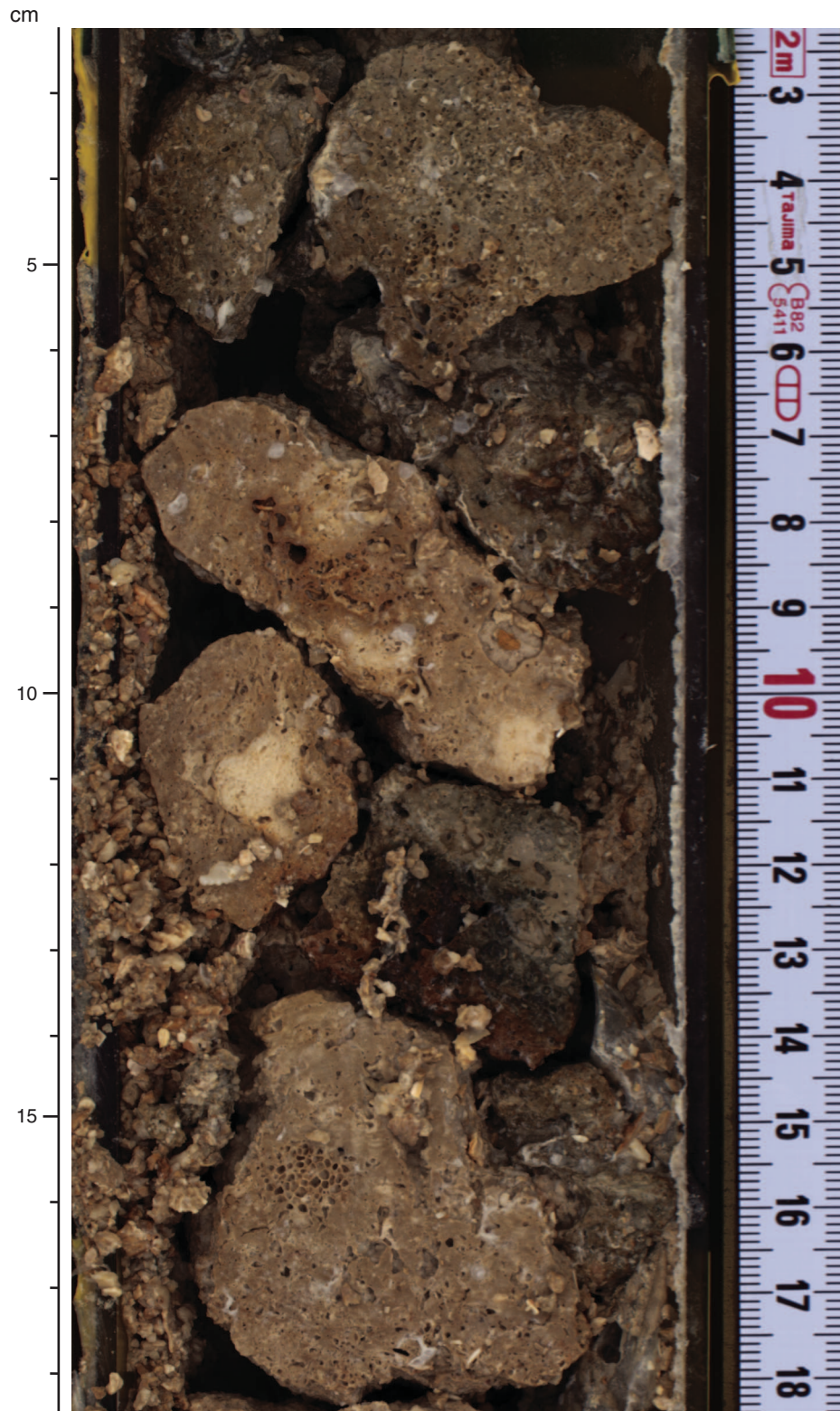


Figure F59. High-resolution line scan image of an eroded piece of *Acropora* encrusted by microbialites (interval 325-M0044A-4R-1, 9–12 cm).



Figure F60. High-resolution line scan image of the base of a branching *Acropora* colony with a thin coralline algal and vermitid crust that is bioeroded by boring bivalves, and again encrusted by a thick microbialite crust (interval 325-M0044A-9R-1, 14–21 cm).



Figure F61. High-resolution line scan image of coralg al framework (medium branching *Porites*) with bivalve borings infilled with internal sediment containing geopetal structures (interval 325-M0044A-8R-1, 15–21 cm).

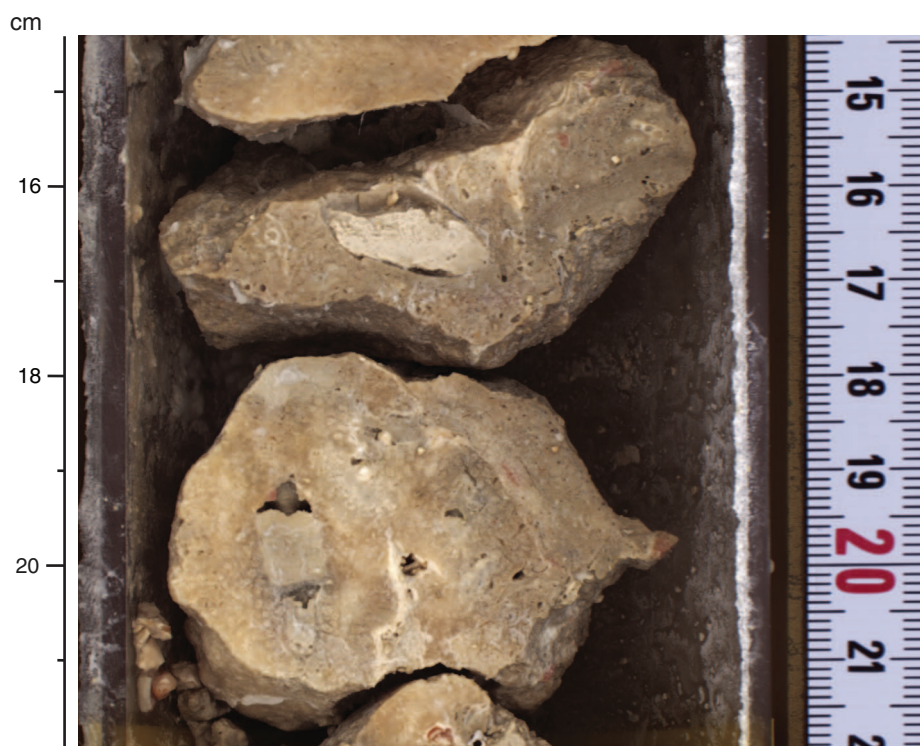


Figure F62. High-resolution line scan image of a medium branching *Acropora* fragment (interval 325-M0044A-7R-1, 4–12 cm).

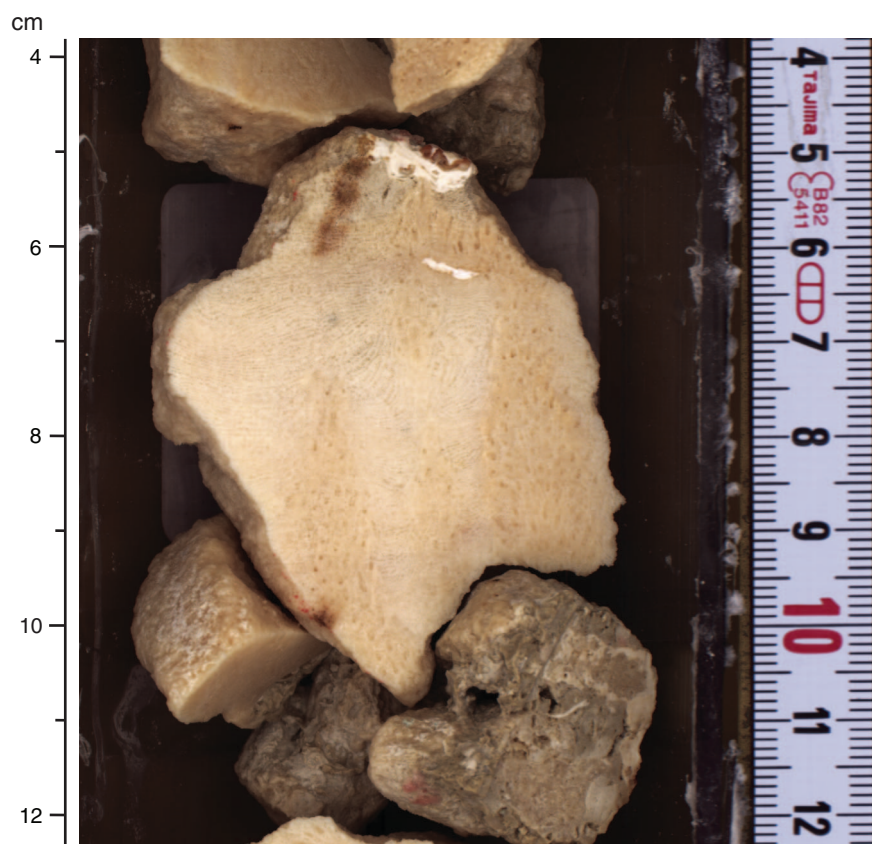


Figure F63. Summary diagram showing data collected on whole cores using the multisensor core logger (MSCL), Hole M0044A.

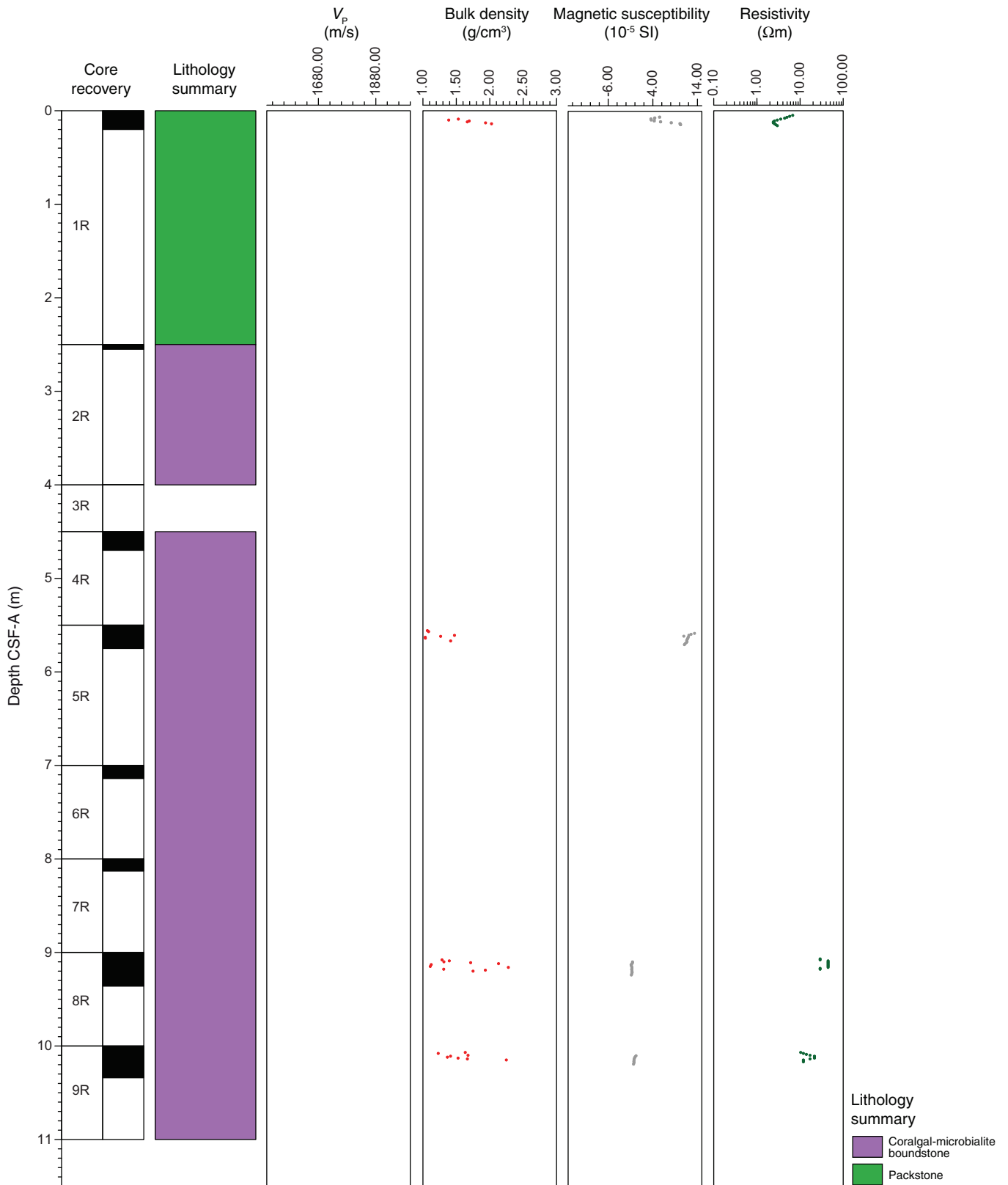


Figure F64. *P*-wave velocity data, Hole M0044A. **A.** Plot of initial, dry, and resaturated *P*-wave velocity measurements on discrete samples vs. depth. Three measurements were taken at each depth and are denoted by a dot. Average values are plotted as an open triangle. **B.** Plot showing discrete *P*-wave velocity vs. discrete bulk density.

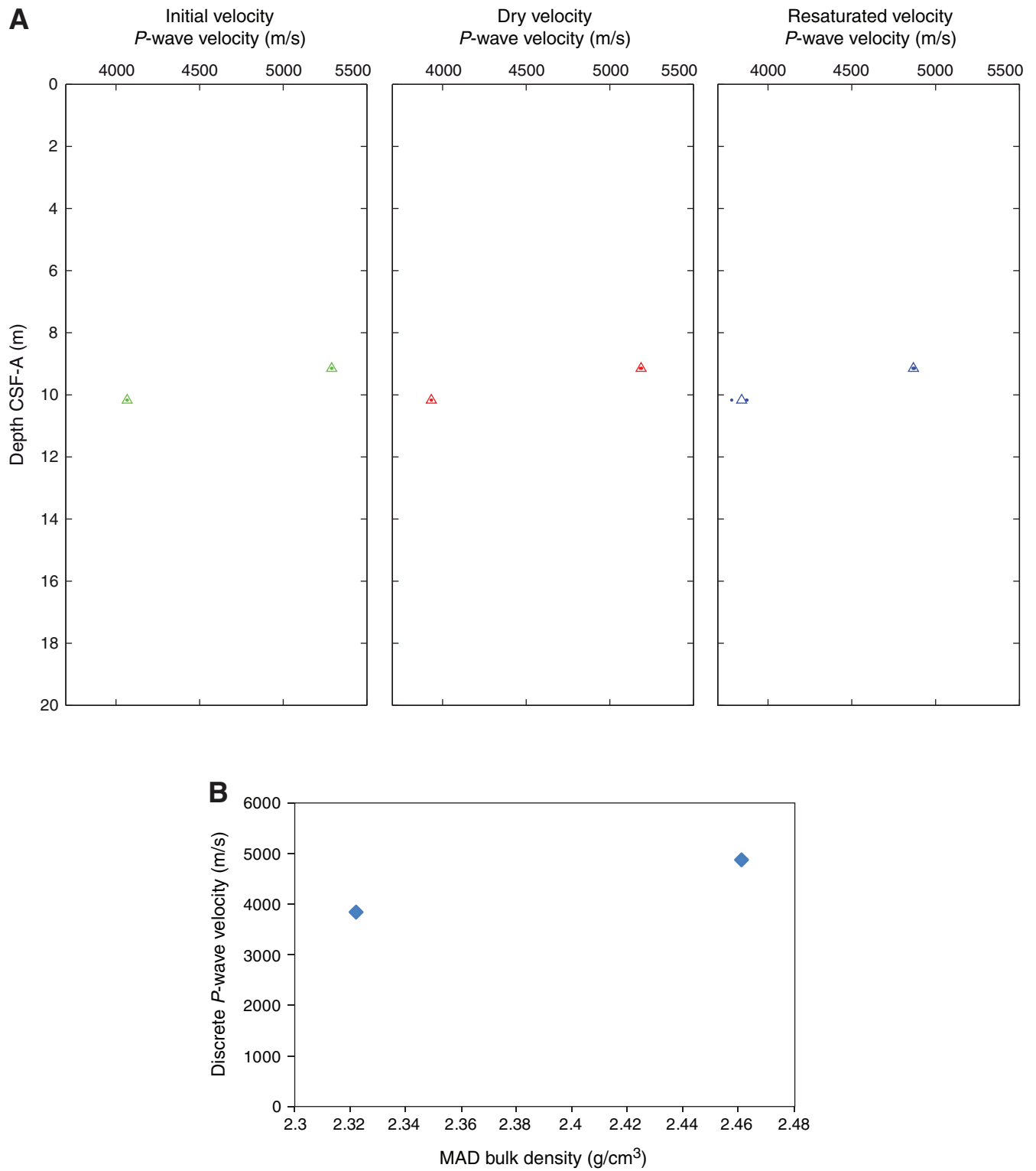


Figure F65. Values of reflectance (L^*), green to red (a^*), and blue to yellow (b^*) indexes, along with ratio a^*/b^* for Hole M0044A.

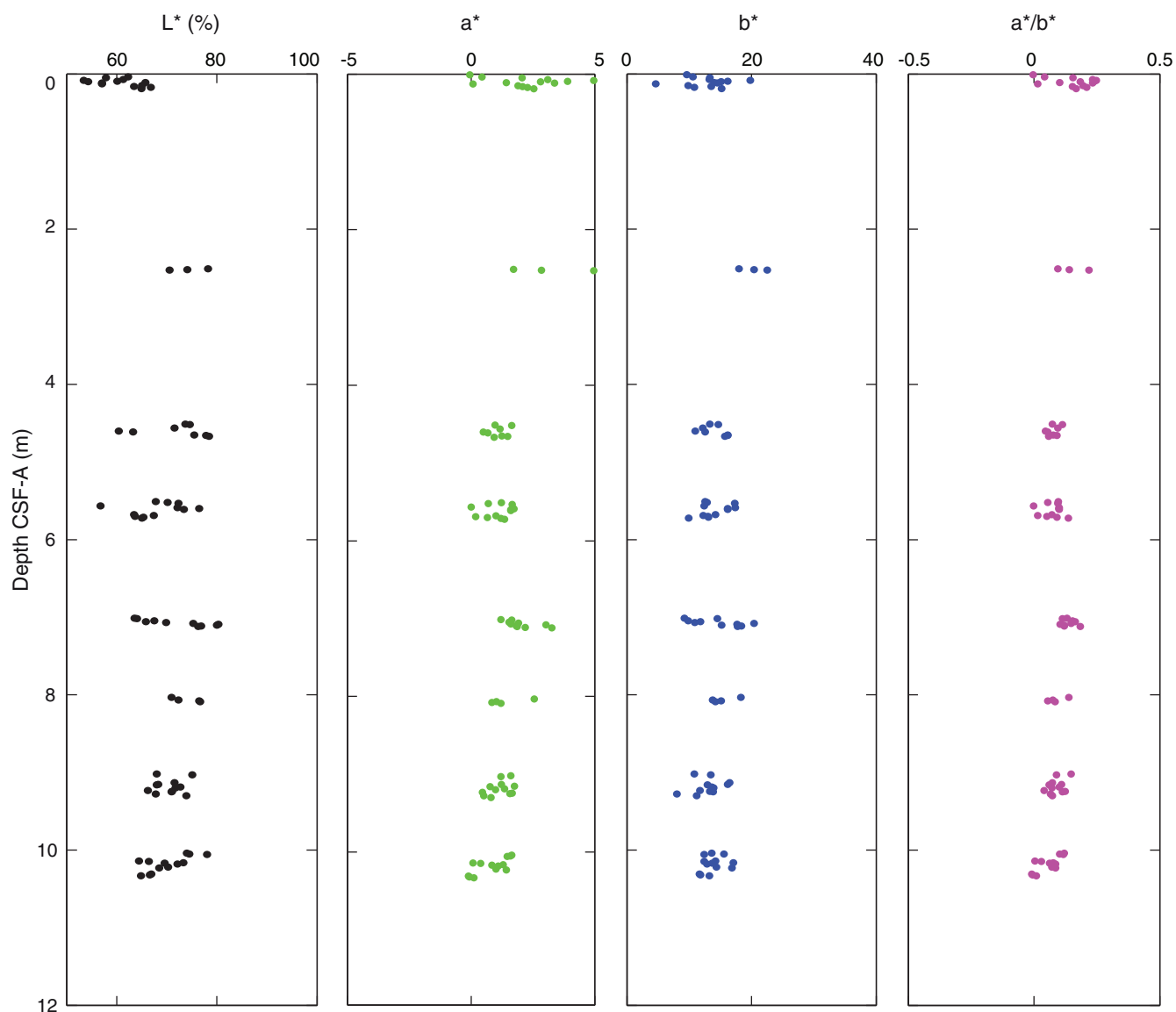


Figure F66. Magnetic susceptibility record for Hole M0044A. Water depth = 105.25 m (LAT).

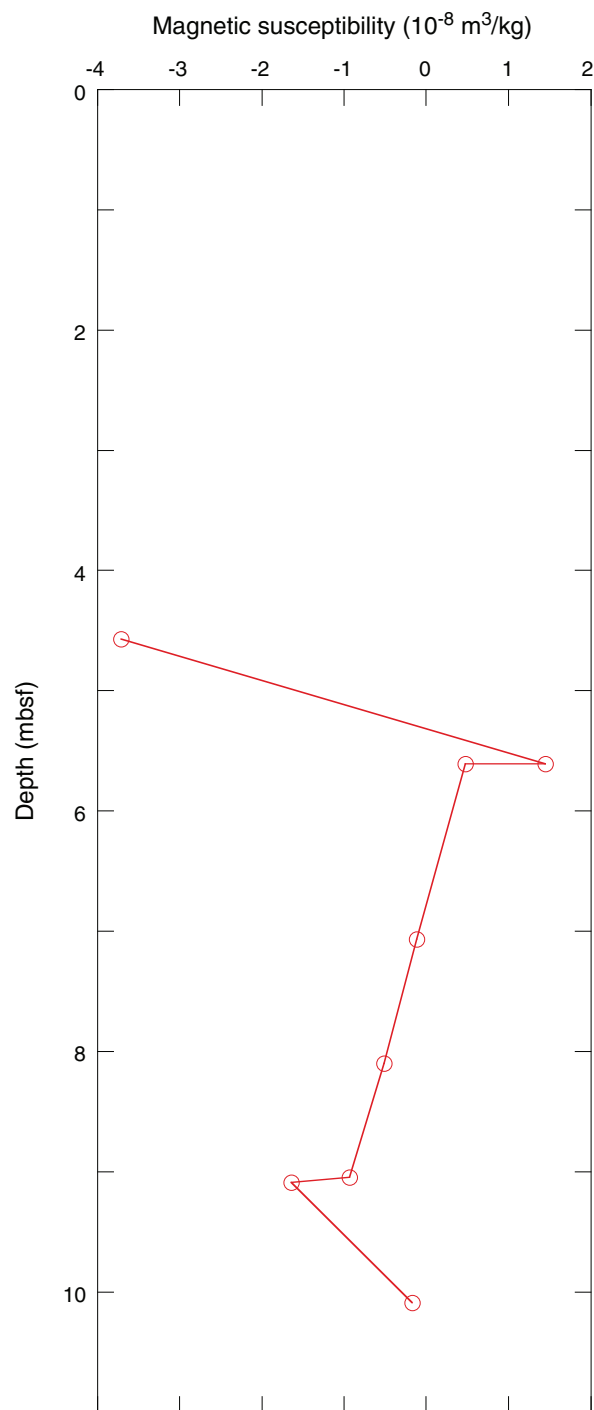


Figure F67. Preliminary chronology for Hole M0044A. Radiocarbon data are presented as graphs with the uncalibrated radiocarbon age and uncertainty shown as the red normal distribution on the ordinate axis and the probability distribution of the calibrated age shown in gray on the abscissa. The marine09 calibration curve is shown in blue. Horizontal bars indicate portions of the age distribution that are significant at the 95.4% confidence interval and the mean age (white circle ± 1 standard deviation) used for the purposes of preliminary dating. All ages are presented as thousands of calendar years BP (1950 AD). See Table T10 in the “Methods” chapter. (See Bronk Ramsey [2009], as well as Bronk Ramsey [2010] at c14.arch.ox.ac.uk/oxcal.html.)

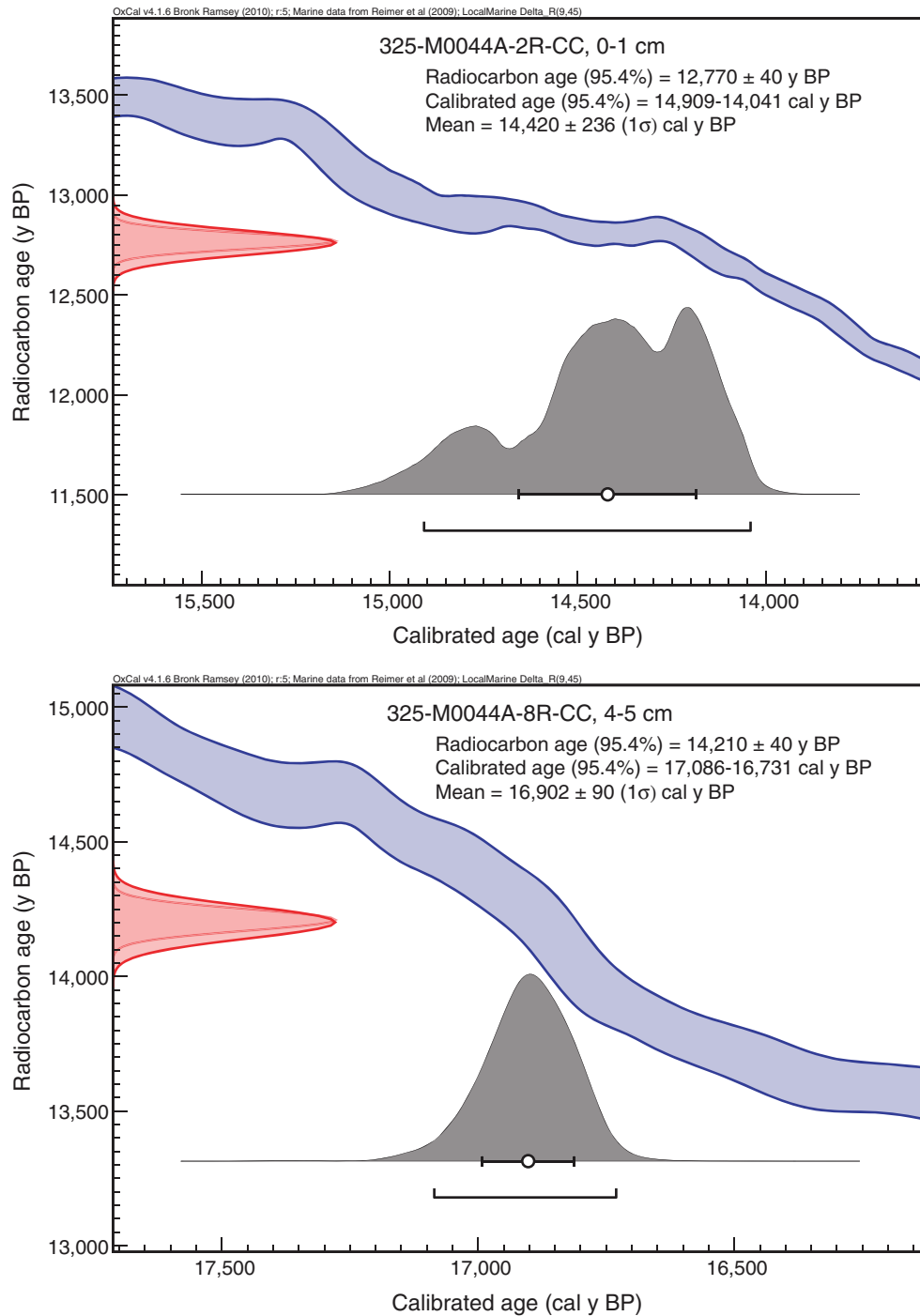


Figure F68. High-resolution line scan image of (upper; 0–7 cm) a submassive coral encrusted by a thick coralline algal crust and (lower; 7–12 cm) a submassive *Montipora*(?) or *Goniopora*(?) (interval 325-M0046A-9R-1, 1–13 cm).

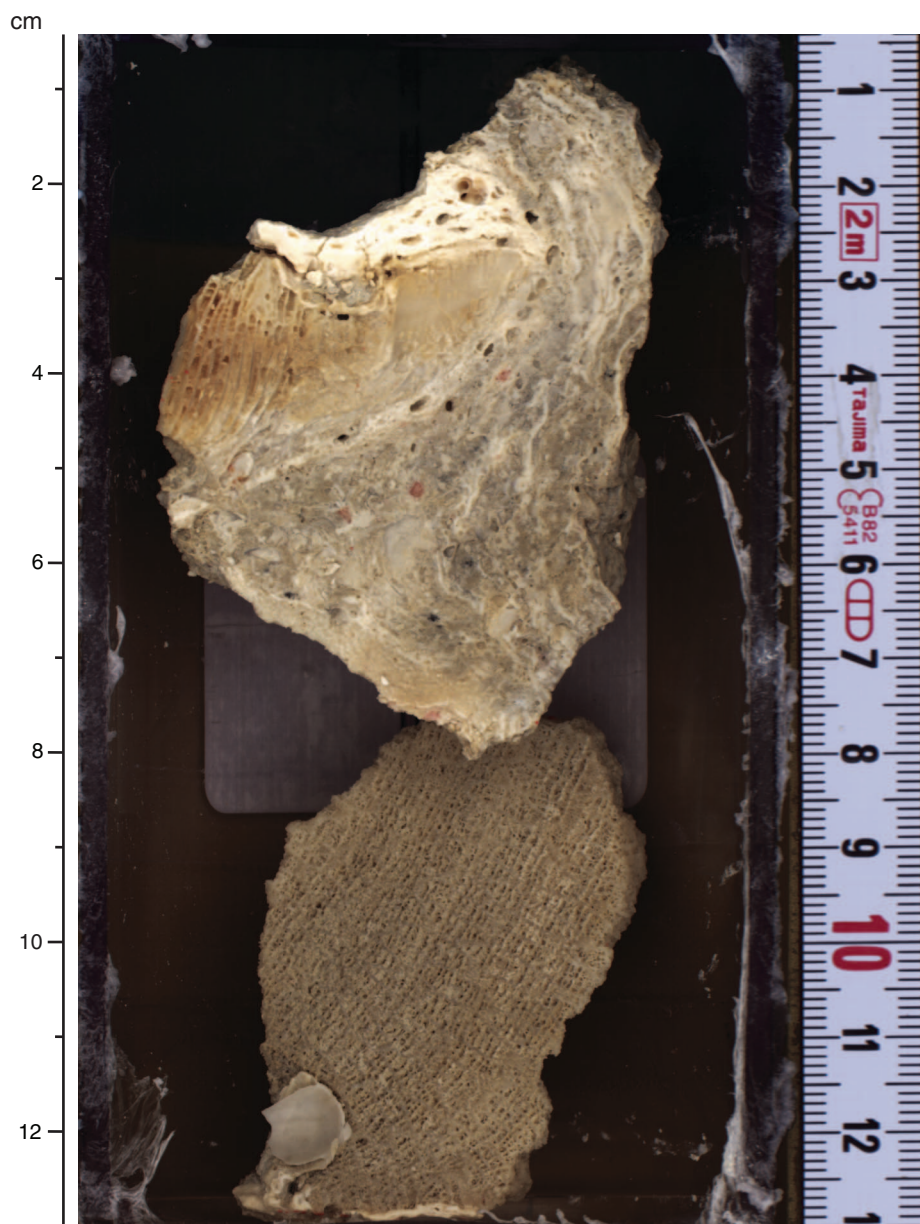


Figure F69. High-resolution line scan image of a bioclastic packstone (4–8 cm) overlying a spiculite (of unknown origin) encrusted by thin coralline algae (interval 325-M0046A-5R-1, 4–11 cm).



Figure F70. High-resolution line scan image of fragments of massive *Echinopora*, fine branching *Seriatopora*, fine to medium branching *Pocillopora*, and fine branching *Acropora* (interval 325-M0046A-11R-CC, 3–13 cm). Other bioclasts include mollusk shells and *Halimeda*.



Figure F71. Summary diagram showing data collected on whole cores using the multisensor core logger (MSCL), Hole M0046A.

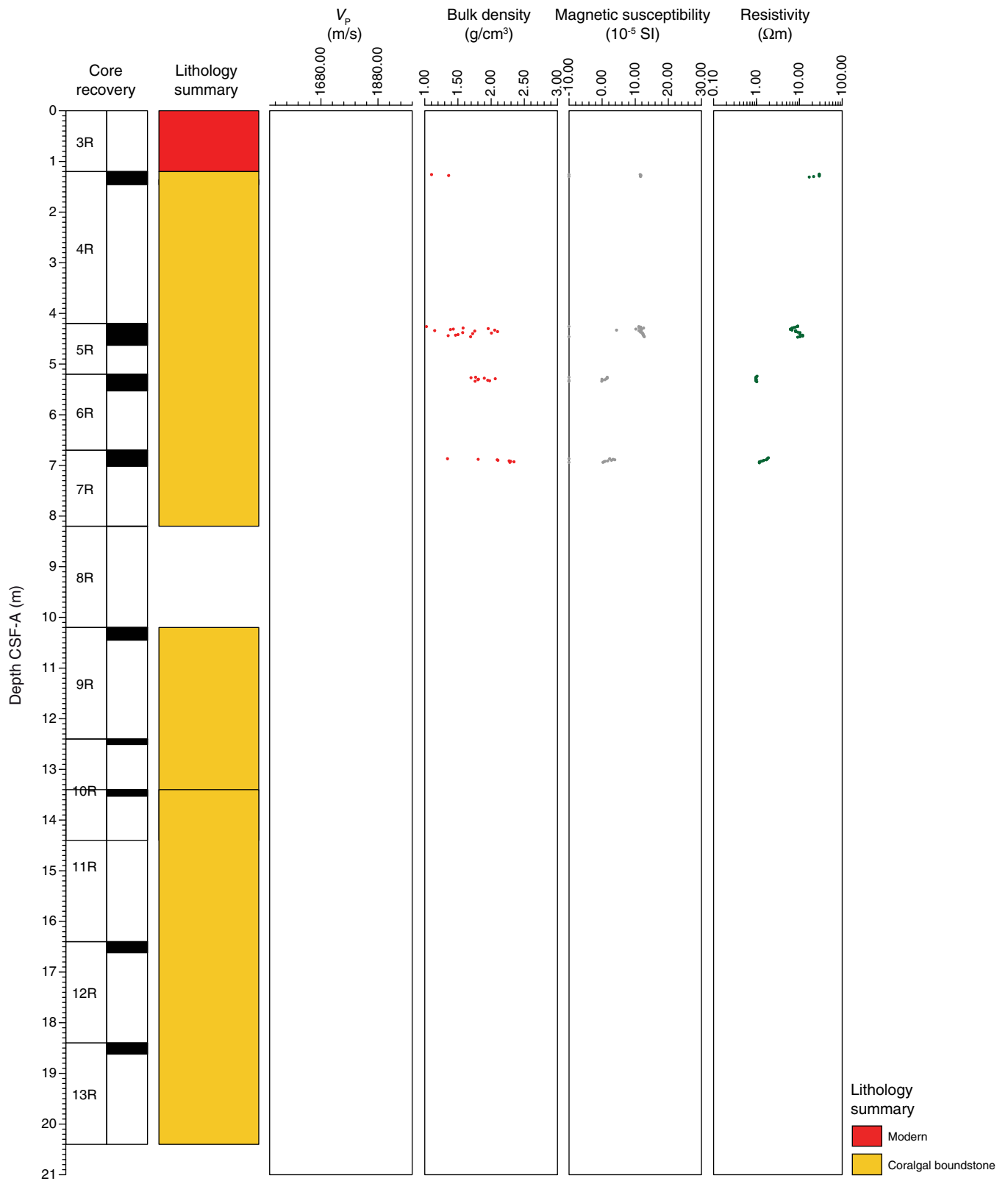


Figure F72. Values of reflectance (L^*), green to red (a^*), and blue to yellow (b^*) indexes, along with ratio a^*/b^* for Hole M0046A.

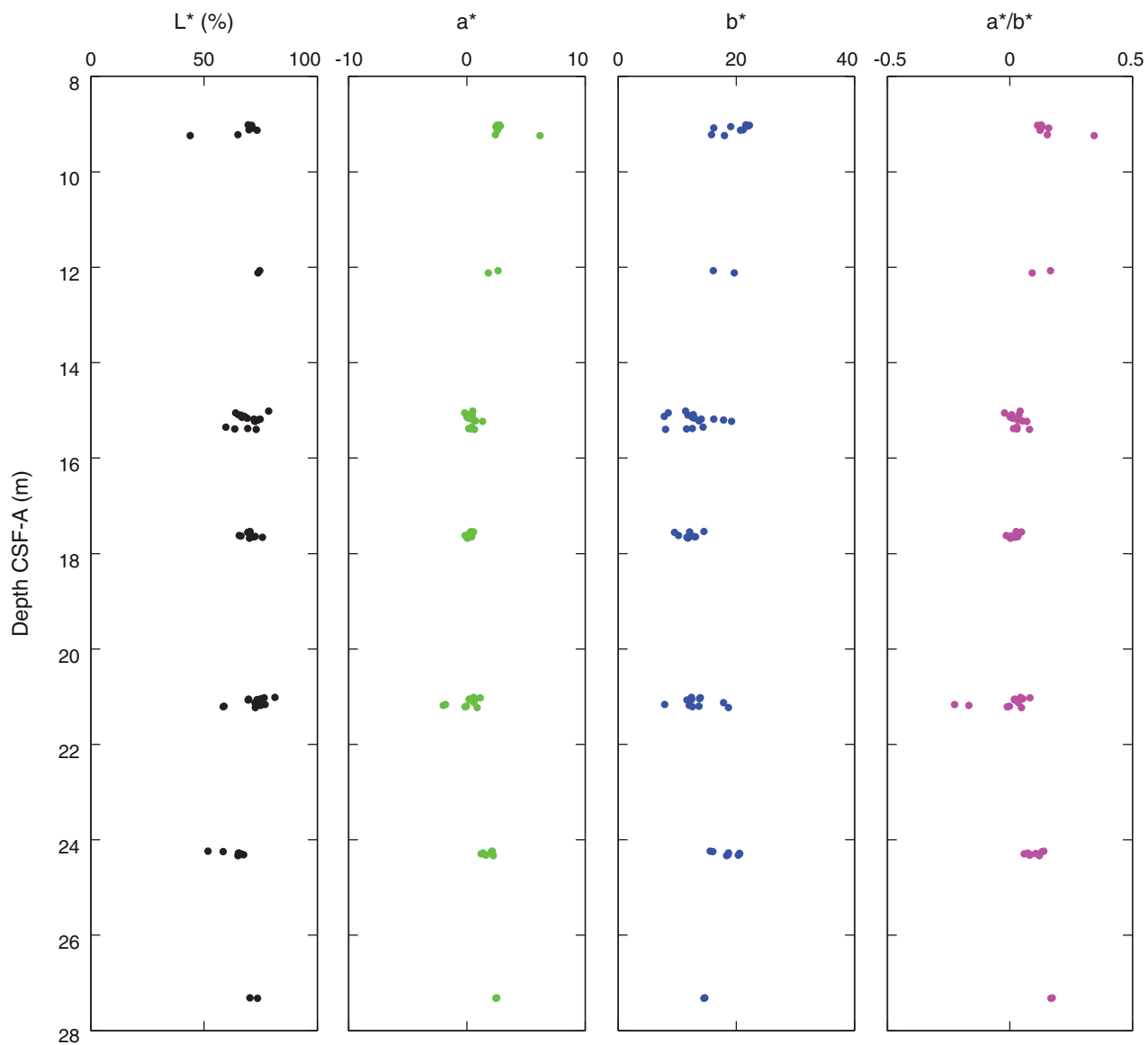


Figure F73. Magnetic susceptibility record for Hole M0046A. Water depth = 106.69 m (LAT). The negative start value of the Y axis is due to Runs 1R and 2R sliding down a pinnacle side and not actually penetrating the seabed. Therefore core depths and associated samples depths were adjusted to account for this.

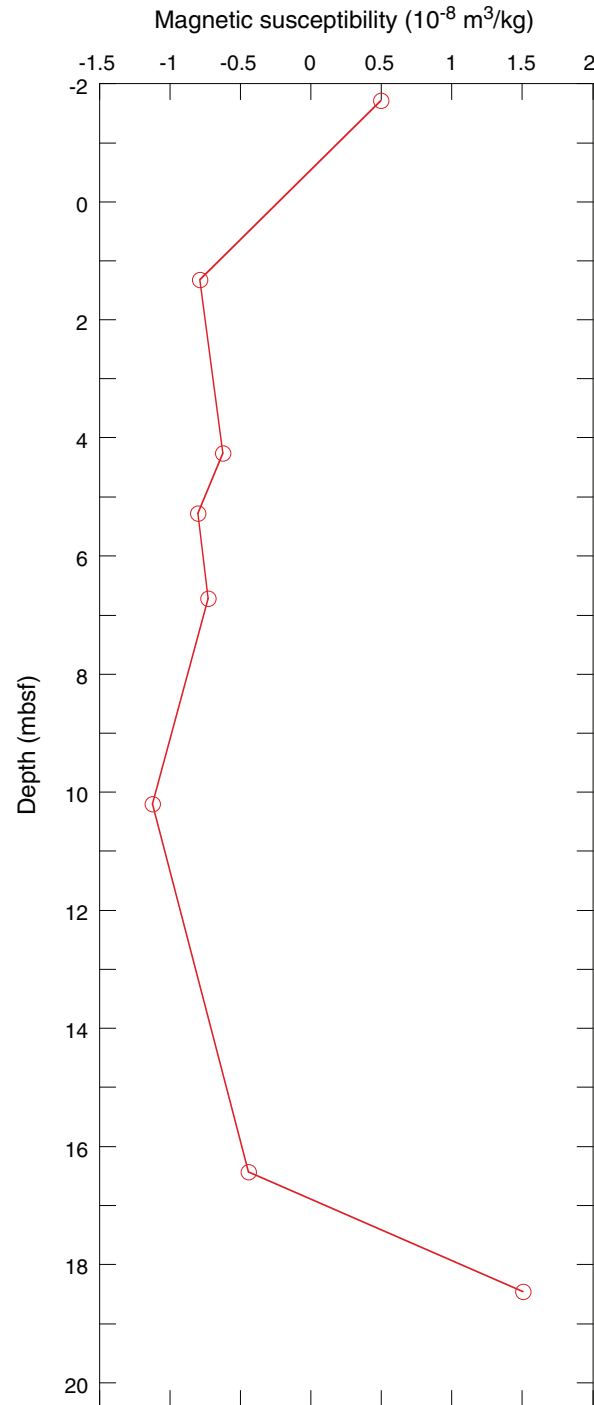


Figure F74. Preliminary chronology for Hole M0046A. Radiocarbon data are presented as graphs with the uncalibrated radiocarbon age and uncertainty shown as the red normal distribution on the ordinate axis and the probability distribution of the calibrated age shown in gray on the abscissa. The marine09 calibration curve is shown in blue. Horizontal bars indicate portions of the age distribution that are significant at the 95.4% confidence interval and the mean age (white circle ± 1 standard deviation) used for the purposes of preliminary dating. All ages are presented as thousands of calendar years BP (1950 AD). See Table T10 in the “Methods” chapter. (See Bronk Ramsey [2009], as well as Bronk Ramsey [2010] at c14.arch.ox.ac.uk/oxcal.html.)

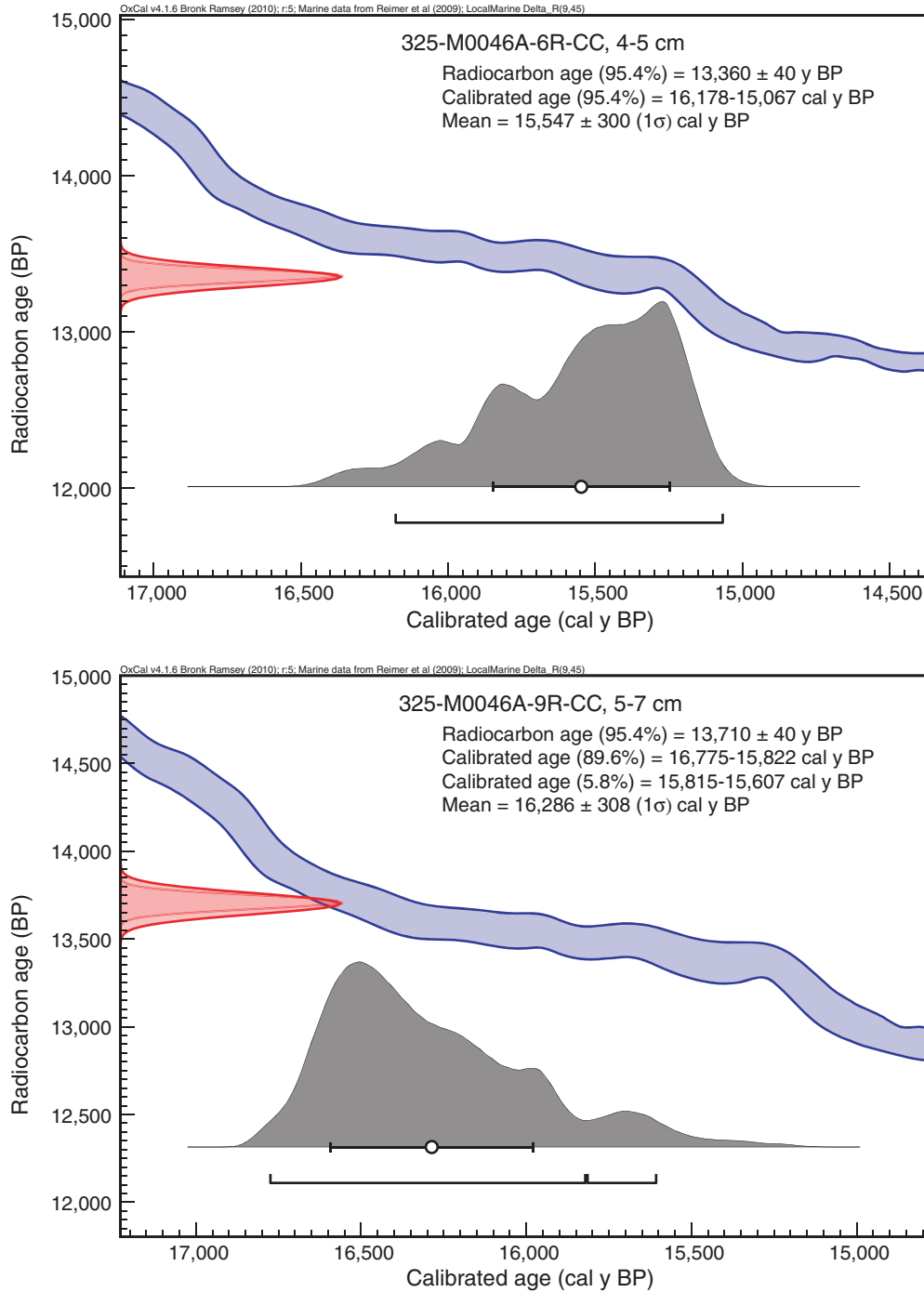


Figure F75. High-resolution line scan image of an altered submassive *Porites* and coralline algae, with black and brown staining (interval 325-M0047A-2R-1, 0–10 cm).

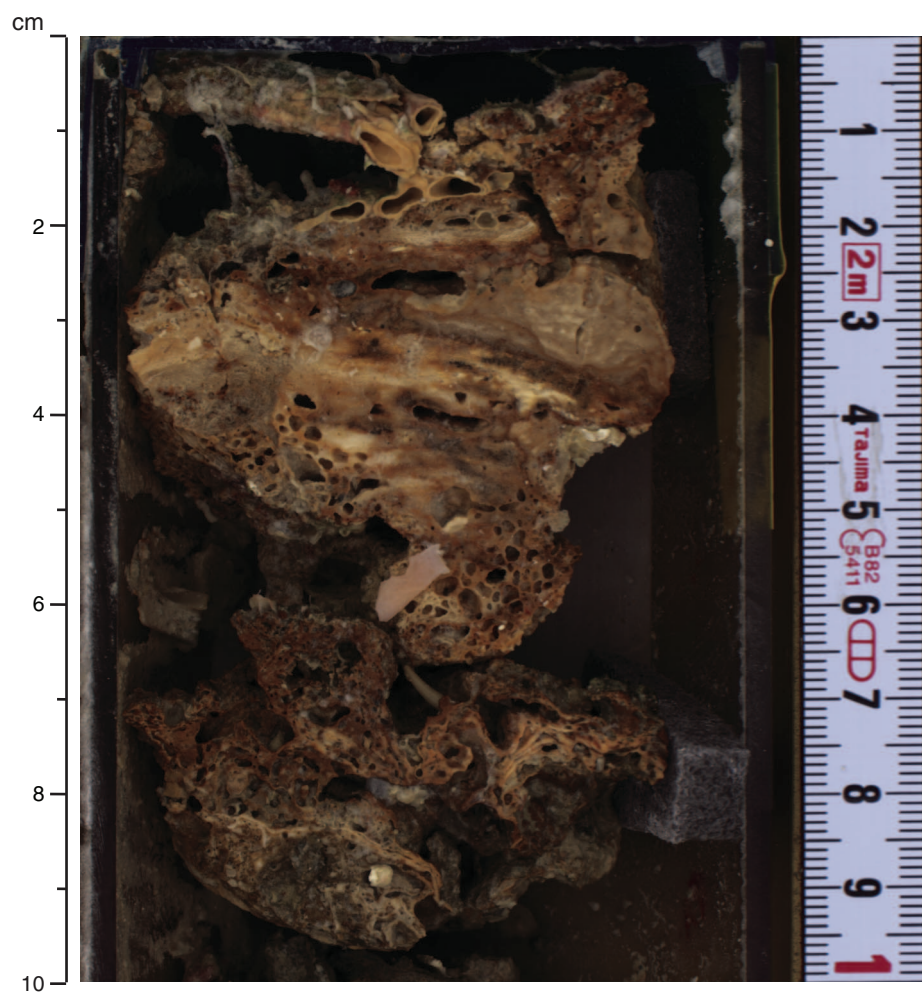


Figure F76. High-resolution line scan image of a medium branching *Acropora* (interval 325-M0047A-10R-1, 1–5 cm).

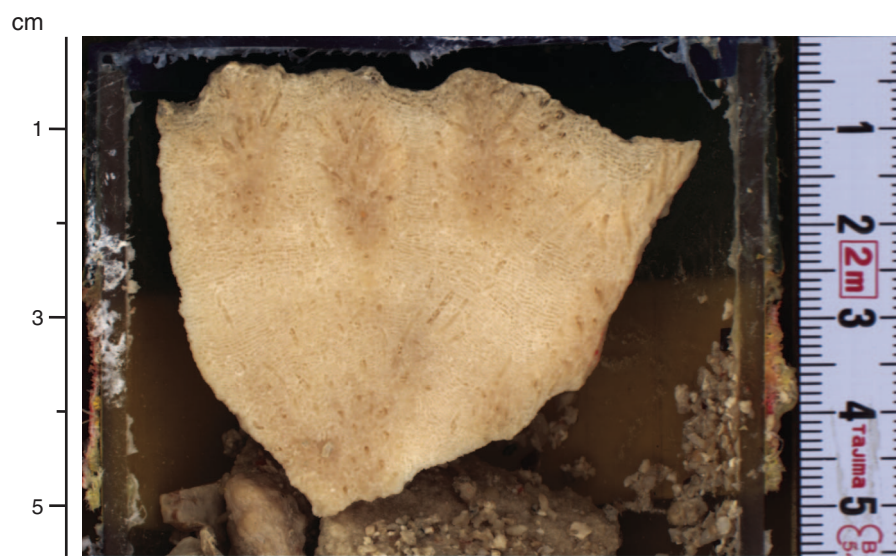


Figure F77. Summary diagram showing data collected on whole cores using the multisensor core logger (MSCL), Hole M0047A.

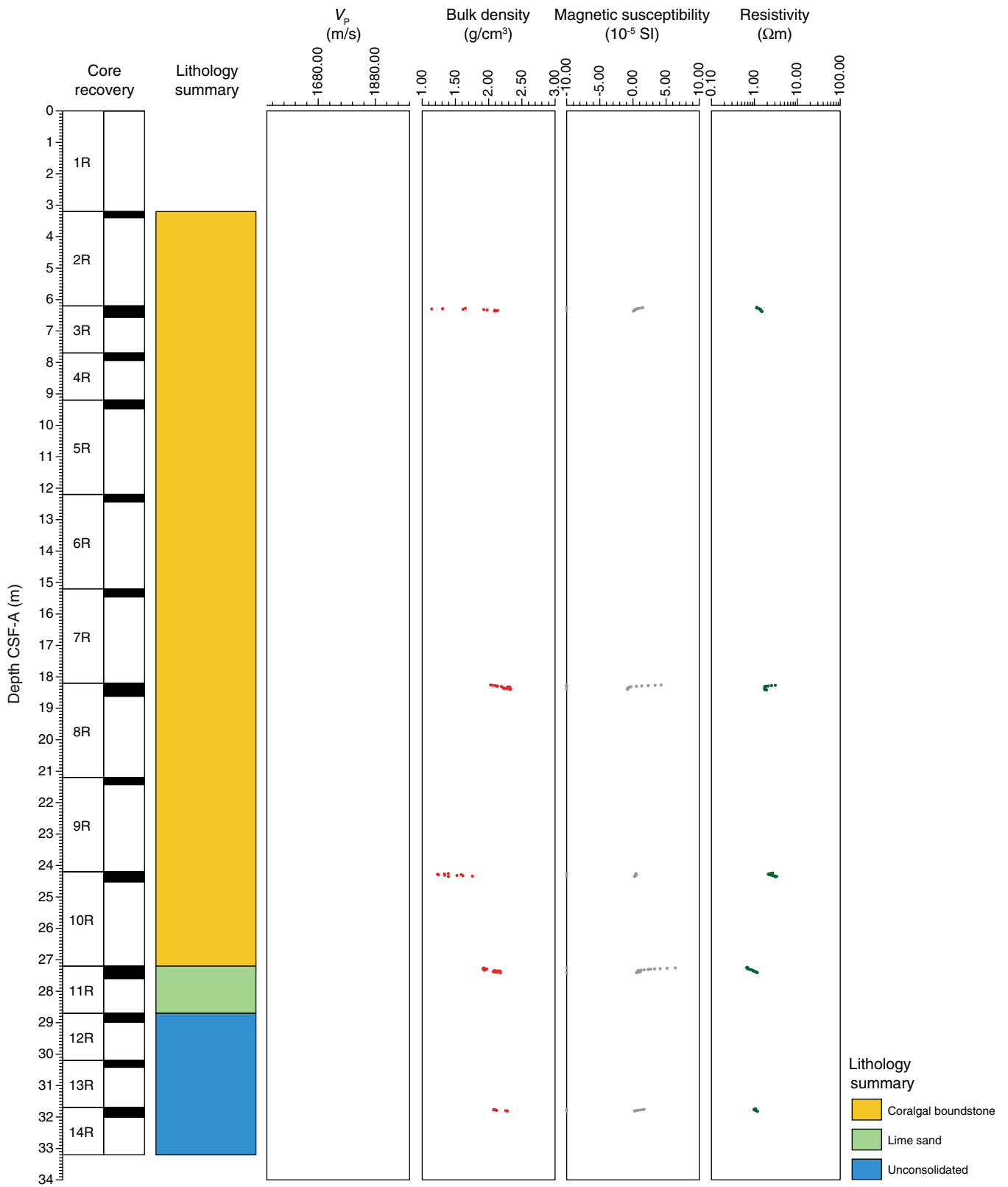


Figure F78. Petrophysical measurements obtained from discrete samples with a pycnometer, Hole M0047A. Bulk density measured on whole cores with the MSCL is shown in red on the bulk density plot.

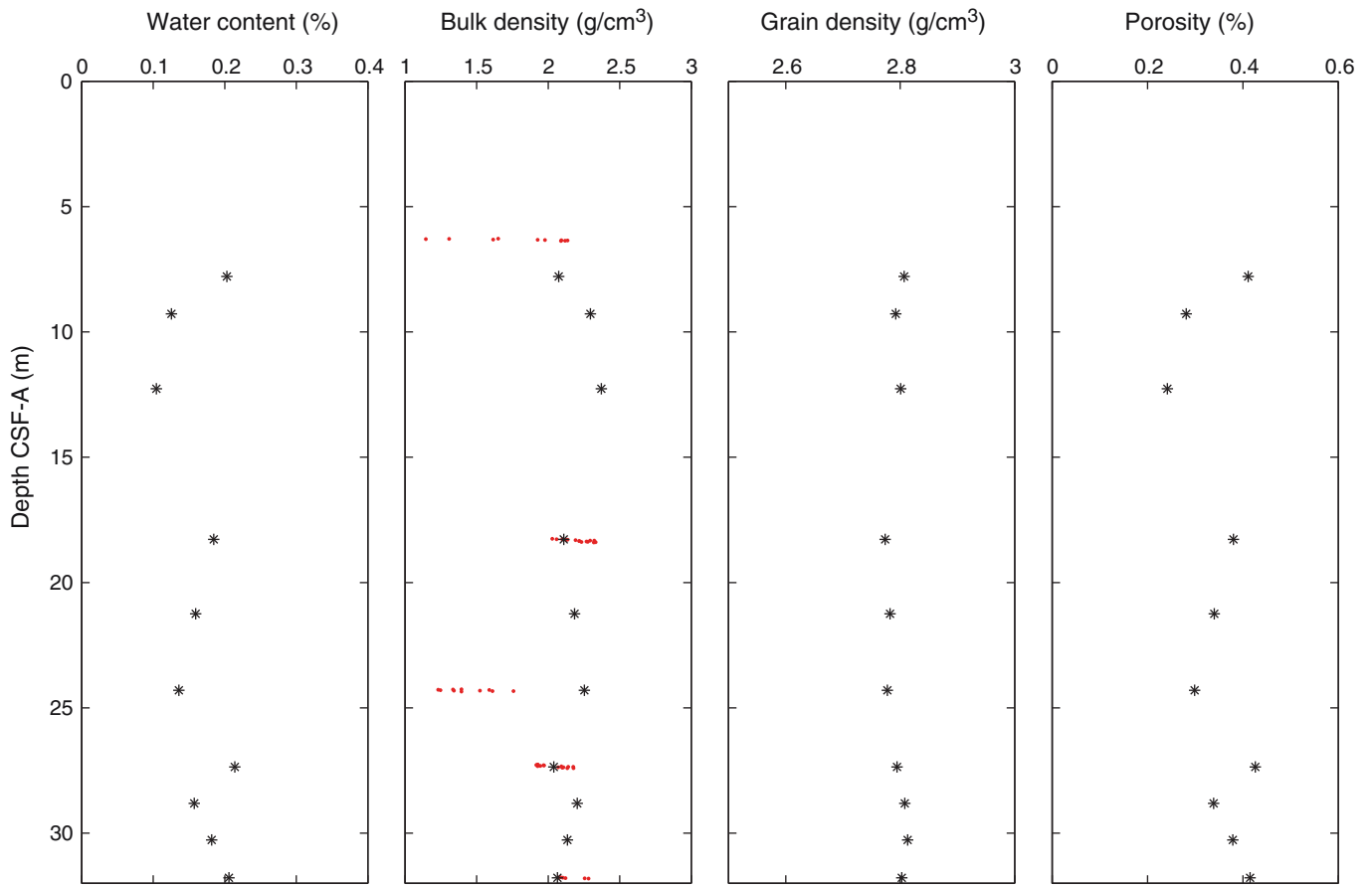


Figure F79. Values of reflectance (L^*), green to red (a^*), and blue to yellow (b^*) indexes, along with ratio a^*/b^* for Hole M0047A.

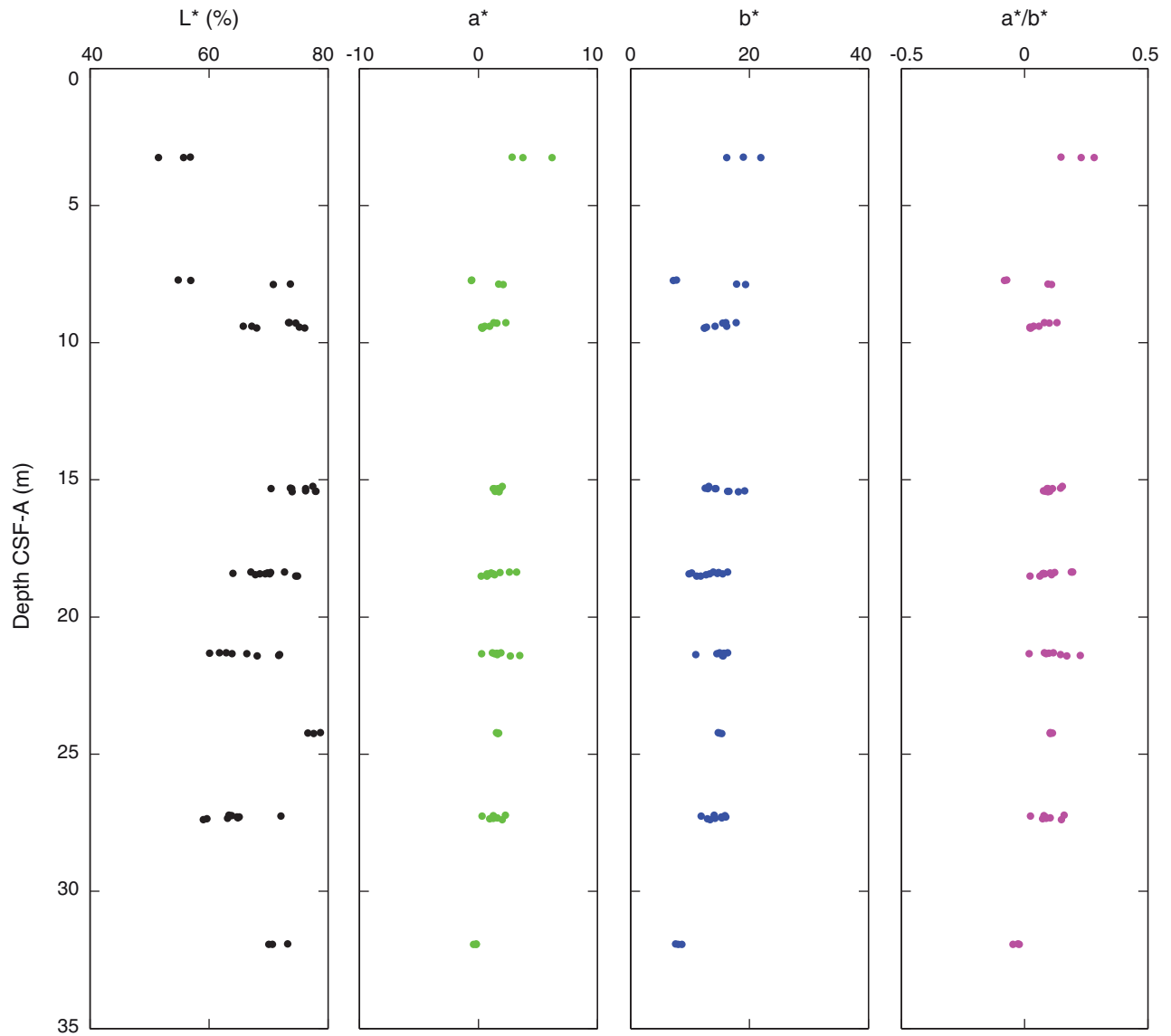


Figure F80. Magnetic susceptibility record for Hole M0047A. Water depth = 99.12 m (LAT).

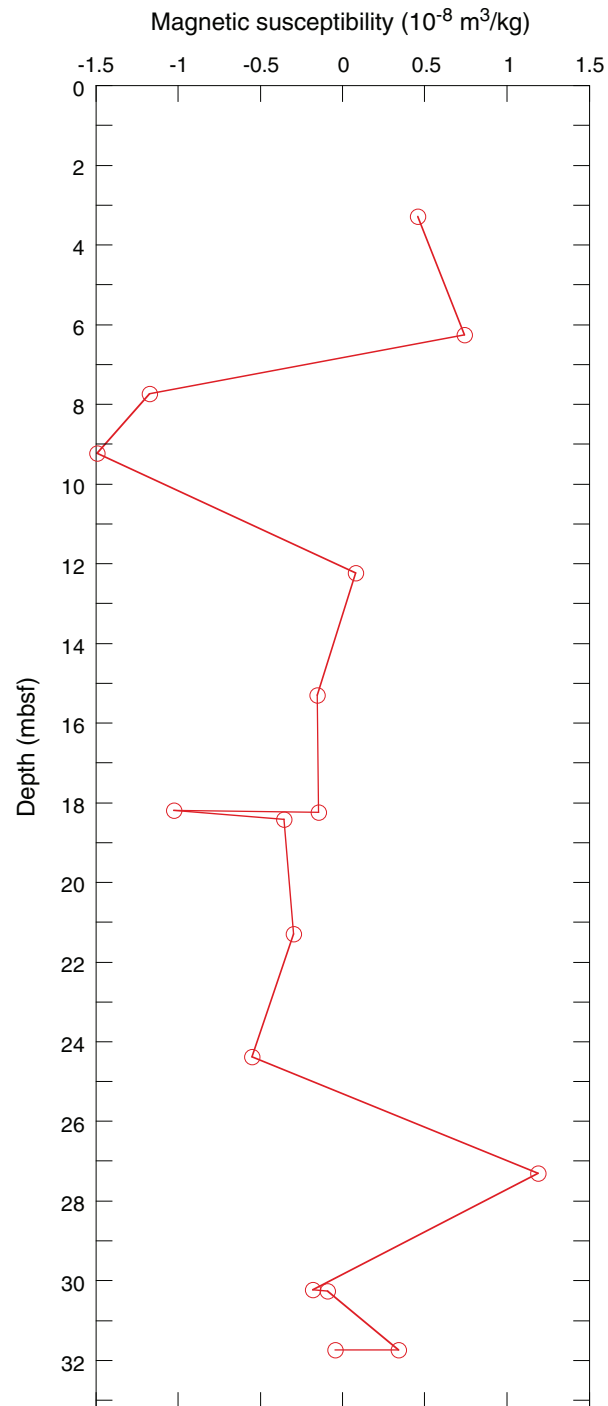


Figure F81. Preliminary chronology for Hole M0047A. Radiocarbon data are presented as graphs with the uncalibrated radiocarbon age and uncertainty shown as the red normal distribution on the ordinate axis and the probability distribution of the calibrated age shown in gray on the abscissa. The marine09 calibration curve is shown in blue. Horizontal bars indicate portions of the age distribution that are significant at the 95.4% confidence interval and the mean age (white circle ± 1 standard deviation) used for the purposes of preliminary dating. All ages are presented as thousands of calendar years BP (1950 AD). See Table T10 in the “Methods” chapter. (See Bronk Ramsey [2009], as well as Bronk Ramsey [2010] at c14.arch.ox.ac.uk/oxcal.html.)

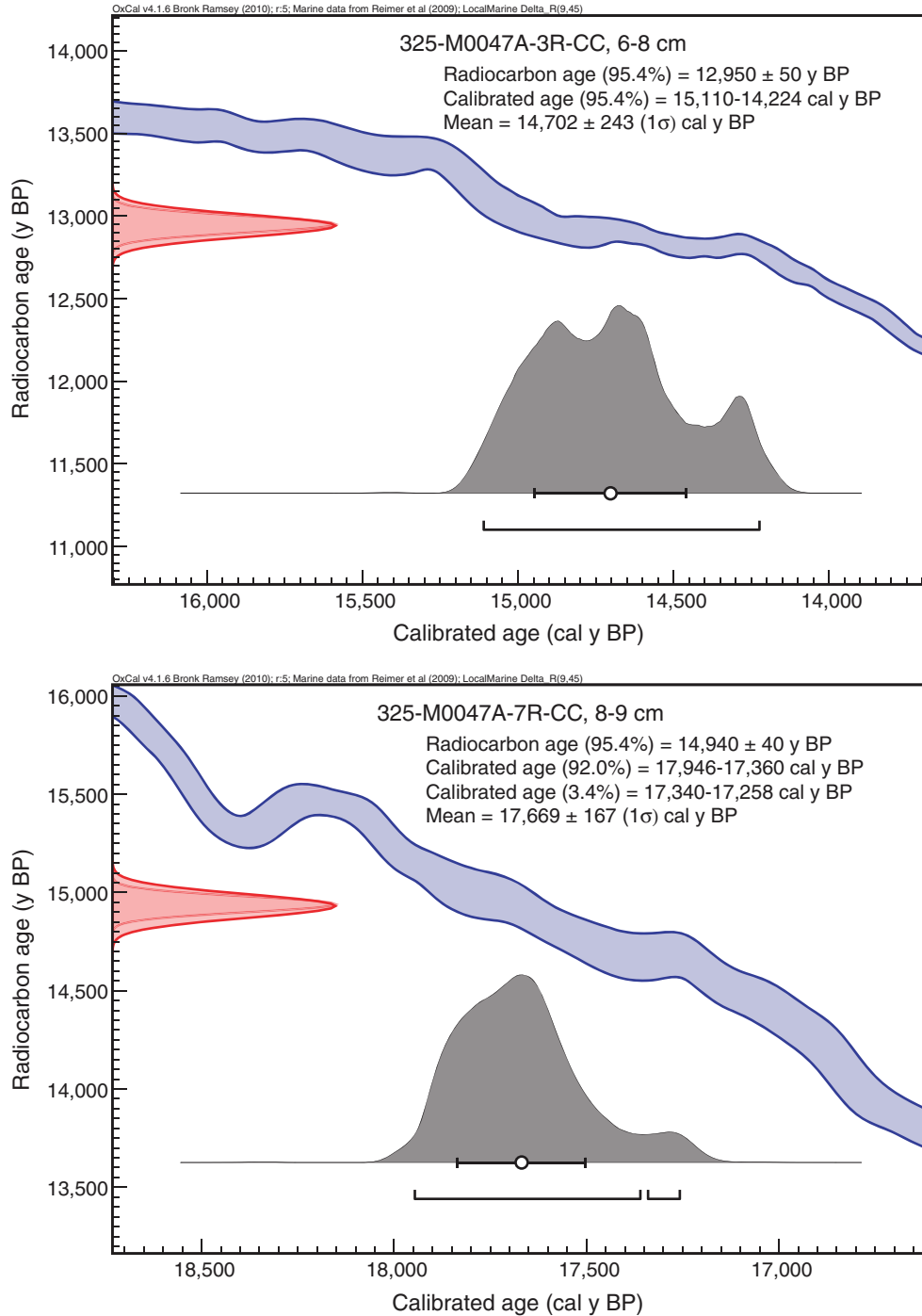


Figure F82. High-resolution line scan image of dark stained fragments of coralline algal boundstone (interval 325-M0048A-3R-1, 6–9 cm).



Figure F83. Summary diagram showing data collected on whole cores using the multisensor core logger (MSCL), Hole M0048A.

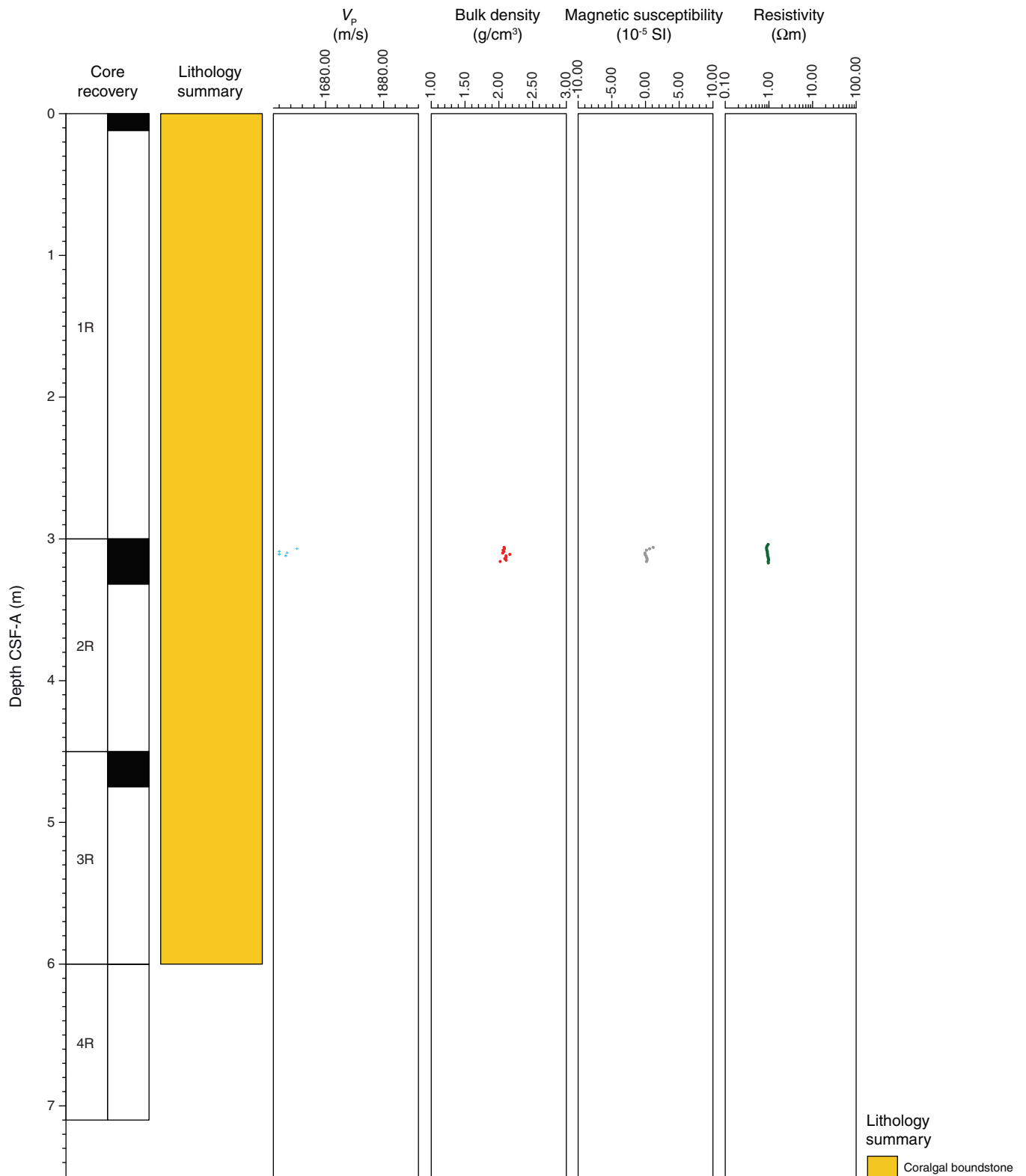


Figure F84. Petrophysical measurements obtained from discrete samples with a pycnometer, Hole M0048A. Bulk density measured on whole cores with the MSCL is shown in red on the bulk density plot.

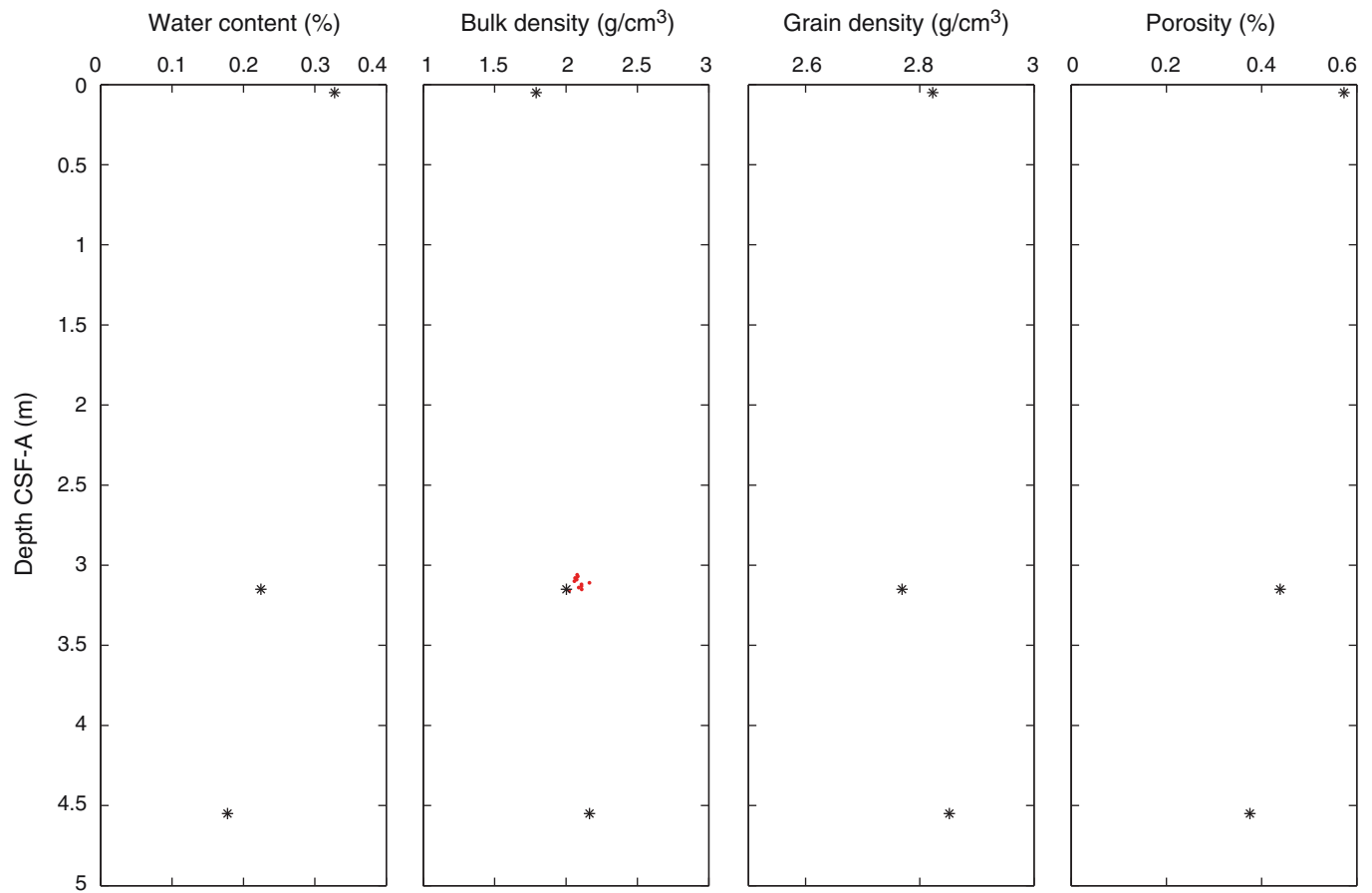


Figure F85. Values of reflectance (L^*), green to red (a^*), and blue to yellow (b^*) indexes, along with ratio a^*/b^* for Hole M0048A.

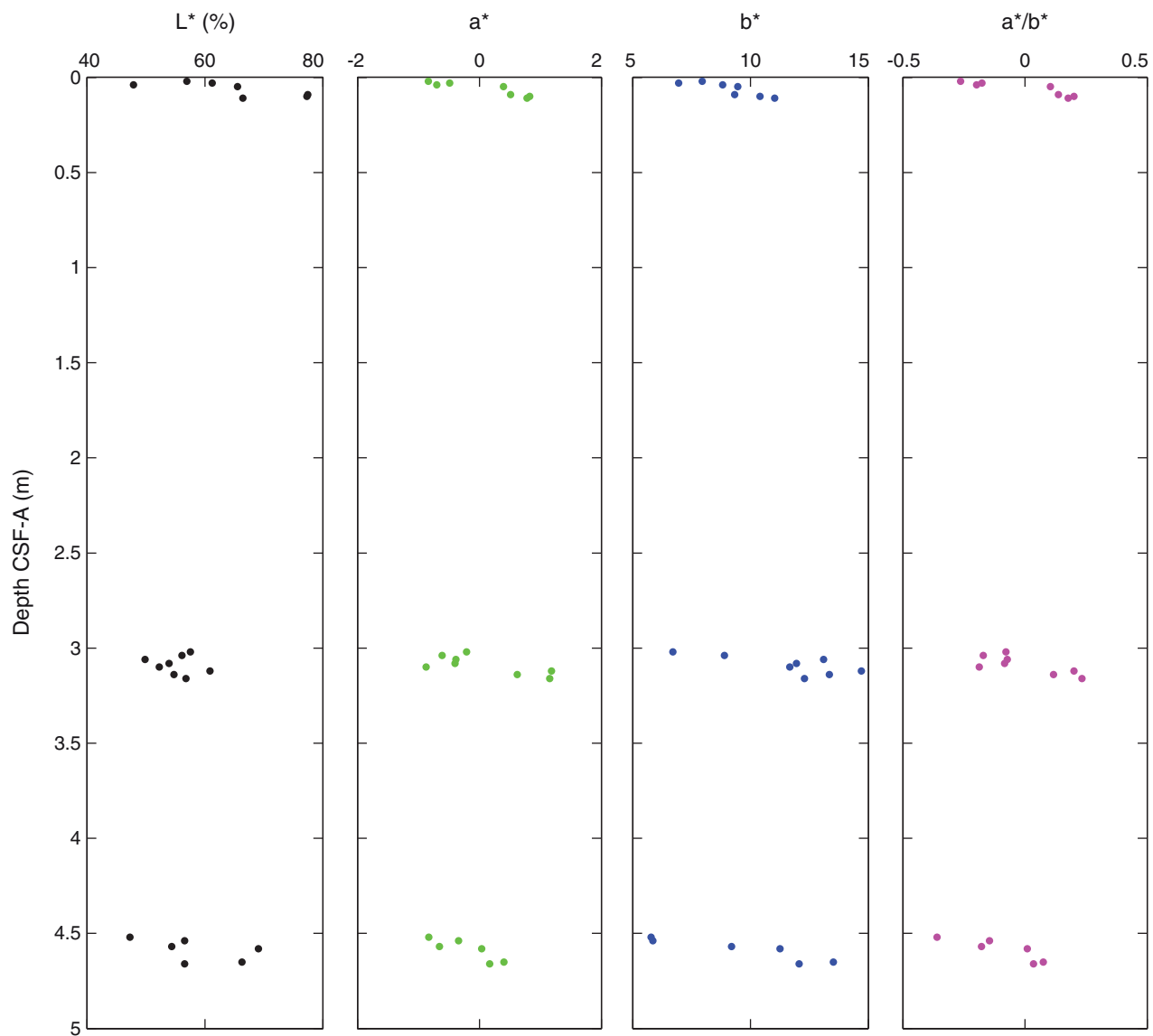


Figure F86. Magnetic susceptibility record for Hole M0048A. Water depth = 97.47 m (LAT).

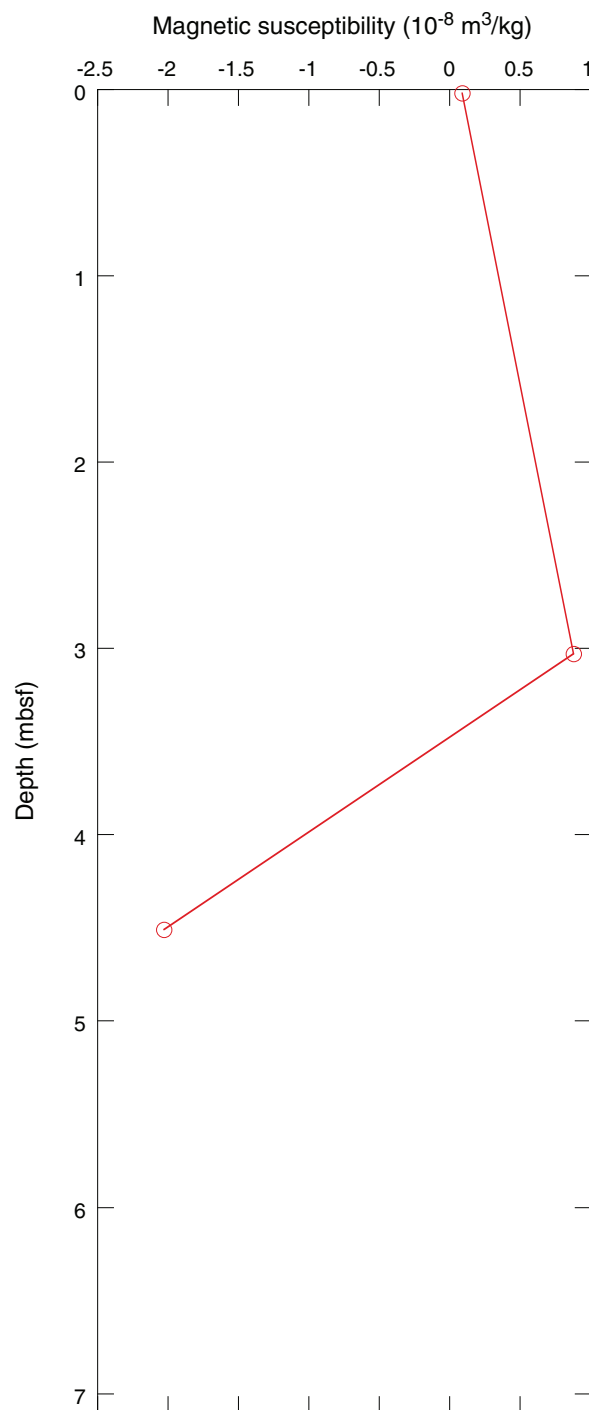


Figure F87. Preliminary chronology for Hole M0048A. Radiocarbon data are presented as graphs with the uncalibrated radiocarbon age and uncertainty shown as the red normal distribution on the ordinate axis and the probability distribution of the calibrated age shown in gray on the abscissa. The marine09 calibration curve is shown in blue. Horizontal bars indicate portions of the age distribution that are significant at the 95.4% confidence interval and the mean age (white circle ± 1 standard deviation) used for the purposes of preliminary dating. All ages are presented as thousands of calendar years BP (1950 AD). See Table T10 in the “Methods” chapter. (See Bronk Ramsey [2009], as well as Bronk Ramsey [2010] at c14.arch.ox.ac.uk/oxcal.html.)

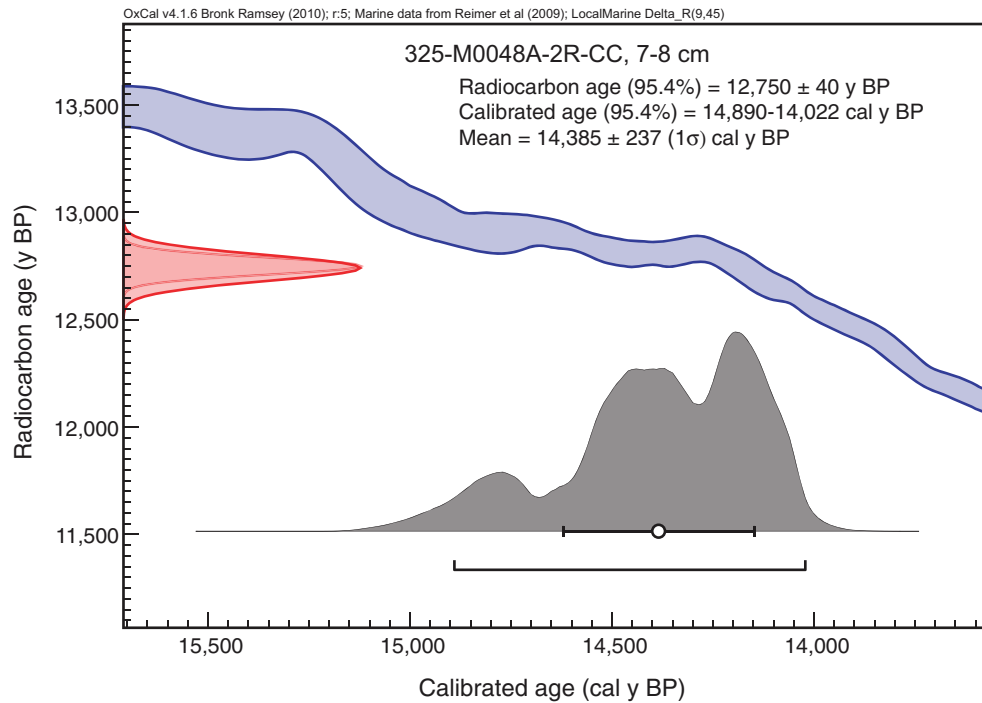


Figure F88. Transect summary showing recovery and main lithostratigraphic units interpreted for transect HYD-02A. Holes are plotted against present-day sea level (LAT taken from corrected EM300 multibeam bathymetry). Distances between holes are indicated on the diagram but are not drawn to horizontal scale.

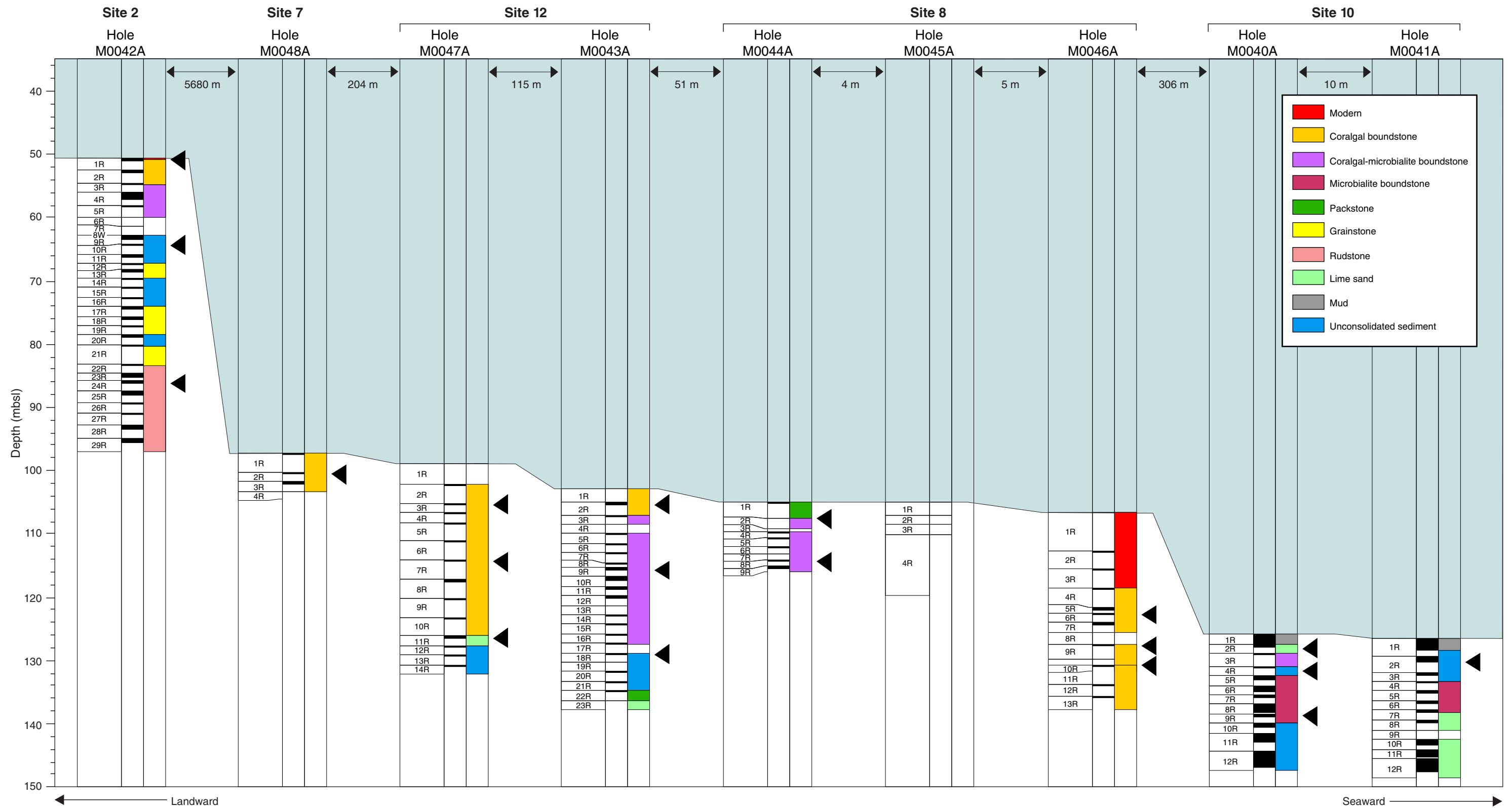


Figure F89. Cross plot showing porosity vs. bulk density measured in discrete samples from transect HYD-02A.

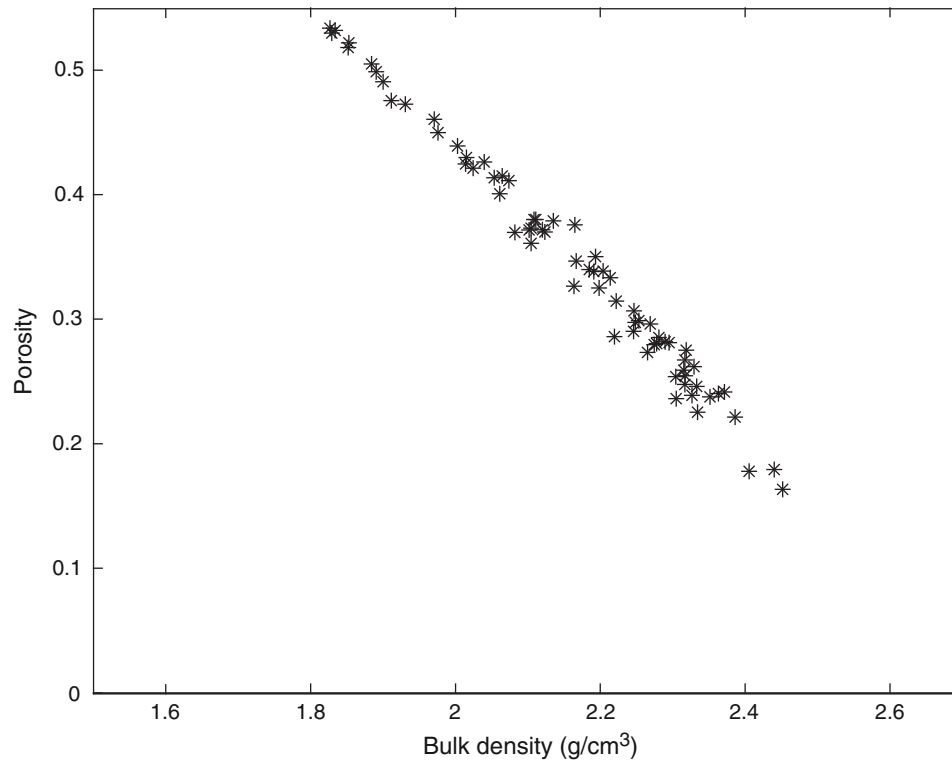


Figure F90. Porosity of discrete samples for all holes measured in transect HYD-02A in order from shallow water to deep water (left to right).

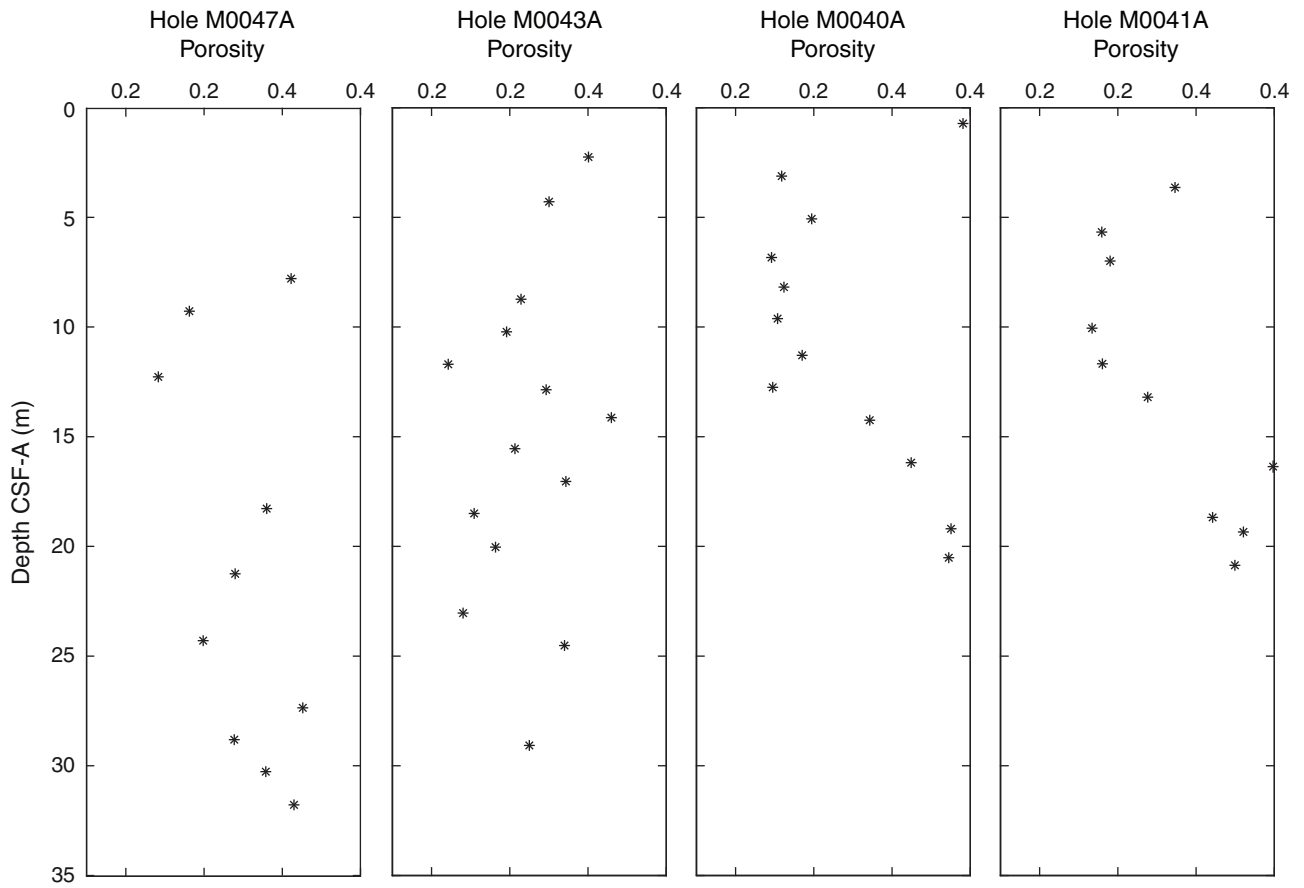


Figure F91. Cross plot of all porosity and V_p measurements from discrete samples analysis from all transect HYD-02A holes.

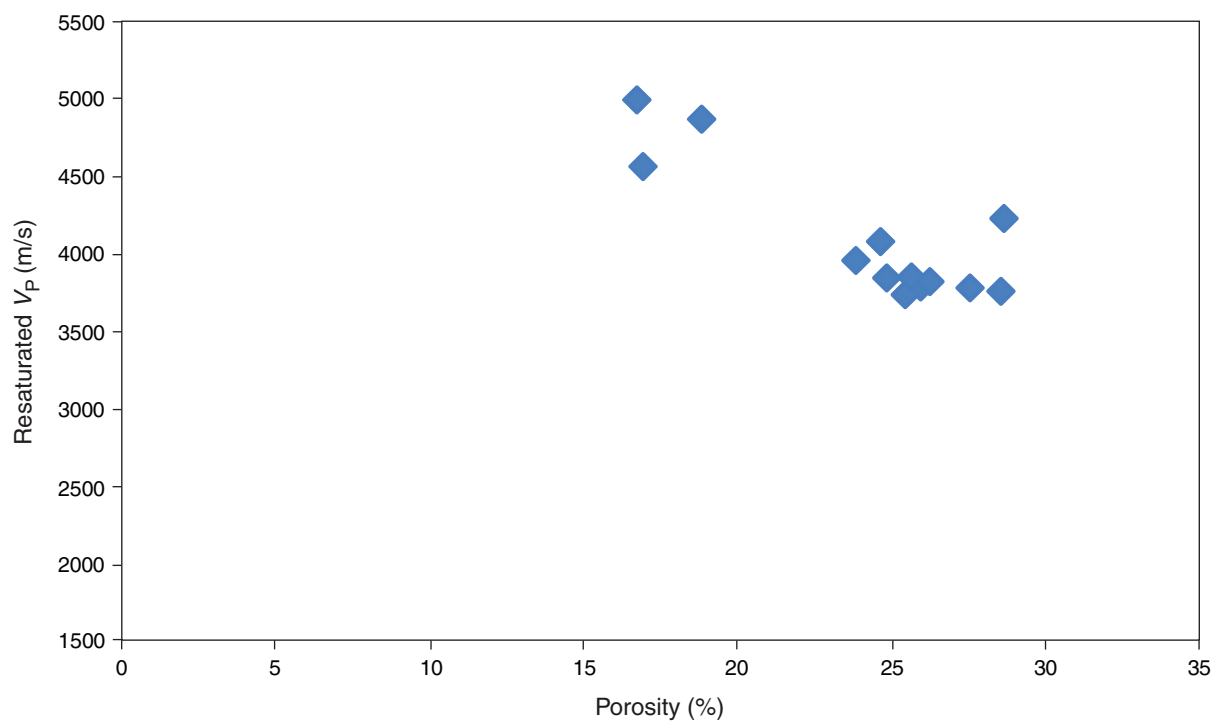




Figure F92. Color reflectance (L^*) for all transect HYD-02A holes in order from shallow water to deep water (left to right).

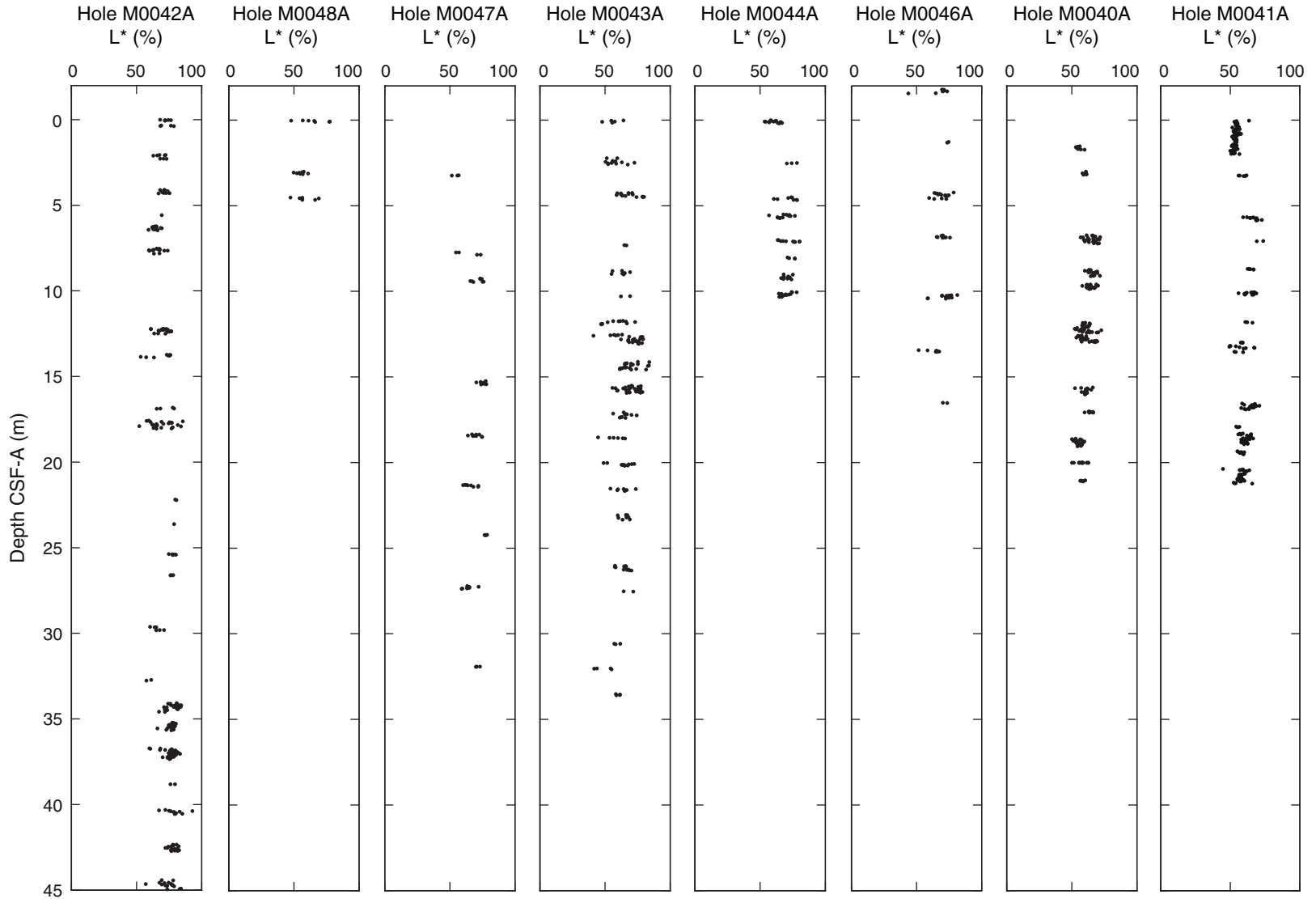


Table T1. Coring summary, transect HYD-02A. (See table notes.) (Continued on next two pages.)

Core	Date (2010)	Time (UTC)	Depth (mbsf)		Length (m)		Recovery (%)	Comments	
			Top	Bottom	Cored	Recovered			
325-M0040A-									
1R	5 Mar	2250	0	1.5	1.5	1.92	128.00	Drill string sank 1.4 m under its own weight with no drilling required.	
2R	5 Mar	2330	1.5	3	1.5	0.17	11.33		
3R	6 Mar	0020	3	5	2	0.24	12.00	Spring core lifter twisted out of shoe—metal in core.	
4R	6 Mar	0230	5	6.5	1.5	0.27	18.00		
5R	6 Mar	0320	6.5	8	1.5	0.77	51.33		
6R	6 Mar	0410	8	9.5	1.5	1.12	74.67		
7R	6 Mar	0450	9.5	11	1.5	0.52	34.67		
8R	6 Mar	0550	11	12.5	1.5	1.43	95.33		
9R	6 Mar	0625	12.5	14	1.5	0.48	32.00		
10R	6 Mar	0715	14	15.5	1.5	0.61	40.67		
11R	6 Mar	0755	15.5	18.5	3	1.6	53.33		
12R	6 Mar	0825	18.5	21.5	3	2.6	86.67		
325-M0041A-									
1R	6 Mar	1005	0	3	3	2.09	69.67	No recovery; assumed to be sand lost on retrieval.	
2R	6 Mar	1040	3	5.4	2.4	0.86	35.83		
3R	6 Mar	1115	5.4	6.9	1.5	0.47	31.33		
4R	6 Mar	1150	6.9	8.4	1.5	0.29	19.33		
5R	6 Mar	1225	8.4	9.9	1.5	0.35	23.33		
6R	6 Mar	1310	9.9	11.4	1.5	0.44	29.33		
7R	6 Mar	1345	11.4	12.9	1.5	0.45	30.00		
8R	6 Mar	1425	12.9	14.6	1.7	0.66	38.82		
9R	6 Mar	1500	14.6	16.1	1.5	0	0.00		
10R	6 Mar	1530	16.1	17.6	1.5	0.96	64.00		
11R	6 Mar	1610	17.6	19.1	1.5	1.33	88.67		
12R	6 Mar	1650	19.1	22.1	3	2.16	72.00		
325-M0042A-									
1R	7 Mar	0330	0	2	2	0.4	20.00		Broken latch head dog—repaired after run.
2R	7 Mar	0405	2	4	2	0.3	15.00		
3R	7 Mar	0500	4	5.5	1.5	0.32	21.33	Change to HQ string after run. API “casing” sank 1.5 m in soft sediments—caused HQ string to vibrate but no damage done. Bit blocked—attempt to free by flushing. API “casing” sinks again—now resting on reentry cone on seabed template causing API string to swab the hole. Trip HQ and continue with API until a hard layer is encountered. Sample recovered from tripped HQ BHA.	
4R	7 Mar	0640	5.5	7.5	2	1.1	55.00		
5R	7 Mar	0705	7.5	9.5	2	0.33	16.50		
6R	7 Mar	1230	9.5	10.7	1.2	0	0.00		
7R	7 Mar	1330	10.7	12.2	1.5	0	0.00		
8W	7 Mar	1500	12.2	12.2	0	0.65	0.00		
9R	7 Mar	1720	12.2	13.7	1.5	0.2	13.33		
10R	7 Mar	1800	13.7	15.2	1.5	0.2	13.33		
11R	7 Mar	1900	15.2	16.7	1.5	0.5	33.33		
12R	7 Mar	1930	16.7	17.5	0.8	0.2	25.00		
13R	7 Mar	2020	17.5	19	1.5	0.57	38.00		
14R	7 Mar	2100	19	20.5	1.5	0.25	16.67		
15R	7 Mar	2135	20.5	22	1.5	0.14	9.33		
16R	7 Mar	2205	22	23.5	1.5	0.2	13.33		
17R	7 Mar	2240	23.5	25	1.5	0.33	22.00		
18R	7 Mar	2320	25	26.5	1.5	0.43	28.67		
19R	8 Mar	0010	26.5	28	1.5	0.27	18.00		
20R	8 Mar	0050	28	29.5	1.5	0.43	28.67		
21R	8 Mar	0130	29.5	32.5	3	0.34	11.33		
22R	8 Mar	0200	32.5	34	1.5	0.39	26.00		
23R	8 Mar	0310	34	35.2	1.2	0.6	50.00		
24R	8 Mar	0355	35.2	36.7	1.5	0.46	30.67		
25R	8 Mar	0435	36.7	38.7	2	0.69	34.50		
26R	8 Mar	0500	38.7	40.2	1.5	0.13	8.67		
27R	8 Mar	0540	40.2	42.2	2	0.38	19.00		
28R	8 Mar	0615	42.2	44.4	2.2	0.56	25.45		
29R	8 Mar	0705	44.4	46.4	2	0.57	28.50	Broken latch head dog—repaired after run.	
325-M0043A-									
1R	9 Mar	0840	0	2.2	2.2	0.17	7.73	Bottom 0.5 m of hole collapsed while running in a new pipe after the first coring run.	
2R	9 Mar	0920	2.2	4.2	2	0.52	26.00	High torque during drilling.	
3R	9 Mar	0955	4.2	5.7	1.5	0.31	20.67	High torque during drilling.	
4R	9 Mar	1030	5.7	7.2	1.5	0	0.00	High torque during drilling.	
5R	9 Mar	1105	7.2	8.7	1.5	0.12	8.00		

Table T1 (continued). (Continued on next page.)

Core	Date (2010)	Time (UTC)	Depth (mbsf)		Length (m)		Recovery (%)	Comments
			Top	Bottom	Cored	Recovered		
6R	9 Mar	1140	8.7	10.2	1.5	0.33	22.00	
7R	9 Mar	1230	10.2	11.7	1.5	0.12	8.00	Shoe jammed with broken coral pieces.
8R	9 Mar	1310	11.7	12.5	0.8	0.24	30.00	
9R	9 Mar	1420	12.5	14	1.5	0.57	38.00	
10R	9 Mar	1510	14	15.5	1.5	0.65	43.33	
11R	9 Mar	1550	15.5	17	1.5	0.5	33.33	
12R	9 Mar	1625	17	18.5	1.5	0.42	28.00	
13R	9 Mar	1700	18.5	20	1.5	0.12	8.00	
14R	9 Mar	1740	20	21.5	1.5	0.2	13.33	
15R	9 Mar	1820	21.5	23	1.5	0.17	11.33	
16R	9 Mar	1900	23	24.5	1.5	0.37	24.67	
17R	9 Mar	1940	24.5	26	1.5	0.2	13.33	
18R	9 Mar	2020	26	27.5	1.5	0.32	21.33	
19R	9 Mar	2100	27.5	29	1.5	0.05	3.33	Large coral piece blocking shoe.
20R	9 Mar	2140	29	30.5	1.5	0.14	9.33	
21R	9 Mar	2220	30.5	32	1.5	0.27	18.00	
22R	9 Mar	2310	32	33.5	1.5	0.15	10.00	
23R	9 Mar	2350	33.5	35	1.5	0.1	6.67	
325-M0044A-								
1R	10 Mar	0320	0	2.5	2.5	0.2	8.00	Fluorescent microspheres.
2R	10 Mar	0405	2.5	4	1.5	0.05	3.33	Switched to spring lifter as lithology very hard.
3R	10 Mar	0555	4	4.5	0.5	0	0.00	Decrease space between shoe and ALN bit to reduce mud flow and so limit unconsolidated material being flushed away.
4R	10 Mar	0700	4.5	5.5	1	0.2	20.00	Mud pressure remains low.
5R	10 Mar	0800	5.5	7	1.5	0.25	16.67	Significant vibration through drill string.
6R	10 Mar	0855	7	8	1	0.14	14.00	Shoe was loose in the inner barrel—reason unknown. Template lowered in water column in an attempt to dampen drill string vibrations.
7R	10 Mar	1000	8	9	1	0.13	13.00	
8R	10 Mar	1100	9	10	1	0.36	36.00	
9R	10 Mar	1615	10	11	1	0.34	34.00	ALN stuck in barrel. During recovery attempt the wireline parted—pipe tripped to recover barrel and overshot.
325-M0045A-								
1R	10 Mar	2130	0	2	2	0	0.00	First attempt at spudding in was aborted as string slipped 3 m rapidly—assumed to have “slid” down the side of a pinnacle/mound.
2R	10 Mar	2205	2	3.5	1.5	0	0.00	
3R	10 Mar	2225	3.5	5	1.5	0	0.00	
4R	10 Mar	2335	5	14.6	9.6	0	0.00	Continued problems with the drill string slipping. Solid drilling encountered between 4.3 and 5 mbsf, but then the string slipped to 14.6 m with no resistance—hole aborted
325-M0046A-								
1R	11 Mar	0130	-10.8	-4.53	6.27	0.13	2.07	Problems with pipe apparently “skipping” down a slope.
2R	11 Mar	0220	-4.53	-1.8	2.73	0.13	4.76	Problems with pipe apparently “skipping” down a slope.
3R	11 Mar	0320	-1.8	1.2	3	0.25	8.33	Problems with pipe apparently “skipping” down a slope.
4R	11 Mar	0420	1.2	4.2	3	0.26	8.67	Coring solid lithology.
5R	11 Mar	0520	4.2	5.2	1	0.43	43.00	
6R	11 Mar	0550	5.2	6.7	1.5	0.33	22.00	
7R	11 Mar	0630	6.7	8.2	1.5	0.32	21.33	
8R	11 Mar	0705	8.2	10.2	2	0	0.00	
9R	11 Mar	0740	10.2	12.4	2.2	0.25	11.36	
10R	11 Mar	0840	12.4	14.4	2	0.11	5.50	Hole collapsed 1 m while recovering barrel.
11R	11 Mar	0920	13.4	16.4	3	0.13	4.33	Top 1 m of core represents infill.
12R	11 Mar	1000	16.4	18.4	2	0.22	11.00	
13R	11 Mar	1035	18.4	20.4	2	0.22	11.00	
325-M0047A-								
1R	11 Mar	1430	0	3.2	3.2	0	0.00	
2R	11 Mar	1510	3.2	6.2	3	0.2	6.67	Contained definite seabed sample at top of core, suggesting first run seabed tag was actually drill string resting on a protrusion which broke off, causing the string to rapidly descend to 3.2 mbsf.
3R	11 Mar	1550	6.2	7.7	1.5	0.37	24.67	
4R	11 Mar	1630	7.7	9.2	1.5	0.24	16.00	
5R	11 Mar	1710	9.2	12.2	3	0.28	9.33	
6R	11 Mar	1800	12.2	15.2	3	0.24	8.00	
7R	11 Mar	1835	15.2	18.2	3	0.26	8.67	
8R	11 Mar	1930	18.2	21.2	3	0.42	14.00	
9R	11 Mar	2030	21.2	24.2	3	0.23	7.67	Decrease space between shoe and ALN bit to reduce mud flow and so limit unconsolidated material being flushed away.

Table T1 (continued).

Core	Date (2010)	Time (UTC)	Depth (mbsf)		Length (m)		Recovery (%)	Comments
			Top	Bottom	Cored	Recovered		
10R	11 Mar	2115	24.2	27.2	3	0.33	11.00	
11R	11 Mar	2200	27.2	28.7	1.5	0.4	26.67	
12R	11 Mar	2240	28.7	30.2	1.5	0.29	19.33	
13R	11 Mar	2325	30.2	31.7	1.5	0.22	14.67	
14R	12 Mar	0015	31.7	33.2	1.5	0.31	20.67	
325-M0048A-								
1R	12 Mar	0405	0	3	3	0.12	4.00	Fluorescent microspheres.
2R	12 Mar	0445	3	4.5	1.5	0.32	21.33	
3R	12 Mar	0520	4.5	6	1.5	0.25	16.67	
4R	12 Mar	0600	6	7.1	1.1	0	0.00	Coring operations aborted because of bad weather—winds >35 kt and heave >2.5 m.

Notes: UTC = Universal Time Coordinated, API = American Petroleum Institute, BHA = bottom-hole assembly, ALN = alien corer (standard rotary corer). Negative depth values indicate depth corrections made during the OSP, to account for the drill string not penetrating the seabed on Runs 1R–3R, thereby indicating progression through the water column and along the side of a topographic high.



Table T2. Physical properties summary, transect HYD-02A. (See table notes.)

Hole	Value	P-wave MSCL (m/s)	P-wave saturated discrete samples (m/s)	Magnetic susceptibility MSCL ($\times 10^{-5}$ SI)	Electrical resistivity MSCL (Ωm)	Bulk density MSCL (g/cm^3)	Bulk density discrete samples (g/cm^3)	Porosity (%)	Grain density (g/cm^3)	Thermal conductivity (W/[m·K])	L* (D65)	a* (D65)	b* (D65)	a*/b*
M0040A	Min	1522	3728	-1.69	0.56	1.01	1.83	25	2.72	1.04	50.27	-1.72	5.35	-0.18
	Max	1829	4073	34.44	26.54	2.44	2.33	53	2.79	1.18	72.73	1.65	15.45	0.12
	Mean \pm SD	1632 \pm 94	3830 \pm 126	2.07 \pm 6.20	4.02 \pm 5.36	1.96 \pm 0.23	2.12 \pm 0.20	37 \pm 11	2.75 \pm 0.02	1.08 \pm 0.06	61.07 \pm 4.83	-0.61 \pm 0.69	10.22 \pm 1.82	-0.06 \pm 0.07
M0041A	Min	1509	3841	-1.00	0.58	1.13	1.83	27	2.74	1.06	44.71	-1.7	4.24	-0.19
	Max	1700	—	67.34	5.03	2.41	2.32	53	2.79	1.09	73.7	1.06	15.01	0.07
	Mean \pm SD	1592 \pm 39	—	1.02 \pm 6.97	0.96 \pm 0.67	2.03 \pm 0.15	2.08 \pm 0.18	39 \pm 10	2.76 \pm 0.02	1.07 \pm 0.02	58.05 \pm 5.19	-1.08 \pm 0.57	10.28 \pm 1.59	-0.11 \pm 0.06
M0042A	Min	1511	3772	-12.42	0.76	1.03	1.51	16	2.70	—	52.1	-0.65	5.06	-0.08
	Max	1866	4223	38.73	40.36	2.49	2.45	72	2.81	—	93.02	3.83	21.48	0.22
	Mean \pm SD	1642 \pm 69	3982 \pm 227	-0.37 \pm 3.75	5.92 \pm 5.53	1.91 \pm 0.33	2.22 \pm 0.22	31 \pm 13	2.74 \pm 0.04	—	73.52 \pm 6.76	1.13 \pm 0.78	14.04 \pm 3.04	0.08 \pm 0.05
M0043A	Min	1527	—	-12.76	0.75	1.05	1.83	22	2.74	—	41.17	-1.3	3.66	-0.29
	Max	1896	—	9.82	93.27	2.40	2.39	53	2.82	—	83.95	3.86	20.24	0.27
	Mean \pm SD	1623 \pm 155	—	0.17 \pm 3.57	6.30 \pm 10.69	1.92 \pm 0.34	2.17 \pm 0.16	35 \pm 9	2.77 \pm 0.02	—	65.29 \pm 8.27	0.57 \pm 0.97	12.04 \pm 2.95	0.04 \pm 0.08
M0044A	Min	—	3874	-0.86	2.39	1.00	2.32	19	2.77	—	53.37	-0.11	4.65	-0.01
	Max	—	4870	13.36	44.84	2.28	2.46	26	2.79	—	80.34	4.95	22.55	0.25
	Mean \pm SD	—	4372 \pm 704	4.20 \pm 5.50	19.73 \pm 16.19	1.51 \pm 0.36	2.39 \pm 0.10	22 \pm 5	2.78 \pm 0.02	—	68.85 \pm 6.33	1.48 \pm 1.02	13.99 \pm 3.01	0.10 \pm 0.06
M0046A	Min	—	—	-0.12	0.96	1.03	—	—	—	—	43.82	-2.01	7.8	-0.23
	Max	—	—	12.76	29.21	2.35	—	—	—	—	81.24	6.19	22.21	0.34
	Mean \pm SD	—	—	6.71 \pm 5.31	7.93 \pm 8.40	1.68 \pm 0.37	—	—	—	—	69.02 \pm 6.36	1.04 \pm 1.30	14.88 \pm 3.85	0.06 \pm 0.08
M0047A	Min	—	—	-0.83	0.66	1.15	2.04	24	2.77	0.98	51.53	-0.59	7.19	-0.08
	Max	—	—	6.38	3.32	2.33	2.37	43	2.81	1.06	78.74	6.18	21.93	0.28
	Mean \pm SD	—	—	0.96 \pm 1.45	1.55 \pm 0.68	1.95 \pm 0.32	2.17 \pm 0.11	35 \pm 6	2.80 \pm 0.01	1.02 \pm 0.06	68.81 \pm 6.62	1.43 \pm 1.12	14.24 \pm 3.01	0.09 \pm 0.07
M0048A	Min	1520	—	-0.08	0.89	2.02	1.79	38	2.77	1.09	47.26	-0.87	5.78	-0.14
	Max	1581	—	1.15	0.99	2.16	2.17	57	2.85	1.09	77.46	1.18	14.72	0.09
	Mean \pm SD	1542 \pm 25	—	0.26 \pm 0.37	0.94 \pm 0.03	2.09 \pm 0.04	1.99 \pm 0.19	46 \pm 10	2.81 \pm 0.04	—	59.29 \pm 8.43	-0.01 \pm 0.68	10.20 \pm 2.61	-0.01 \pm 0.07

Notes: MSCL = multisensor core logger. SD = standard deviation. — = no measurement taken.

Table T3. Larger benthic foraminifera in cores from the transect HYD-02A. (See table note.)

Hole, core, section, interval (cm)	Abundance	Preservation	<i>Alveolinella</i>	<i>Amphistegina</i>	<i>Baculogypsina</i>	<i>Calcarina</i>	<i>Cycloclypeus</i>	Elphidiidae	<i>Gypsina</i>	<i>Heterostegina</i>	<i>Homotrema</i>	<i>Lenticulina</i>	<i>Marginopora</i>	<i>Miliolida</i>	<i>Operculina</i>	<i>Planorbulinella</i>	<i>Rotalida</i>	Soritinae	<i>Sphaerogypsina</i>	<i>Textulariida</i>
325-																				
M0040A-1R-1, 80–85	Ab																			
M0040A-10R-1, 20–25	C	Moderate/fragmented/abraded													x		x			
M0040A-11R-1, 70–75	C	Good to moderate/fragmented													x					
M0040A-12R-1, 70–75	R	Good		x										x	x					
M0040A-12R-2, 50–55	R	Good												x	x					
M0041A-1R-1, 14–19	R	Good		x										x	x					
M0041A-1R-2, 70–75	Ab																			
M0041A-8R-1, 40–45	C	Good to abraded	x	x																
M0041A-10R-1, 34–39	C	Fragmented	x	x				x												
M0041A-11R-1, 55–60	R	Good to fragmented																		
M0041A-12R-1, 64–69	R	Good to fragmented													x	x				
M0041A-12R-2, 24–29	R	Good to fragmented													x	x				
M0042A-1R-1, 14–19	Ab																			
M0042A-13R-1, 26–31	R	Abraded		x						x										
M0042A-29R-CC, 0–5	Ab																			
M0043A-2R-1, 20–25	R	Fragmented		x						x										
M0043A-18R-1, 10–15	A	Fragmented/abraded			x	x														
M0043A-23R-CC, 5–10	R	Fragmented													x					
M0046A-6R-CC, 5–10	Ab																			
M0047A-3R-1, 10–15	R	Good		x																
M0047A-11R-1, 10–15	A	Abraded			x	x														x
M0047A-14R-CC, 0–5	R	Fragmented							x											
M0048A-1R-1, 0–5	R	Fragmented/encrusted	x	x			x													
M0048A-3R-CC, 7–12	R	Good		x																

Note: Abundance: A = abundant, C = common, R = rare, Ab = Absent.



Table T4. Geochemical data relating to interstitial water collected from transect HYD-02A. (Continued on next page.)

Hole, core, section, interval (cm)	Depth (mbsf)	Sample ID	pH	Alk (mM)	NH ₄ (μM)	Ca (mM)	Si (μM)	Sr (μM)	Mg (mM)	B (μM)	K (mM)	S (mM)	Na (mM)	Ba (nM)	Li (μM)	Al (μM)	As (nM)
325-																	
M0040A-1R-1, 75	0.75	S19	7.77	2.65	45	10.6	103.3	105.3	53.1	427	10.33	28.7	467	76	25.6	41.9	68
M0040A-1R-2, 21	1.72	S20	7.71	3.04	42	10.6	107.1	108.5	53.4	433	10.41	28.8	470	74	26.3	40.4	0
M0040A-10R-1, 36	14.36	S21	7.81	3.44	61	9.8	81.3	96.6	51.5	455	10.13	26.4	442	74	28.8	40.4	0
M0040A-12R-1, 92	19.42	S22	7.70	2.79	30	10.6	91.9	114.1	53.4	443	10.28	29.2	446	74	25.3	47.2	0
M0041A-1R-1, 27	0.27	S23	7.64	2.75	27	10.3	97.5	98.5	52.8	451	10.48	28.7	465	71	24.8	44.1	0
M0041A-8R-1, 42	13.32	S24	7.76	2.94	30	10.5	69.1	110.1	53.5	451	10.29	28.8	466	82	26.2	42.3	0
M0041A-10R-1, 72	16.82	S25	7.72	2.84	34	10.5	72.8	111.9	53.6	446	10.28	29.4	472	70	27.4	42.2	138
M0041A-11R-1, 60	18.20	S26	7.71	2.61	32	10.6	69.6	115.1	53.8	441	10.27	29.7	457	75	25.2	39.4	0
M0041A-12R-1, 29	19.39	S27	7.67	2.81	29	10.6	76.4	116.3	53.8	442	10.31	29.1	469	74	25.3	44.0	28
M0041A-12R-1, 130	20.40	S28	7.67	2.56	30	10.6	80.9	116.8	53.8	445	10.32	28.9	472	80	26.0	44.0	0
M0042A-13R-1, 36	17.86	S29	7.70	4.42	2	11.5	29.1	102.9	49.5	421	9.87	26.1	424	94	24.6		
M0042A-29R-1, 25	44.65	S30	7.64	5.25	0	14.6	57.5	103.7	39.9	421	9.69	18.5	427	127	24.5	46.1	0
M0043A-2R-1, 33	2.53	S31	7.84	3.11	0	10.0	42.0	81.8	53.4	455	10.25	28.4	459	75	25.4	50.3	0
M0043A-10R-1, 26	14.26	S32	7.61	5.05	40												
M0043A-18R-1, 7	26.07	S33	7.95	7.06	0												
M0043A-18R-1, 15	26.15	S34	7.79	3.34	32	10.4	41.1	97.5	52.4	432	10.03	27.3	441	71	24.1	44.0	183
M0046A-13R-CC, 3	29.37	S35	7.73	6.59	10	9.1	38.5	65.3	53.9	447	10.01	26.8	449	62	26.9	37.1	70
M0046A-13R-CC, 6	29.34	S36	7.71	4.98	39												
M0047A-8R-1, 14	18.34	S37	7.77	5.17	14												
M0047A-8R-1, 20	18.40	S38	7.69	4.01	30	10.0	38.9	96.9	52.1	432	9.92	27.3	438	67	24.5	48.9	0
Hole, core, section, interval (cm)	Depth (mbsf)	Sample ID	Be (nM)	Cd (nM)	Co (nM)	Cr (nM)	Cu (nM)	Fe (μM)	Mn (μM)	Mo (nM)	Ni (nM)	P (μM)	Pb (nM)	Ti (nM)	V (nM)	Zn (μM)	Zr (nM)
325-																	
M0040A-1R-1, 75	0.75	S19	167	0	0	0	0	0.98	0.29	0	0	2.65	0	50	7	3.87	256
M0040A-1R-2, 21	1.72	S20	54	0	0	0	0	1.24	0.28	0	0	1.55	0	0	0	3.37	262
M0040A-10R-1, 36	14.36	S21	94	0	0	0	0	1.03	0.01	0	38	4.09	0	0	531	3.74	222
M0040A-12R-1, 92	19.42	S22	135	0	0	0	0	1.87	0.06	0	12	2.37	0	5	0	5.37	308
M0041A-1R-1, 27	0.27	S23	102	11	23	0	0	1.18	0.25	0	0	3.95	0	0	0	3.36	295
M0041A-8R-1, 42	13.32	S24	141	0	0	0	0	0.94	0.02	0	2	1.15	0	0	133	3.96	257
M0041A-10R-1, 72	16.82	S25	71	0	0	0	0	0.96	0.05	0	0	32.92	0	0	153	3.27	238
M0041A-11R-1, 60	18.20	S26	93	0	0	0	0	1.64	0.03	0	0	1.19	0	0	65	3.53	262
M0041A-12R-1, 29	19.39	S27	108	0	0	0	0	1.32	0.02	0	36	1.86	2	0	0	3.87	327
M0041A-12R-1, 130	20.40	S28	103	0	0	0	0	2.24	0.04	0	36	0.78	0	1	87	3.66	228
M0042A-13R-1, 36	17.86	S29															
M0042A-29R-1, 25	44.65	S30	80	0	0	0	0	1.40	0.12	189	101	7.41	0	0	0	3.83	308
M0043A-2R-1, 33	2.53	S31	58	0	121	0	0	1.03	0.10	0	133	1.33	0	0	150	3.55	341
M0043A-10R-1, 26	14.26	S32															
M0043A-18R-1, 7	26.07	S33															
M0043A-18R-1, 15	26.15	S34	99	0	47	0	0	1.10	0.05	0	161	2.97	0	0	0	4.44	330
M0046A-13R-CC, 3	29.37	S35		0	22	0	0	0.87	0.01	306	36	8.21	0	0	1528	2.92	412
M0046A-13R-CC, 6	29.34	S36															
M0047A-8R-1, 14	18.34	S37	123														
M0047A-8R-1, 20	18.40	S38		0	0	0	0	0.83	0.00	0	0	3.24	0	0	537	3.61	347



Table T4 (continued).

Hole, core, section, interval (cm)	Depth (mbsf)	Sample ID	Cl (mM)	Br (μ M)	SO ₄ (mM)
325-					
M0040A-1R-1, 75	0.75	S19	570	890	29.8
M0040A-1R-2, 21	1.72	S20	565	907	29.8
M0040A-10R-1, 36	14.36	S21	541	871	27.1
M0040A-12R-1, 92	19.42	S22	564	899	29.8
M0041A-1R-1, 27	0.27	S23	566	897	29.8
M0041A-8R-1, 42	13.32	S24	567	901	29.6
M0041A-10R-1, 72	16.82	S25	569	903	29.6
M0041A-11R-1, 60	18.20	S26	563	908	29.7
M0041A-12R-1, 29	19.39	S27	552	890	29.1
M0041A-12R-1, 130	20.40	S28	569	920	30.1
M0042A-13R-1, 36	17.86	S29	538	867	26.7
M0042A-29R-1, 25	44.65	S30	517	835	19.2
M0043A-2R-1, 33	2.53	S31	563	914	29.3
M0043A-10R-1, 26	14.26	S32			
M0043A-18R-1, 7	26.07	S33			
M0043A-8R-1, 15	26.15	S34	552	890	29.0
M0046A-13R-CC, 3	29.37	S35			
M0046A-13R-CC, 6	29.34	S36			
M0047A-8R-1, 14	18.34	S37			
M0047A-8R-1, 20	18.40	S38	549	891	28.6